STRUCTURE AND REACTIVITY OF O-LITHIATED SPECIES: SPECTROSCOPIC AND COMPUTATIONAL INVESTIGATIONS OF SOLUTION STRUCTURE AND REACTION MECHANISM

A Dissertation

Presented to the Faculty of the Graduate School

of Cornell University

In Partial Fulfillment of the Requirements for the Degree of

Doctor of Philosophy

by

Angela Margaret Bruneau

January 2014

STRUCTURE AND REACTIVITY OF O-LITHIATED SPECIES: SPECTROSCOPIC AND COMPUTATIONAL INVESTIGATIONS OF SOLUTION STRUCTURE AND REACTION MECHANISM

Angela Margaret Bruneau, Ph.D.

Cornell University 2014

Solution structural characterization of organolithium aggregates has been advanced through the efforts of Collum and coworkers. These characterizations necessarily precede detailed mechanistic studies, and may guide the engineering of new aggregates of interest. Amino alkoxides used as chiral auxiliaries by Merck and DuPont have been characterized through the use of the method of continuous variations at high temperatures. The results are corroborated by low temperature NMR data, X-ray structures, and DFT computations. Chiral mixed aggregates of lithium hexamethyldisilazide and amino alkoxides of potential synthetic utility were discovered in the course of this work, and their structure elucidated through a new extension of the Method of Continuous Variations. In an effort to extend the utility of amino alkoxides as chiral auxiliaries, mixtures of achiral enolates and phenolates with amino alkoxides were explored.

A detailed mechanistic study of an aza aldol addition is presented in Chapter II herein. Following structural studies, detailed mechanistic studies are performed to understand the origins of product ratios, and correlations between rate and reaction conditions that are necessary for optimization. This mechanistic

study is presented in the context of previous assumptions about the aggregation dynamics along the reaction coordinate, and is the first mechanistic study of an aza aldol addition. The dimer-based reaction was uncloaked through the use of in-situ ReactIR, rapid inject NMR, and DFT computations.

BIOGRAPHICAL SKETCH

Angela Margaret Bruneau was born in Richmond, California to Ann Elizabeth Moffitt and Ronald Roger Bruneau on August 17, 1981. Her family moved to South Florida early in her childhood where she attended several grade schools following the opening and closing of gifted programs before opting to graduate early in 1997. Angela worked in real estate from 1997-1999 before taking a job in computer operations where she worked full time for five years while learning computer programming and simultaneously attending community college full-time for the last three years. In 2005 Angela transferred to the University of California Berkeley to study chemistry. There she worked in the laboratory of Professor Jean M. J. Fréchet at the Lawrence Berkeley National Laboratory on projects in dendrimer synthesis and templated [2]catenane synthesis, and published her first scientific work in 2008. Angela graduated with a B.S. in Chemistry from the University of California Berkeley in 2008, and moved to cooler weather in Ithaca, NY to enter a doctoral program at Cornell University. Under the mentorship of Professor David B. Collum, Angela wrote two research papers in the field of physical organic chemistry concerning the aggregate structures and reaction mechanisms of O-lithiated species. In 2013 Angela graduated with her Ph.D. in Chemistry from Cornell University, and will begin a career with ExxonMobil in Paulsboro, NJ in 2014.

This work is dedicated to my mother, Ann Elizabeth Moffitt, who is my rock, my biggest fan, and the most loving person that I know; to my doting father, Ronald Bruneau, may he rest in peace; to my loving brother, Michael Bruneau; and to my life partner, Kyle Nouri, and our son, Aimon Nouri, who make all of my days infinitely brighter.

ACKNOWLEDGMENTS

First I would like to first thank my advisor, Professor David B. Collum, who has been tremendously supportive throughout my graduate career. Working with Dave has helped to shape me both personally and professionally, and I cannot thank him enough for our interactions. I would also like to acknowledge my colleagues, who have each helped me grow as a teacher, a student, a team leader, and a team player in the last five years. Past group members: Tim DeVries, Alex Hoepker, Joseph Renny, Josie Gruver, Lehka Gupta, Anandarup Goswami, Hari Subramanian, and Shannon Oseback. Current Group Members: Laura Tomasevich, Jun Liang, Michael Houghton, Jacqueline Perodeau, Evan Tallmadge, Kyoung-Joo Jin, and Russell Algera. I would further like to thank my committee members, Geoffrey Coates and William Dichtel, for their strong support, and other key Cornell Faculty and Instructors that have helped me in various ways in the course of my time at Cornell: Dr. Thomas Ruttledge, Professor Brian Crane, Professor Chad Lewis, and Professor Bruce Ganem. The support staff at Cornell has been absolutely indispensable, and I thank them profusely for their assistance: Patricia Hine, Denise Wurtenburg, Josh Wakeman, Larry Stull, Dave Neish, Anthony Condo, and especially Ivan Keresztez, who has spent countless hours with me on the NMR, and to whom I owe my magnet shimming artistry. Of course, most of all I want to thank Cornell University and the University of California Berkeley, my alma mater, for challenging and supporting me in my studies.

TABLE OF CONTENTS

Biographical Sketch	iii
Dedication	iv
Acknowledgements	v
Table of Contents	vi
List of Figures	vii
List of Tables	xi
Chapter I: Solution Structures of Lithium Amino Alkoxides Used in Highly Enantioselective 1,2-Additions	1
Appendix I: Supporting Information for Chapter I	19
a. NMR Spectroscopic Studies	19
b. MCV (Job) Plots	30
c. X-Ray Crystal Structure	32
d. DFT Computations	38
References I.	52
Chapter II: Azaaldol Condensation of a Lithium Enolate Solvated by *N,N,N′,N′*-Tetramethylethylenediamine: Dimer-Based 1,2-Addition to Imines	58
Appendix II: Supporting Information for Chapter II	73
a. NMR Spectroscopic Studies	74
b. NMR and IR Kinetic Studies	82
c. DFT Computations	92
References II.	115
Chapter III: Lithium Amino alkoxide-Lithium Enolate Mixed Aggregates	125
References III.	136

LIST OF FIGURES

Figure 1.1.	ORTEP of **5a**.	6
Figure 1.2.	^{6}Li NMR spectrum of a 1:1 mixture of **2a** and **2b** in toluene recorded at +60 ºC.	8
Figure 1.3.	Job plot of **2a** and **2b** for 0.10 M mixtures in toluene at +60 ºC.	9
Figure 1.4.	^{6}Li NMR spectrum of 1:1 mixture of [^{6}Li,^{15}N]LiHMDS (0.10 M) and **2a** (0.10 M) in toluene at -30 ºC.	11
Figure 1.5.	^{6}Li NMR spectra for mixtures of [^{6}Li]LiHMDS (0.10 M) with varying **2a**:**2b** ratio in toluene.	12
Figure 1.6.	Job plot of mixed ladders **12a** (**A_2**), **12b** (**B_2**), and **12c** (**AB**) in toluene at -30 ºC.	13
Figure A1.1.	^{6}Li NMR spectra of [^{6}Li]**2a** (0.10 M) in toluene from **-**80 ºC to +25 ºC.	20
Figure A1.2.	^{6}Li NMR spectra of [^{6}Li]**2b** (0.10 M) in toluene from **-**80 ºC to +25 ºC.	21
Figure A1.3.	^{6}Li NMR spectra of [^{6}Li]**3a** (0.10 M) in toluene from **-**80 ºC to +25 ºC.	21
Figure A1.4.	^{6}Li NMR spectra of [^{6}Li]**3b** (0.10 M) in toluene from **-**80 ºC to +25 ºC.	22
Figure A1.5.	^{6}Li NMR spectra of 1:1 [^{6}Li]**2a** (0.050 M) and [^{6}Li]**2b** (0.050 M) in toluene from -80 ºC to +60 ºC.	23
Figure A1.6.	^{6}Li NMR spectra of 1:1 [^{6}Li]**2a** (0.050 M) and [^{6}Li]**2b** (0.050 M) in THF (6.0 M) and toluene cosolvent from -100 ºC to +40 ºC.	24
Figure A1.7.	^{6}Li NMR spectra of 1:1 [^{6}Li]**2a** (0.050 M) and [^{6}Li]**2b** (0.050 M) in pyridine (1.2 M) and toluene cosolvent from -100 ºC to +40 ºC.	25

Figure A1.8. ^{6}Li NMR spectra for 0.10 M solutions of [^{6}Li]**2a** and [^{6}Li]**2b** in toluene with varying X_{2a} at +60 °C. 26

Figure A1.9. ^{6}Li NMR spectra for 0.10 M solutions of [^{6}Li]**3a** and [^{6}Li]**3b** in toluene with varying X_{3b} at +80 °C. 27

Figure A1.10. Job plot of [^{6}Li]**2a**/[^{6}Li]**2b**. Relative integrals measured at +60 °C are plotted vs measured mole fraction of [^{6}Li]**2a**. 28

Figure A1.11. Job plot of [^{6}Li]**3a**/[^{6}Li]**3b**. Relative integrals at +80 °C are plotted vs measured mole fraction of [^{6}Li]**3b**. 28

Figure A1.12. ^{6}Li NMR spectrum of **12b** at -80 °C. 29

Figure A1.13. ^{15}N NMR spectrum of **12b** at -80 °C. 30

Figure A1.14. ^{6}Li NMR spectra for 0.10 M solutions of [^{6}Li]**12a** and [^{6}Li]**12b** in toluene with varying X_{12b}. 30

Figure A1.15. Job plot of [^{6}Li]**12a**/[^{6}Li]**12b** in toluene. Relative integrals measured are plotted vs measured mole fraction of [^{6}Li]**12b**. 31

Figure A1.16. X-ray crystal structure of **2b**. 32

Figure A1.17. Relative free energies of **7a, 7b** and **13a, 13b**. 38

Figure 2.1. Curve fitting for the condensation of enolate **2** with equimolar imine **1** in TMEDA/toluene at -60°C. 62

Figure 2.2. Plot of k_{obsd} versus **[2]** for condensation with **1** under pseudo first order conditions in TMEDA/toluene at -60°C. 63

Figure 2.3. Plot of kobsd versus **[TMEDA]**$_{free}$ for condensation of 1 and 2 under pseudo first order conditions in TMEDA/toluene at -60°C. 64

Figure 2.4. Computed transition structures of stoichiometry $[(ROLi)_2(TMEDA)_2(imine)]^{‡}$. 65

Figure A2.1. ^{1}H NMR spectrum of **4** in $CDCl_3$. 74

Figure A2.2. ^{13}C NMR spectrum of **4** in $CDCl_3$. 75

Figure A2.3. ^{1}H NMR spectrum of [^{15}N]**4** in $CDCl_3$. 76

Figure A2.4. ^{13}C NMR spectrum of [^{15}N]**4** in $CDCl_3$. 77

Figure A2.5. ^{6}Li NMR spectrum of a 0.10 M solution of [^{6}Li,^{15}N]**3** in TMEDA/toluene at -60 °C. 78

Figure A2.6. ^{15}N NMR spectrum of a 0.10 M solution of [^{6}Li,^{15}N]**3** in TMEDA/toluene at -60 °C. 79

Figure A2.7. ^{19}F NMR spectrum of a 0.10 M solution of [6Li,15N]**3** in TMEDA/toluene at -60 °C. 80

Figure A2.8. ^{6}Li NMR spectrum of a solution of stoichiometric [^{6}Li,^{15}N]**3** and enolate [^{6}Li]**2** in TMEDA/toluene at -60 °C. 81

Figure A2.9. Representative ^{6}Li NMR spectroscopic analysis of the condensation of lithium enolate **2** with varying concentrations of imine **1** in TMEDA/toluene at -60°C. 82

Figure A2.10. Representative ^{19}F NMR spectroscopic analysis of the pseudo first order condensation of lithium enolate **2** with imine **1** in TMEDA/toluene at -60 °C. 83

Figure A2.11. Condensation of the lithium enolate **2** (0.10 M) with imine **1** (0.005 M) in 0.55 M TMEDA/toluene at -60 °C. 84

Figure A2.12. Curve fitting for the condensation of lithium enolate **2** with stoichiometric imine **1** in TMEDA/toluene at -60 °C. 85

Figure A2.13. Plot of k_{obsd} versus [**2**] for its condensation with imine **1** (0.005 M) in TMEDA/toluene at -60 °C. 86

Figure A2.14. Plot of k_{obsd} versus [**TMEDA**] for the condensation of enolate **2** and imine **1** in toluene cosolvent at -60 °C. 87

Figure A2.15. Representative curve fitting of initial rates for the stoichiometric condensation of lithium enolate **2** with imine **1** in TMCDA/toluene at -60 °C. 88

Figure A2.16. Representative curve fitting for the condensation of lithium enolate **2** (0.10 M) with imine **1** (0.005 M) in TMCDA/toluene at -60 °C. 89

Figure A2.17. Plot of k_{obsd} versus [**2**] for its condensation with imine **1** in TMCDA/toluene at -60 °C. 90

Figure A2.17. Plot of k_{obsd} versus [TMCDA] in toluene cosolvent for the condensation of lithium enolate **2** (0.10 M) with imine **1** (0.005 M) at -60 ° C. 91

Figure 3.1. ^{6}Li NMR spectra of 0.10 M mixtures of [^{6}Li]acetophenone enolate and **1** at -80 °C. 127

Figure 3.2. ^{6}Li NMR spectra of 0.10 M mixtures of [^{6}Li]naphthol phenolate and **1** at -80 °C. 128

Figure 3.3. ^{6}Li NMR spectra of 0.10 M mixtures of [^{6}Li]cyclohexanone enolate and **2** at -80 °C. 129

Figure 3.4. ^{6}Li NMR spectra of 0.10 M mixtures of [^{6}Li]naphthol phenolate and **2** at -80 °C. 130

Figure 3.5. ^{6}Li NMR spectra of 0.10 M mixtures of [^{6}Li]1-indanone enolate and **2** at -80 °C. 131

Figure 3.6. ^{6}Li NMR spectra of 0.10 M mixtures of [^{6}Li]4-fluorophenolate and **2** at -80 °C. 132

Figure 3.7. ^{6}Li NMR spectra of 0.10 M mixtures of [^{6}Li]acetophenone enolate and **2** at -80 °C. 133

LIST OF TABLES

Table A1.1.	Crystal Data and Structure Refinement for **2b**.	33
Table A1.2.	ORTEP coordinates for **2b**.	34
Table A1.3.	Optimized geometries, coordinates, and energies for observed tetramer **7b**.	39
Table A1.4.	Optimized geometries, coordinates, and energies for unobserved tetramer **9b**.	42
Table A1.5.	Optimized geometries, coordinates, and energies for unsubstituted tetramer **13a**.	45
Table A1.6.	Optimized geometries, coordinates, and energies for unsubstituted tetramer **13b**.	47
Table A1.7.	Optimized geometries, coordinates, and energies for observed tetramer **8a**.	49
Table A2.1.	Optimized ground state geometry, coordinates, and energy for imine **1**.	92
Table A2.2.	Optimized ground state geometry, coordinates, and energy for TMEDA dichelated dimer of lithium enolate **2**.	93
Table A2.3.	Optimized transition structure geometry, coordinates, and energy for TMEDA dichelated open dimer **5a**.	95
Table A2.4.	Optimized transition structure geometry, coordinates, and energy for TMEDA monochelated open dimer **5b**.	97
Table A2.5.	Optimized transition structure geometry, coordinates, and energy for TMEDA unchelated open dimer **5c**.	99
Table A2.6.	Optimized transition structure geometry, coordinates, and energy for TMEDA dichelated closed dimer **5d**.	101
Table A2.7.	Optimized transition structure geometry, coordinates, and energy for TMEDA monochelated closed dimer **5e**.	103
Table A2.8.	Optimized transition structure geometry, coordinates, and energy for TMEDA unchelated closed dimer **5f**.	105

Table A2.9. Optimized transition structure geometry, coordinates, and energy for TMEDA unchelated nitrogen-containing dimer **5g**. 107

Table A2.10. Optimized transition structure geometry, coordinates, and energy for unsolvated anion of triple ions **5h** and **7b**. 108

Table A2.11. Optimized geometry, coordinates, and energy for TMEDA dichelated lithium cation of triple ion **5h**. 110

Table A2.12. Optimized transition structure geometry, coordinates, and energy for TMCDA disolvated open dimer **7a**. 111

Table A2.13. Optimized geometry, coordinates, and energy for TMCDA dichelated lithium cation of triple ion **7b**. 113

CHAPTER I

Solution Structures of Lithium Amino Alkoxides Used in Highly Enantioselective 1,2-Additions

Abstract

Lithium ephedrates and norcarane-derived lithium amino alkoxides used to effect highly enantioselective 1,2-additions on large scales have been characterized in toluene and tetrahydrofuran. The method of continuous variations in conjunction with ^{6}Li NMR spectroscopy reveals that the lithium amino alkoxides are tetrameric. In each case, low-temperature ^{6}Li NMR spectra show stereoisomerically pure homoaggregates displaying resonances consistent with an S_4-symmetric cubic core rather than the alternative D_{2d} core. These assignments are supported by density functional theory computations and conform to X–ray crystal structures. Slow aggregate exchanges are discussed in the context of amino alkoxides as chiral auxiliaries.

Introduction

The idea of exploiting organolithium mixed aggregates to control organolithium reactivity and selectivity lurked for several decades,[1] but it moved to center stage in the early 1980s largely owing to contributions of Seebach and coworkers.[2] In a dramatic application of aggregate-based stereocontrol, the process group at Merck has shown that two equiv each of lithium cyclopropylacetylide **1** and lithium ephedrate **2b** effect the 1,2-addition in eq 1 in 98% enantioselectivity.[3] Synthesis of more than 50,000 kg of reverse transcriptase inhibitor efavirenz (Sustiva, Stocrin) using this protocol quashed any doubt about the practicality of stoichiometric amino alkoxide auxiliaries.[4] Subsequently, DuPont Pharmaceuticals prepared more than 2000 kg of a second-generation reverse transcriptase inhibitor using a seemingly analogous 1,2-addition of lithium acetylide **1** to quinazolinone **4** with an extraordinary 99.5% enantioselectivity (eq 2).[5] In this case, however, optimal selectivity was obtained using a 3:1 mixture of norcarane-derived amino alkoxide **3a** and **1**.

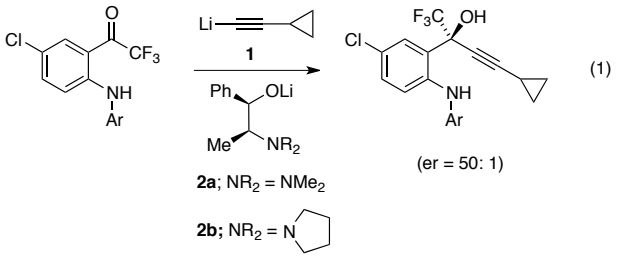

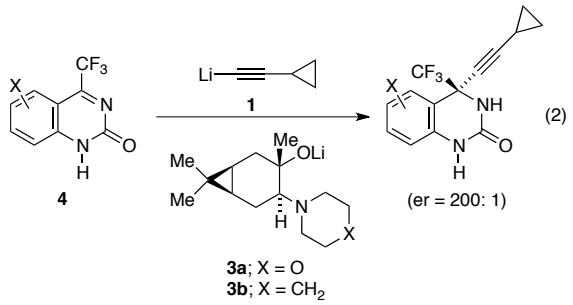

A Cornell–Merck collaboration traced the high enantioselectivity in eq 1 to reaction of substrate with 2:2 $(ROLi)_2(R'Li)_2$ mixed tetramer **5**.[6] A subsequent Cornell–DuPont collaboration attributed the enantioselectivity in eq 2 to external attack of acetylide on 3:1 $(ROLi)_3(substrate)_1$ mixed tetramer **6**.[7] In both reactions, aging the reaction near ambient temperature before addition at low temperature was key to attaining high selectivity.

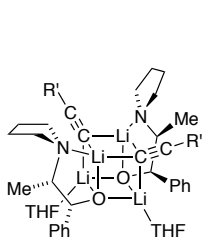

5

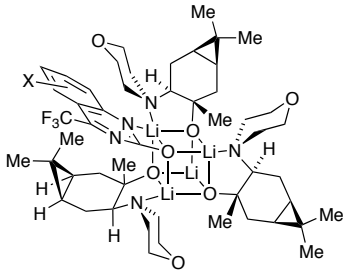

6

During these structural and mechanistic studies, the solution structures of the amino alkoxide homoaggregates proved elusive. The problem emanated from the difficulties associated with characterizing O-lithiated species in solution, wherein high symmetry and lack of O–Li coupling preclude direct NMR spectroscopic analysis.[8] Arnett and coworkers have previously reported a crystal structure of ephedrate **2a** displaying an S_4-symmetric tetrameric core, but their efforts to determine the solution structure were less conclusive.[9]

Considerable inroads have now been made toward characterizing the structures of O-lithiated species in solution.[8,10,11,12] Using a combination of ^{6}Li NMR spectroscopy, the method of continuous variations (MCV),[8,12,13] and density functional theory computations, we show herein that amino alkoxides **2a,b** and **3a,b** form exclusively unsolvated homotetramers **7a,b** and **8a,b**.[11,12,14] Several

intraaggregate exchanges[12,15] are shown to be remarkably slow. In conjunction with ^{6}Li–^{15}N double-labeling studies, the application of MCV is extended to distinguish lithium hexamethyldisilazide-lithium amino alkoxide dimers **11** and the corresponding ladders **12**[16]—a structural ambiguity arising from opaque O–Li linkages that has dogged us for many years.[12b,17] We also provide a more nuanced view of the benefits of catalytic lithium salts on the enantioselectivities observed by DuPont investigators.

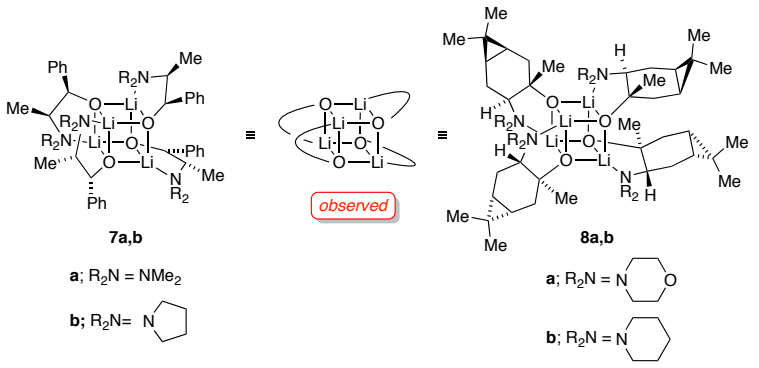

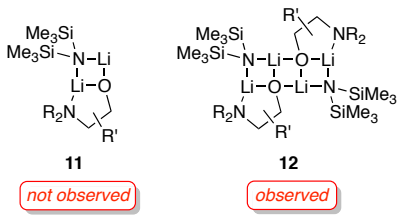

Results

Homoaggregation. Lithium alkoxides **2a,b** and **3a,b** were generated in toluene by treating the corresponding alcohols[3e,18] with 1.0 equiv of labeled lithium hexamethyldisilazide ([^{6}Li]LiHMDS).[19] To facilitate the narrative, we note at the outset that the data support cubic tetramers **7a,b** and **8a,b** bearing S_4-symmetric cores.

Low-temperature ^{6}Li NMR spectroscopy of all four alkoxides reveals two resonances (1:1) that coalesce above –15 °C to afford a single sharp resonance above 0 °C consistent with a single aggregate containing two magnetically inequivalent lithium nuclei. Note that S_4-symmetric cubic tetramers **7a,b** and **8a,b** would show such a pair, whereas D_{2d} tetramers **9a,b** and **10a,b** would each display a single ^{6}Li resonance. The coalescence temperature in toluene (approximately –20 °C for all four alkoxides) is higher than that in neat THF ($T_{coalesc}$ ≈ –35 °C), suggesting that THF assists the exchange. We attribute these behaviors to a degenerate rearrangement of the chelates about the cubic tetramer frameworks of **7a,b** and **8a,b** (eq 3).

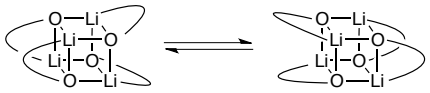

(3)

Despite the THF dependence on the *rate* of chelate exchange, we conclude that THF is coordinated only transiently based on a simple and powerful diagnostic probe as follows.[12] Pyridine strongly coordinates lithium nuclei and shifts ^{6}Li resonances markedly (0.5 to >1.0 ppm) downfield even in neat THF solutions.[12c,20] Amino alkoxides **2a,b** and **3a,b** showed no measurable change in

chemical shift in solutions of 1.2 M pyridine/toluene compared with that in THF/toluene or toluene solutions, demonstrating that the chelates occupy all available coordination sites.

The assignment of **7a** is consistent with a crystal structure by Arnett and coworkers.[9] The assignment of **7b** was corroborated by an X–ray crystal structure of **5a** showing the S_4-symmetric cubic tetramer core (Figure 1; supporting information).

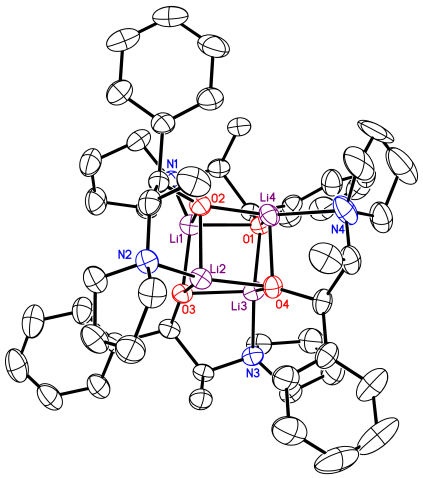

Figure 1.1. ORTEP of **5a** as fully chelated tetramer bearing an S_4-symmetric cubic core.

Heteroaggregation and MCV. Assignment of **2a,b** and **3a,b** as tetramers **7a,b** and **8a,b** relied critically on MCV.[8,12,13] In this experiment, the high symmetries of the lithium alkoxides are disrupted by forming ensembles of homo- and heteroaggregates (eq 4).[21,22] The number and symmetries of the heteroaggregates and the dependence of the distribution on the mole fraction ($X_{\mathbf{A}}$ or $X_{\mathbf{B}}$) attest to the structures of the homoaggregates, $\mathbf{A}_n$ and $\mathbf{B}_n$. In most previous applications of MCV, cubic tetramers appear as a series of five homo- and

heteroaggregates with the characteristic resonance counts illustrated in Chart 1.[8,12]

$$\mathbf{A}_n + \mathbf{B}_n \Longrightarrow \mathbf{A}_n + \mathbf{A}_{n-1}\mathbf{B}_1 + \mathbf{A}_{n-2}\mathbf{B}_2 + \ldots\mathbf{B}_n \qquad (4)$$

Chart 1

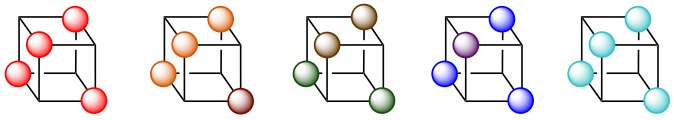

$\mathbf{A}_4$ $\mathbf{A}_3\mathbf{B}_1$ (3:1) $\mathbf{A}_2\mathbf{B}_2$ (2:2) $\mathbf{A}_1\mathbf{B}_3$ (1:3) $\mathbf{B}_4$

Characterization of the alkoxides as tetramers using MCV is illustrated with **2a** and **2b** emblematically. Mixtures of **2a** and **2b** in a 1:1 ratio in toluene or THF give intractable NMR spectra at low temperature. The complexity inherent to ensembles is exacerbated by the stereochemistry of chelation (discussed in detail below). On warming, however, the resonances coalesce to afford a sharp 5-peak ensemble at +60 °C consistent with a tetramer ensemble—$\mathbf{A}_4$, $\mathbf{A}_3\mathbf{B}_1$, $\mathbf{A}_2\mathbf{B}_2$, $\mathbf{A}_1\mathbf{B}_3$, and $\mathbf{B}_4$—with each stoichiometry appearing as a single resonance (Figure 2). The apparent *intraaggregate* Li–Li exchange[8,12,15,20a] is well precedented and has been useful in characterizing O-lithiated species, but it is usually significantly more facile. The exchange shows minor acceleration by THF relative to toluene. The aggregates were monitored in the high temperature limit with varying proportions of **2a** and **2b** and fixed total alkoxide concentration. The relative integrations of the five distinct aggregates are plotted versus measured mole fractions[23] ($X_\mathbf{A}$ or $X_\mathbf{B}$) of the two components in Figure 3. The curves result from a parametric fit as described previously.[8,12] the number of aggregates and quality of

the fit confirm the tetramer assignment. In conjunction with the symmetry of the homoaggregates at low temperature and solvent-independent chemical shift, MCV completes the assignment of alkoxides **2a** and **2b** as solvent-free tetramers **8a** and **8b**.

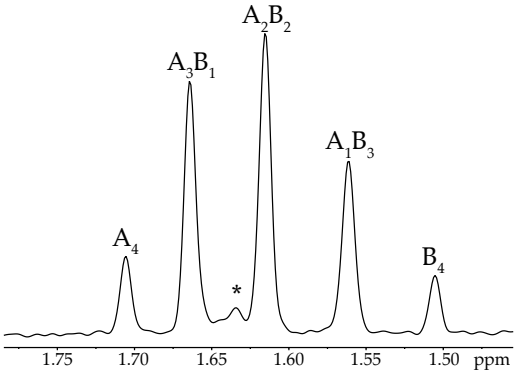

Figure 1.2. ^{6}Li NMR spectrum of a 1:1 mixture of lithium ephedrates **2a** and **2b** in toluene recorded at +60 °C. The labels indicate the relative $\mathbf{A}_m\mathbf{B}_n$ stoichiometries. The asterisk denotes an unknown impurity.

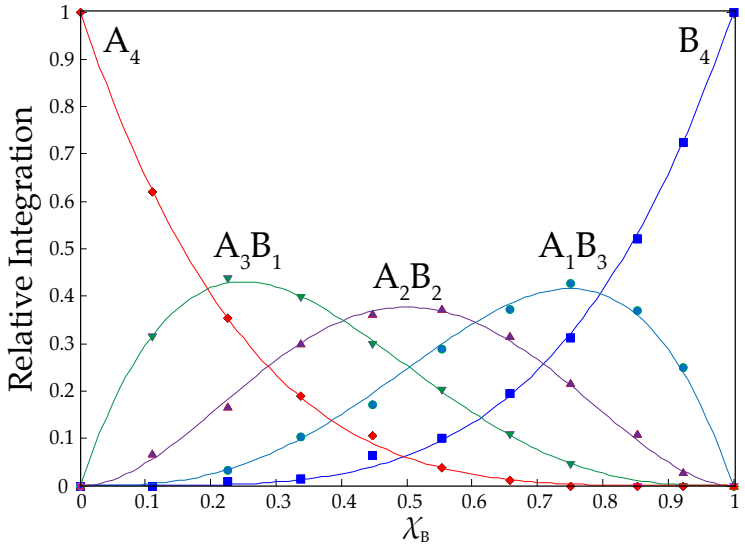

Figure 1.3. Job plot showing the relative integrations of tetrameric homo- and heteroaggregates versus measured mole fractions[23] of **2a** (X_A) for 0.10 M mixtures of lithium ephedrates [^{6}Li]**2a** (**A**) and [^{6}Li]**2b** (**B**) in toluene at +60 °C.

Studies of norcarane-derived alkoxides **3a** and **3b** afforded results fully analogous to those of **2a** and **2b** in every respect, supporting unsolvated cubic tetramers **8a** and **8b**. Relatively minor quantitative differences include slightly faster chelate exchanges and slightly slower intraaggregate Li–Li site exchanges.

The stereochemical preference for S_4 rather than D_{2d} cubic cores was examined using density functional theory computations at the B3LYP level of theory with the 6–31G(d) Pople basis set.[24] Free energies were calculated from an MP2-derived single-point energy [6–31G(d) basis set] and a B3LYP-derived thermal correction [6–31G(d)] at 195 K and 1 atm. The 21 kcal/mol preference for the S_4 form in **7b** (eq 5) is fully consistent with the experimental data. Although we often use computations only qualitatively, this difference is *very* large for isodesmic[25] stereoisomers. Computations of a sterically less congested variant in

which the phenyl and methyl moieties along the backbone of ephedrate **2a** were omitted show a reduced but still sizeable 7 kcal/mol preference for the S_4 core (eq 6).

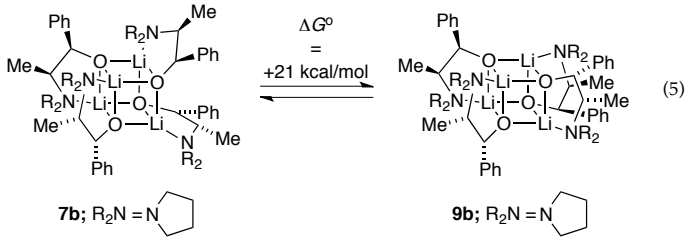

(5)

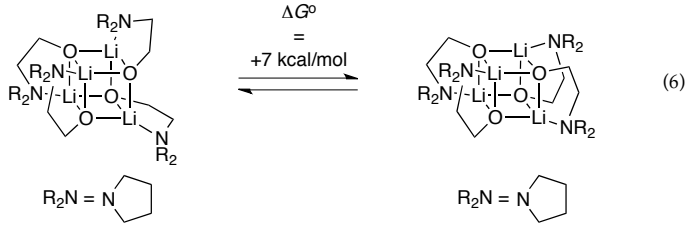

(6)

Lithium alkoxide–LiHMDS mixed aggregates. During the studies described above, we detected lithium alkoxide–LiHMDS mixed aggregates that formed quantitatively with 1.0 equiv of excess LiHMDS.[22] For example, lithium ephedrate **2a** with 1.0 equiv excess [^{6}Li,^{15}N]LiHMDS displays two ^{6}Li doublets in a 1:1 ratio (J_{Li-N} = 1.0 Hz) and a single resonance appearing as a quintet in the ^{15}N NMR spectrum (Figure 4). The data are consistent with the basic mixed dimer subunits **11a,b** or the corresponding ladder **12a**. Once again, the spectroscopically opaque Li–O linkages posed a problem, and MCV offered the solution.

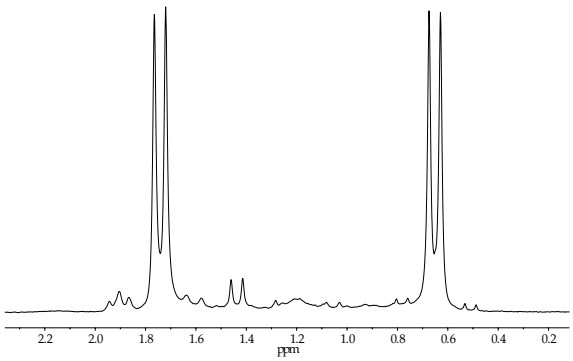

Figure 1.4. ^{6}Li NMR spectrum recorded on a 1:1 mixture of [^{6}Li,^{15}N]LiHMDS (0.10 M) and lithium amino alkoxides **2a** (0.10 M total concentration) in toluene cosolvent at –30 °C.

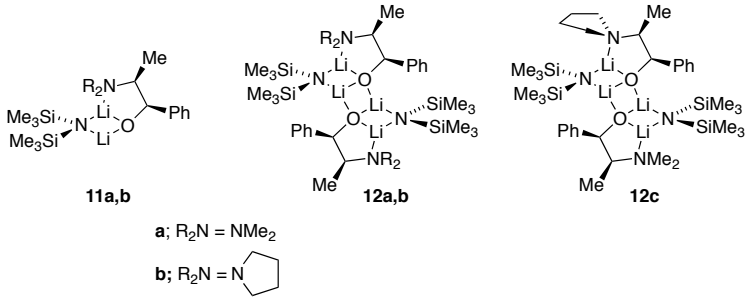

Mixtures of lithium ephedrates **2a** and **2b** in toluene at varying proportions but constant lithium alkoxide titer in the presence of 1.0 equiv of LiHMDS afford ^{6}Li spectra showing the two original resonance pairs along with additional resonances consistent with mixed ladder **12c**. The downfield ensemble is not well resolved, yet the upfield resonances clearly show **12a** and **12b** along with two resonances (1:1) attributed to mixed ladder **12c**. We suspect that the well-resolved upfield resonances correspond to those bearing the dialkylamino chelates. Maintaining the total concentration of excess LiHMDS at 0.10 M and the total alkoxide titer at 0.10 M while varying proportions (mole fractions) of the

two alkoxides afforded a mole fraction-dependent distribution consistent with ladders **12a**, **12b**, and **12c**. The resulting Job plot is illustrated in Figure 6. The resonance counts and quality of the fit confirm the 1:1 association of two mixed dimeric subunits and the overall ladder motif.

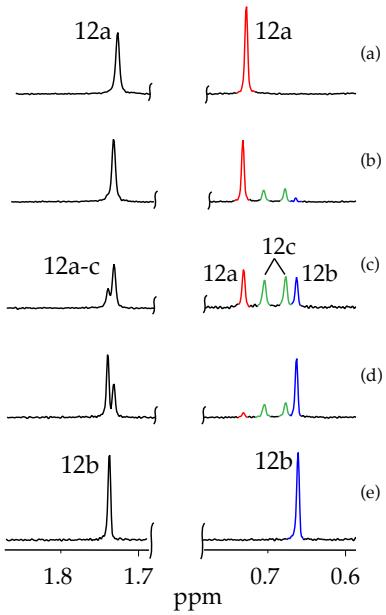

Figure 1.5. ^{6}Li NMR spectra recorded on mixtures of [^{6}Li]LiHMDS (0.10 M) and lithium amino alkoxides **2a** and **2b** (0.10 M total concentration) in toluene cosolvent at –30 °C: (a) 0.10 M [^{6}Li]**2b**; (b) 0.080 M [^{6}Li]**2b** and 0.020 M [^{6}Li]**2a**; (c) 0.050 M [^{6}Li]**2b** and 0.050 M [^{6}Li]**2a**; (d) 0.020 M [^{6}Li]**2b** and 0.080 M [^{6}Li]**2a**; and (e) 0.10 M [^{6}Li]**2a**.

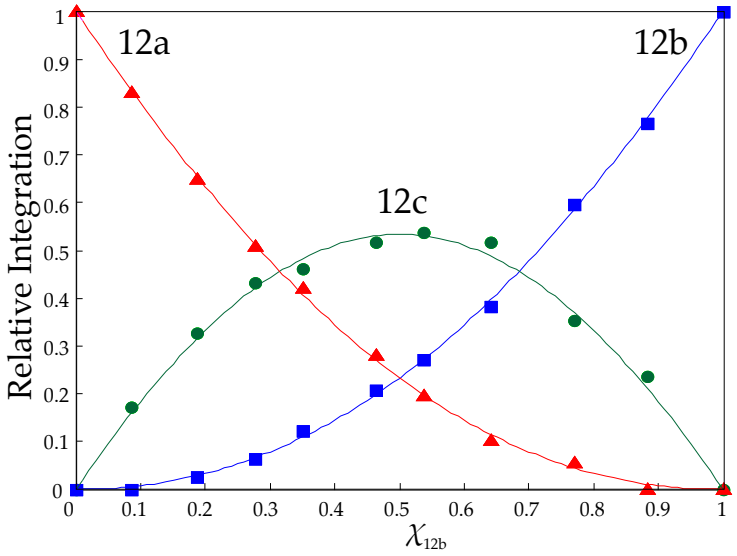

Figure 1.6. Job plot showing the relative integrations of mixed ladders **12a** (**A**$_2$), **12b** (**B**$_2$), and **12c** (**AB**) versus measured mole fractions of **2b**–LiHMDS (X_B) in mixtures containing 0.10 total amino alkoxide and 0.10 M LiHMDS at –30 °C.

Discussion

Synthetically important lithium amino alkoxides pose an interesting challenge for structural organolithium chemists. Arnett and coworkers have shown that crystalline 2a is cubic tetramer 9a, but their efforts to determine the solution structure were less conclusive. Messy ^{6}Li NMR spectra cast doubt on the colligative measurements, which are notoriously sensitive to impurities.[8] We previously studied amino alkoxides 2a and 3a using NMR spectroscopy and gleaned no useful information.[6,7] The current paper describes how a combination of ^{6}Li NMR spectroscopy and MCV allowed us to characterize 2a,b and 3a,b as stereochemically pure cubic tetramers 9a,b and 10a,b. Computational studies suggest that the S_4-symmetric cubic core is inherently more stable than the D_{2d} core, a preference that is amplified by the substituents along the chelate

backbone (eqs 4 and 5). During these studies, we made a number of observations and achieved some tactical developments in MCV that call for further elaboration.

In the low temperature limit, all four homoaggregates display two distinct resonances that, with warming, coalesce into a single resonance owing to facile degenerate isomerizations of the chelates (eq 3). Although this observation proved critical to complete the structural assignments, it foreshadowed severe technical problems with the use of MCV. In typical applications of MCV to characterize tetramer ensembles (eq 4), we would observe three heteroaggregates of stoichiometries—3:1, 2:2, and 1:3—displaying resonance counts and integrations reflecting the symmetries (Chart 1).[12] The amino alkoxides, by contrast, show a markedly increased resonance count arising from stereochemical complexity (Chart 2). The homoaggregates each show two rather than the usual one resonance. The 3:1 and 1:3 heterotetramers exist as two distinct diastereomers each displaying *eight* resonances total. There are potentially *four* diastereomeric 2:2 heterotetramers—two C_2-symmetric diastereomers displaying two resonances each and two C_1-symmetric diastereomers containing four discrete lithium resonances each. Thus, the tetramer ensemble in the slow exchange limit would include 32 resonances in total. It is not shocking, therefore, that ensembles generated from **2a/2b** or **3a/3b** pairings are intractable in the low temperature limit.

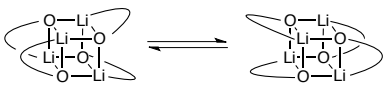

(6)

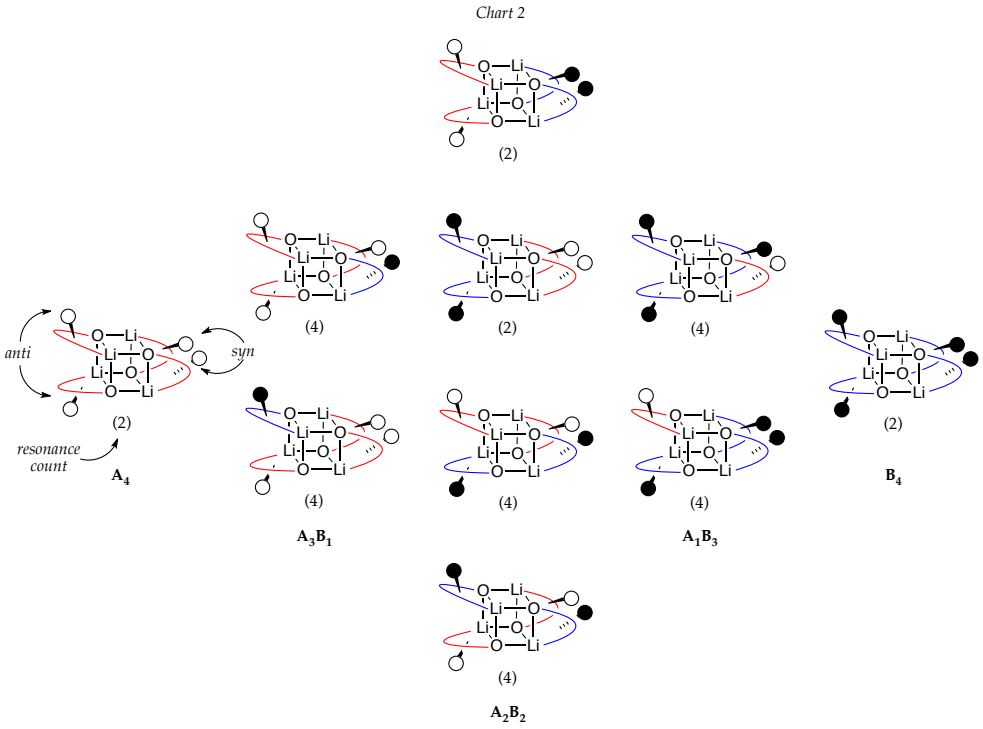

Two general classes of intraaggregate exchanges would, in principle, simplify the spectra. Chelate–chelate exchange (eq 3) without further deepseated adjustments within the cubic core would reduce the complexity of Chart 2 to the simpler distribution depicted in Chart 1 and lower the ^{6}Li resonance count from 32 to eight. Intraaggregate exchange of all ^{6}Li nuclei[12,15] within each aggregate would further symmetrization, causing the five-aggregate ensemble to appear as five discrete ^{6}Li singlets. In practice, warming the samples appeared to elicit rapid chelate exchange, but we could not readily observe all eight resonances at a single temperature owing to differential exchange rates of the different aggregates. Warming of the samples to 60–70 °C, however, elicited the hoped-for rapid intraaggregate Li–Li site exchanges. We have examined structures in the

limit of rapid intraaggregate exchange before,[12,20a] but the temperatures required for vicinal amino alkoxides are remarkably high.

We previously noted the maxim "like aggregates with like."[12] Ensembles generated from lithium alkoxides and related O-lithiated species of differing aggregation states resist heteroaggregation, affording no heteroaggregates whatsoever or an ensemble of homo- and heteroaggregates that deviates significantly from statistical.[12] The most compelling assignments stem from structurally related ROLi/R'OLi pairs. At the outset, however, we thought that pairing structurally very different alkoxides would be required to obtain sufficient resolution in the ^{6}Li NMR spectra. Nonetheless, the **2a**/**2b** and **3a**/**3b** pairs differing marginally at the dialkylamino appendages provide convincing results.[26] More heterogeneous pairing of lithium ephedrate and norcarane-derived lithium alkoxides—**2**/**3** pairs—also appeared to provide tetramer ensembles, but rapid intraaggregate demanded very high (>80 °C) temperatures.

Mounting evidence suggests that cubic tetramers of enolates and related O-lithiated species are far more robust (less dynamic) than we ever suspected.[27,28] Effects of aging (warming–cooling cycles) and catalytically active lithium salts on aggregate equilibrations may profoundly influence stereo- and regiochemical outcomes. Both chelate–chelate and Li–Li site exchanges are observed at lower temperatures in THF than in toluene, indicating a role of THF.

During the studies of homoaggregates we detected lithium alkoxide–LiHMDS mixed aggregates in toluene. (LiHMDS does not form mixed aggregates in THF.[29]) The connectivities obtained from ^{6}Li–^{15}N double-labeling studies do not distinguish cyclic dimer **11** from ladder **12**, a distinction that has eluded us

previously.[17] We used MCV to reveal that mixtures of LiHMDS and alkoxides afford mixed ladders (**12a–c**). The chirality of these mixed aggregates may also pique curiosity among those interested in enantioselective reactions of lithium amides.

Conclusion

We have shown that cubic tetramers are a dominant form of several lithium amino alkoxides. This study and others[28] suggest that such tetramers composed of O-lithiated species are very robust. It is not difficult to imagine, therefore, that practitioners using lithium enolates to achieve stereocontrolled carbon–carbon bond formation have been thwarted by undetected aging and salt effects.

The importance of lithium amino alkoxides as auxiliaries in organolithium chemistry has grown markedly in the absence of any structural insights whatsoever.[3,4,5] Notably, structural studies of aggregates underlying the Merck chemistry (eq 1)[6] have played a direct role in the *development* of the protocols subsequently used at DuPont (eq 2).[5,7] In this context, we note a curious observation that may prove important. Inserting lithium salts into the cubic tetramers of **7a** and **8a** to form the mixed tetramers **5** and **6** central to Merck's and DuPont's enantioselective additions requires disruption of the chelate orientations of the S_4 core structure of homoaggregates **7a** and **8a**. We wonder: would mixed aggregates that allow three of the four chelates in the S_4 core to remain intact (eq 7) offer a more generalized control of stereochemistry? Studies are, of course, ongoing.

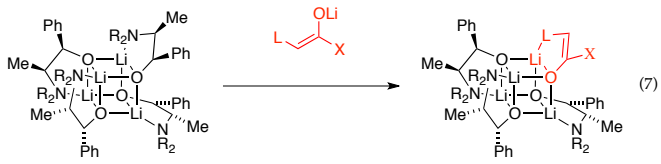

(7)

Experimental Section

Reagents and Solvents. Toluene, THF, and pyridine were distilled from blue solutions containing sodium benzophenone ketyl. The toluene contained approximately 1% tetraglyme to dissolve the ketyl. [^{6}Li]LiHMDS and [^{6}Li,^{15}N]LiHMDS were prepared and recrystallized using modified literature protocols.[19] Air- and moisture-sensitive materials were manipulated under argon using standard glove box, vacuum line, Schlenk, and syringe techniques. NMR samples were prepared using protocols described previously.[12c] ^{6}Li NMR spectra were typically recorded on a 500 or 600 MHz spectrometer with the delay between scans set to >5 x T1 to ensure accurate integrations. Chemical shifts are reported relative to a 0.30 M ^{6}LiCl/MeOH standard at -80 °C.

Acknowledgments. We thank the National Institutes of Health (GM077167) for support and Merck and Bristol–Myers Squibb (formerly DuPont) for a number of amino alcohols.

APPENDIX I

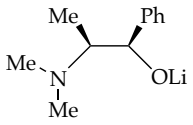

2a

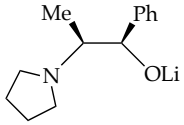

2b

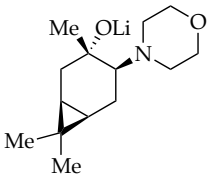

3a

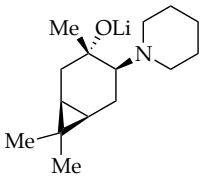

3b

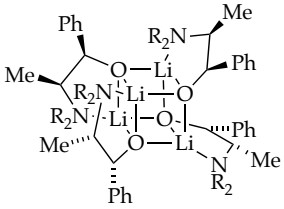

7a,b

a; $R_2N = NMe_2$; **b;** R_2N= 

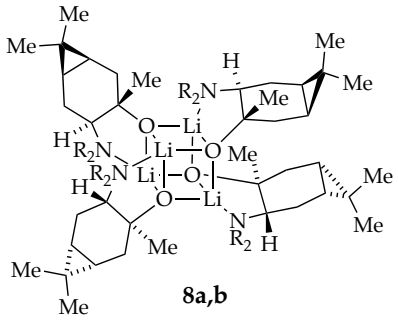

8a,b

a; R_2N =  **b**; R_2N =

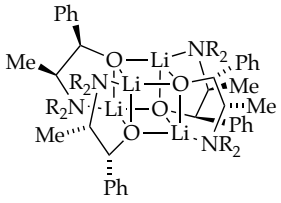

9a,b

a; $R_2N = NMe_2$; **b;** R_2N= 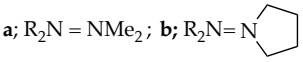

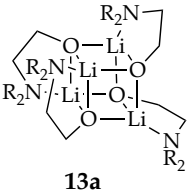

13a

R_2N =

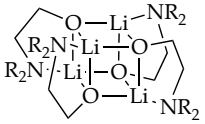

13b

R_2N = 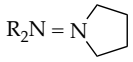

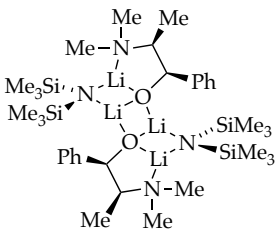

12a

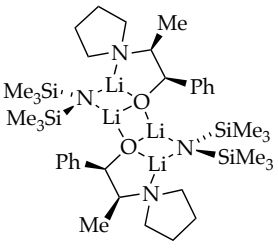

12b

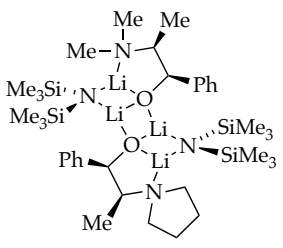

12c

a. NMR Spectroscopic Studies

i. Experimental Methods

NMR tubes were prepared under air-free conditions using Schlenk techniques and air-tight syringe. Stock solutions were prepared with same concentration in separate flame-dried vessels under argon using freshly distilled solvents and dry reagents. Syringe was used to transfer materials to flame-dried NMR tube under argon, and the tube was sealed under partial vacuum using a torch. Tubes were aged for at least 50 minutes at room temperature prior to spectral collection, and were stored at -90 °C. Spectra were collected after tuning and manual shimming at each temperature, each tube referenced to [^{6}Li]LiCl at -80°C as 0.00 ppm for ^{6}Li NMR.

ii. NMR Spectroscopic Data

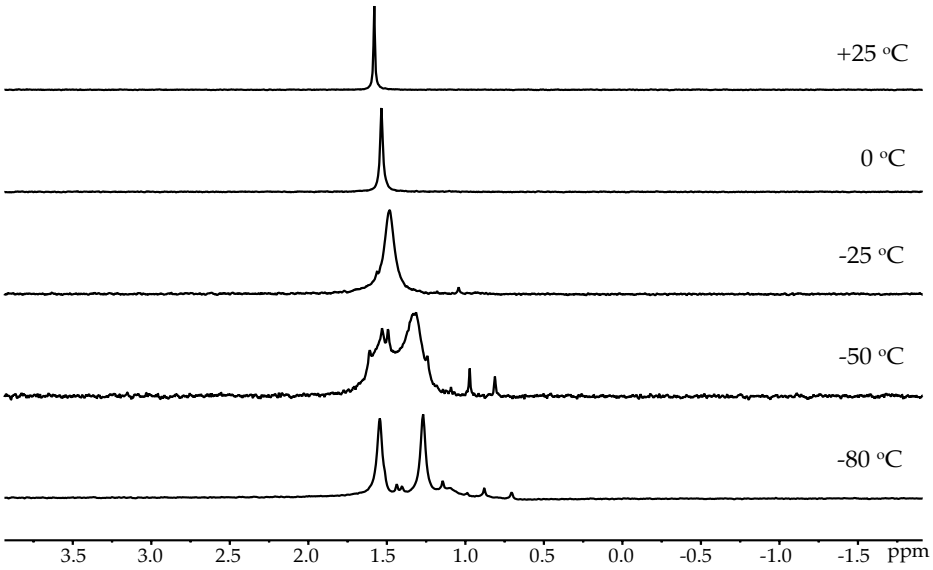

Figure A1.1. ^{6}Li NMR spectra of [^{6}Li]**2a** (0.10 M) in toluene showing coalescence with increasing temperature and evidence of structural asymmetry of the homoaggregate at low temperature.

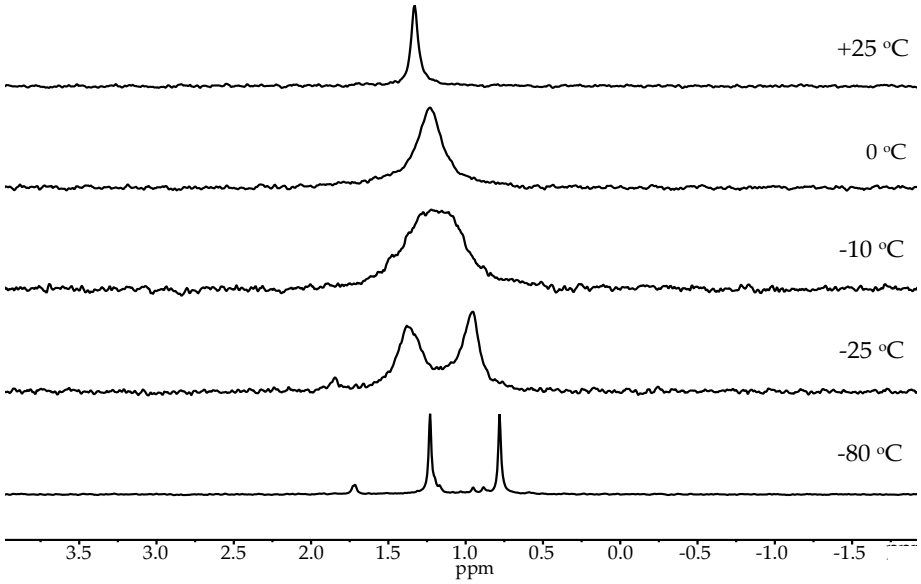

Figure A1.2. ^{6}Li NMR spectra of [^{6}Li]**2b** (0.10 M) in toluene showing coalescence with increasing temperature and evidence of structural asymmetry of the homoaggregate at low temperature.

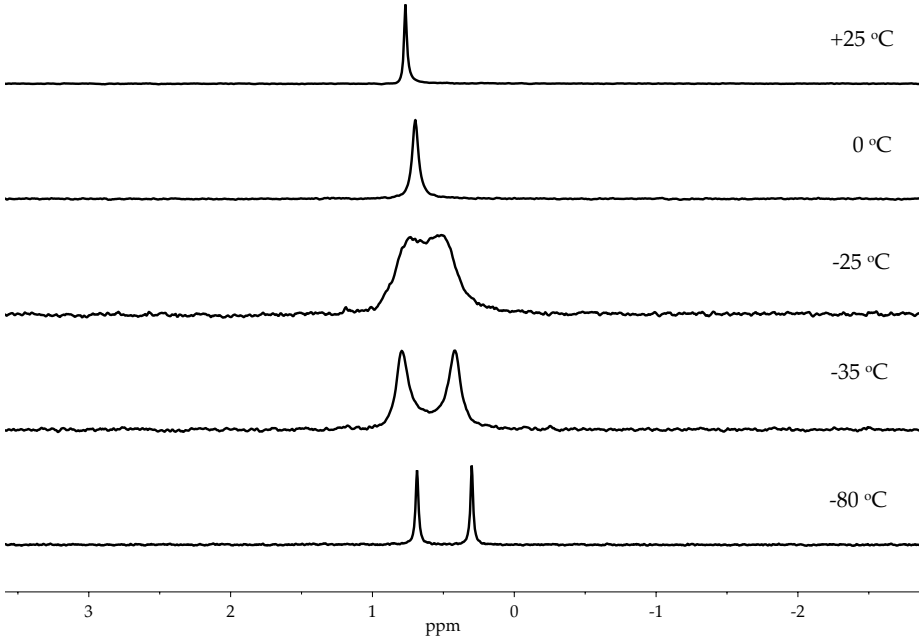

Figure A1.3. ^{6}Li NMR spectra of [^{6}Li]**3a** (0.10 M) in toluene showing coalescence with increasing temperature and evidence of structural asymmetry of the homoaggregate at low temperature.

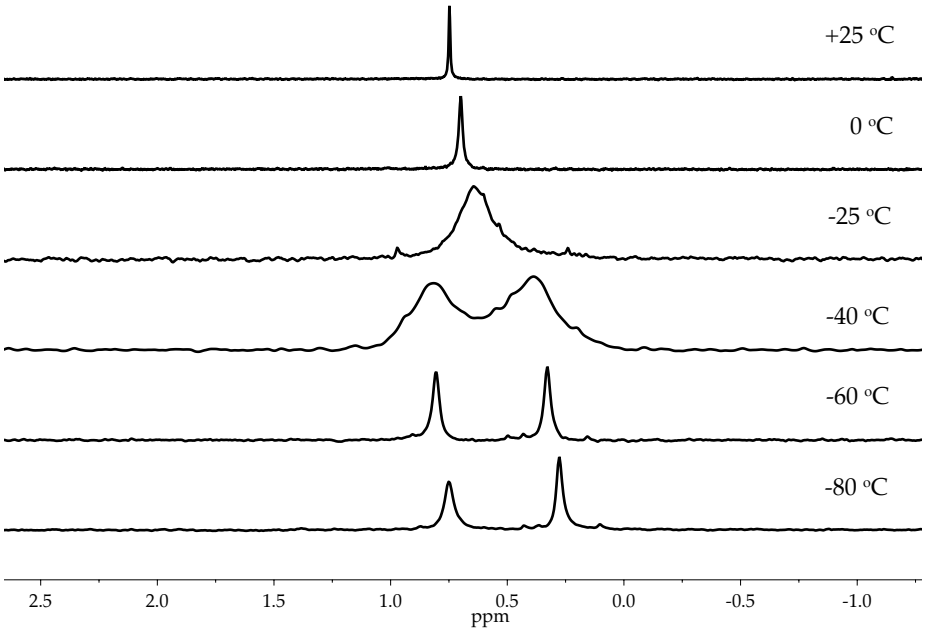

Figure A1.4. ^{6}Li NMR spectra of [^{6}Li]**3b** (0.10 M) in toluene showing coalescence with increasing temperature and evidence of structural asymmetry of the homoaggregate at low temperature.

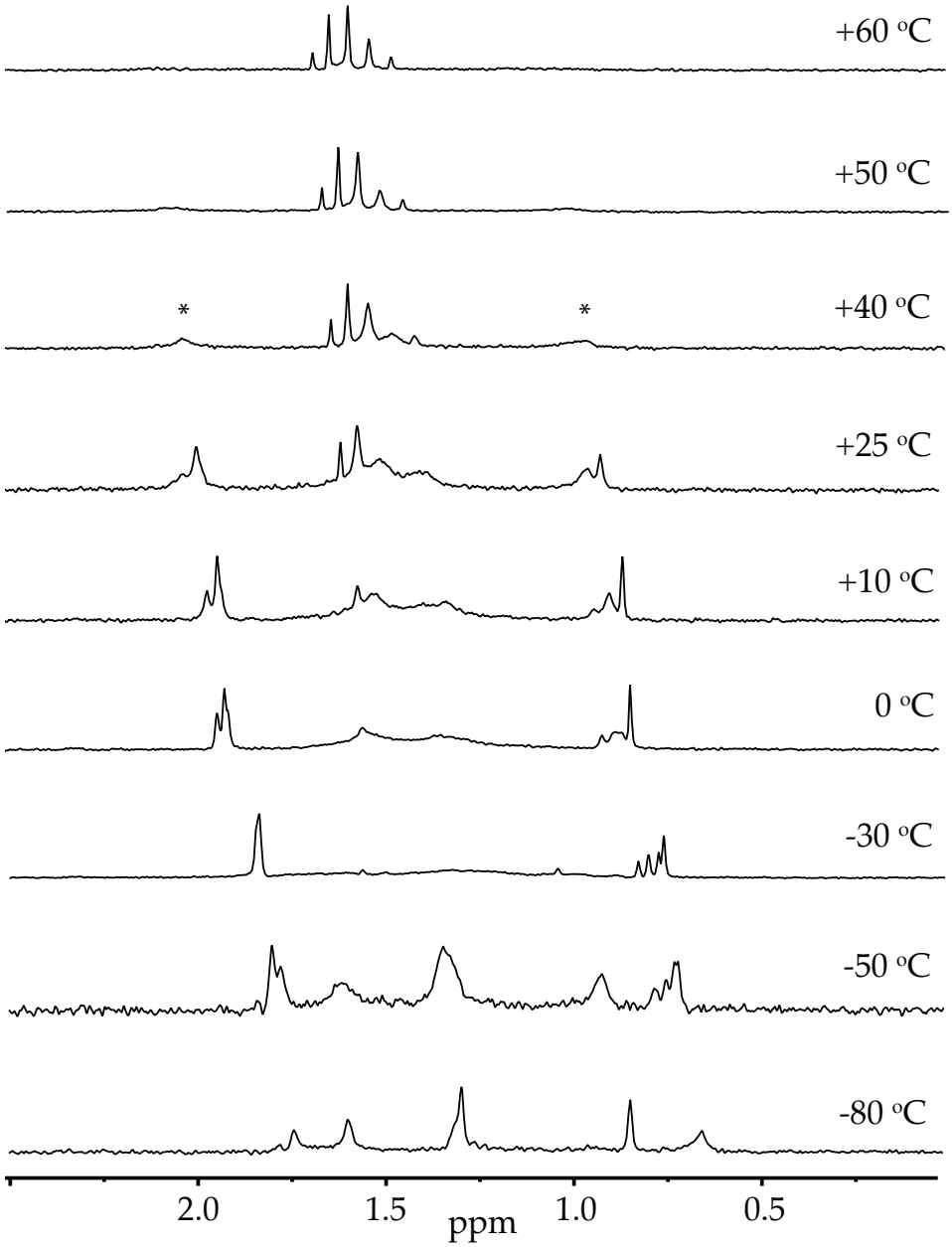

Figure A1.5. ^{6}Li NMR spectra of [^{6}Li]**2a** (0.050 M) and [^{6}Li]**2b** (0.050 M) with 0.020 M excess [^{6}Li]LiHMDS in toluene showing coalescence behavior with changing temperature. Asterisks (*) denote mixed aggregates of amino alkoxides and [^{6}Li]LiHMDS that occur under conditions of excess base (see figures 12-15).

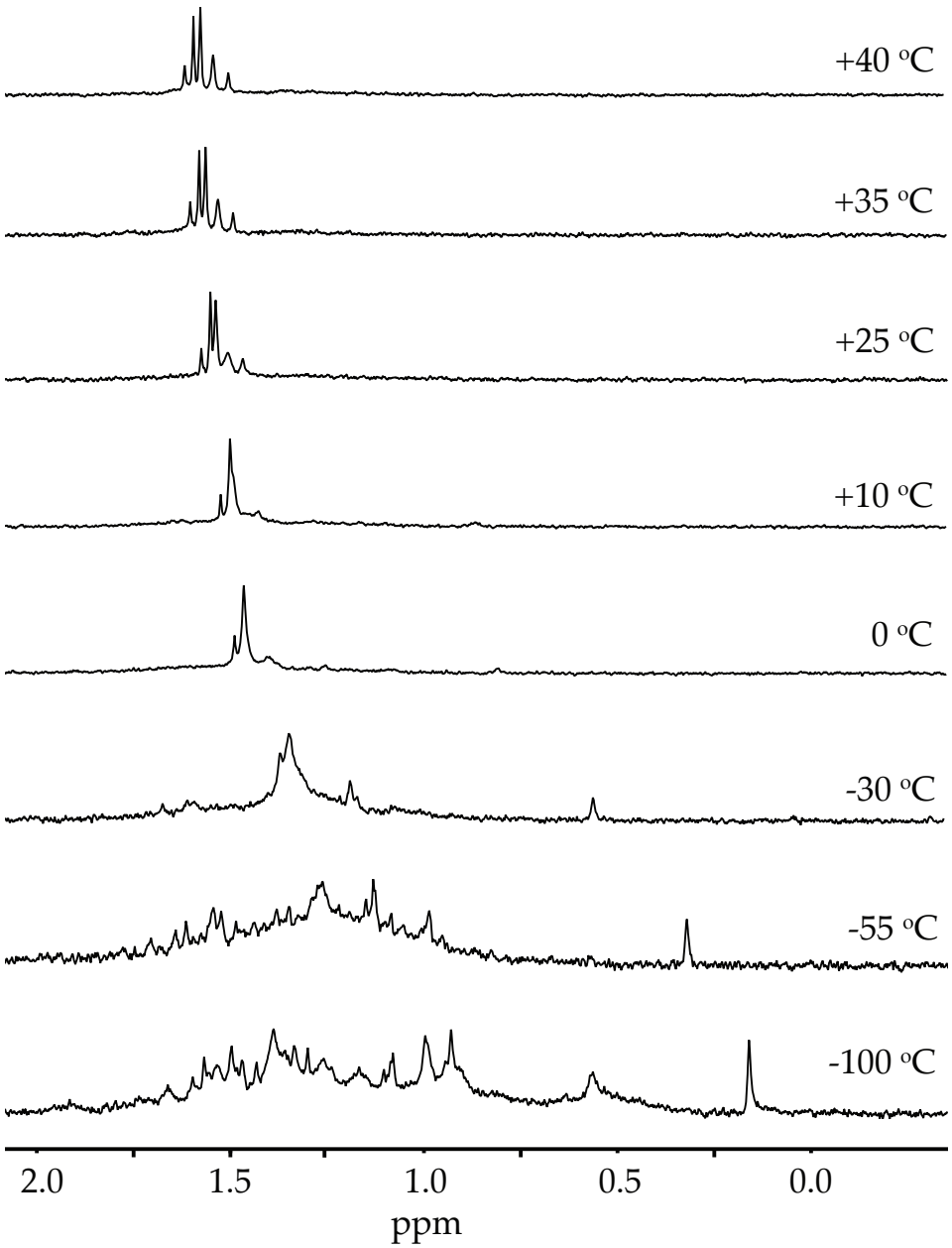

Figure A1.6. ^{6}Li NMR spectra of [^{6}Li]**2a** (0.050 M) and [^{6}Li]**2b** (0.050 M) with 0.020 M excess [^{6}Li]LiHMDS in THF (6.0 M) with toluene cosolvent showing coalescence behavior with changing temperature. The coalescence temperature is approximately 20 °C lower than in pure toluene.

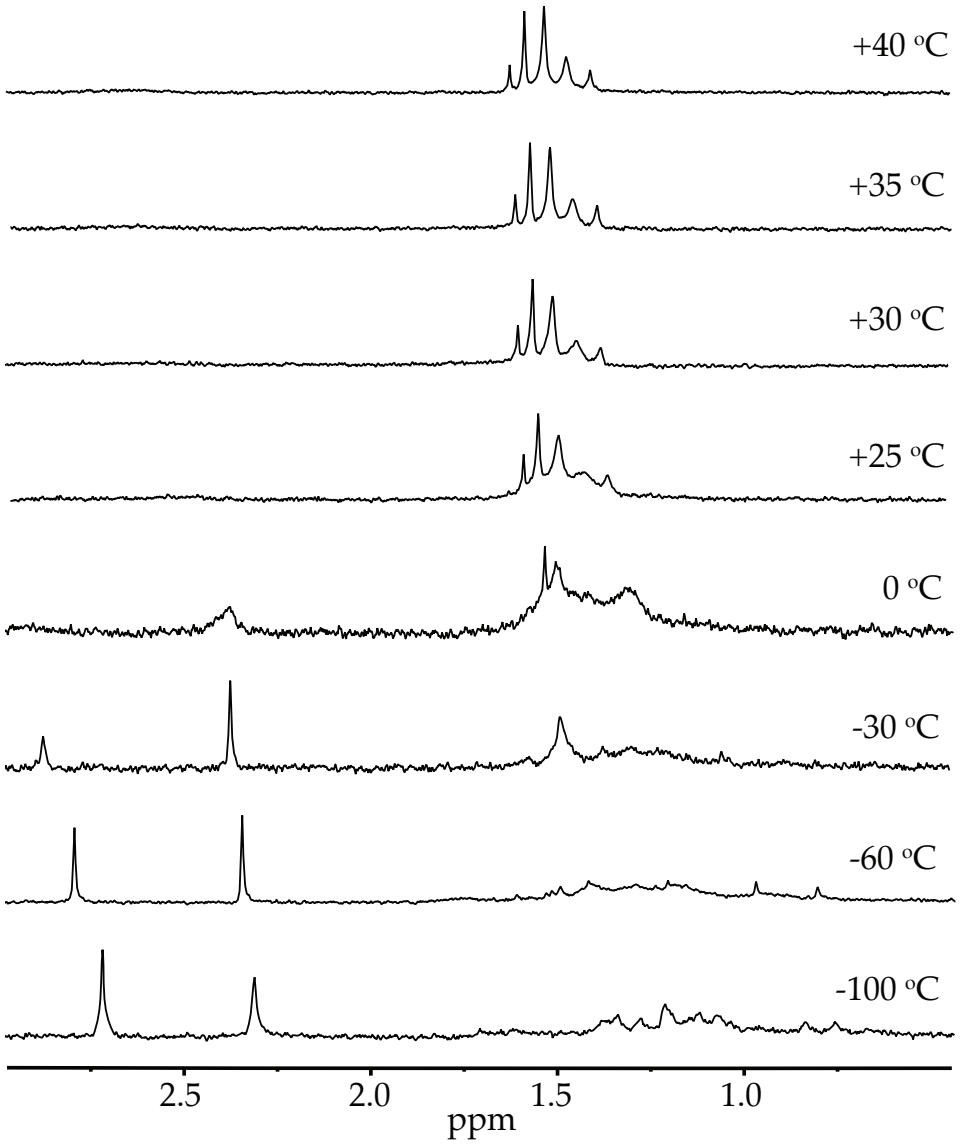

Figure A1.7. ^{6}Li NMR spectra of [^{6}Li]**2a** (0.050 M) and [^{6}Li]**2b** (0.050 M) with 0.020 M excess [^{6}Li]LiHMDS in pyridine (1.20 M) with toluene cosolvent showing coalescence behavior with changing temperature. The coalescence temperature is approximately 20 °C lower than in pure toluene.

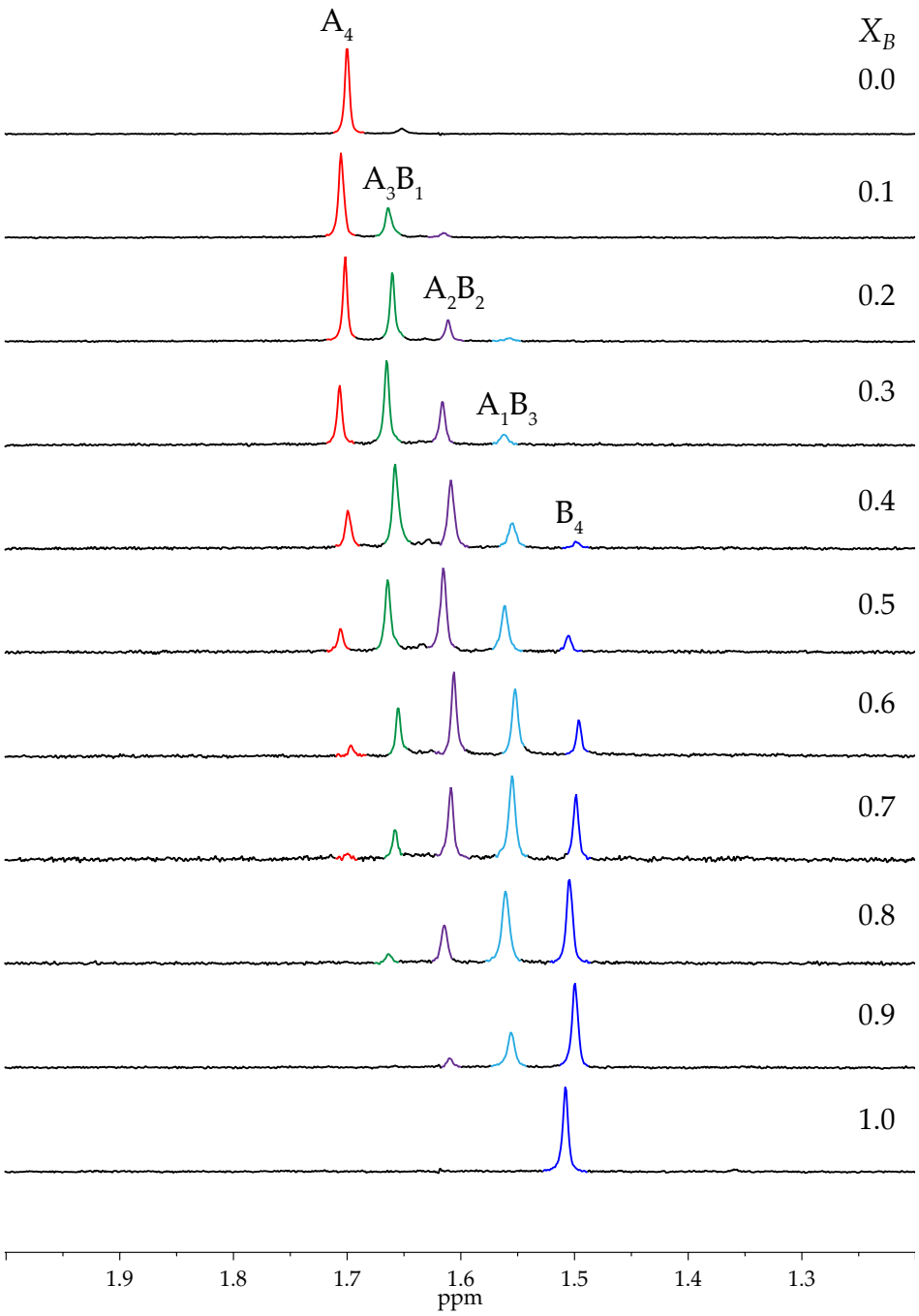

Figure A1.8. ^{6}Li NMR spectra of 0.10 M solutions of amino alkoxides [^{6}Li]**2b** (**A**) and [^{6}Li]**2a** (**B**) with varying mole fractions of **B** (X_B) in toluene at +60 °C.

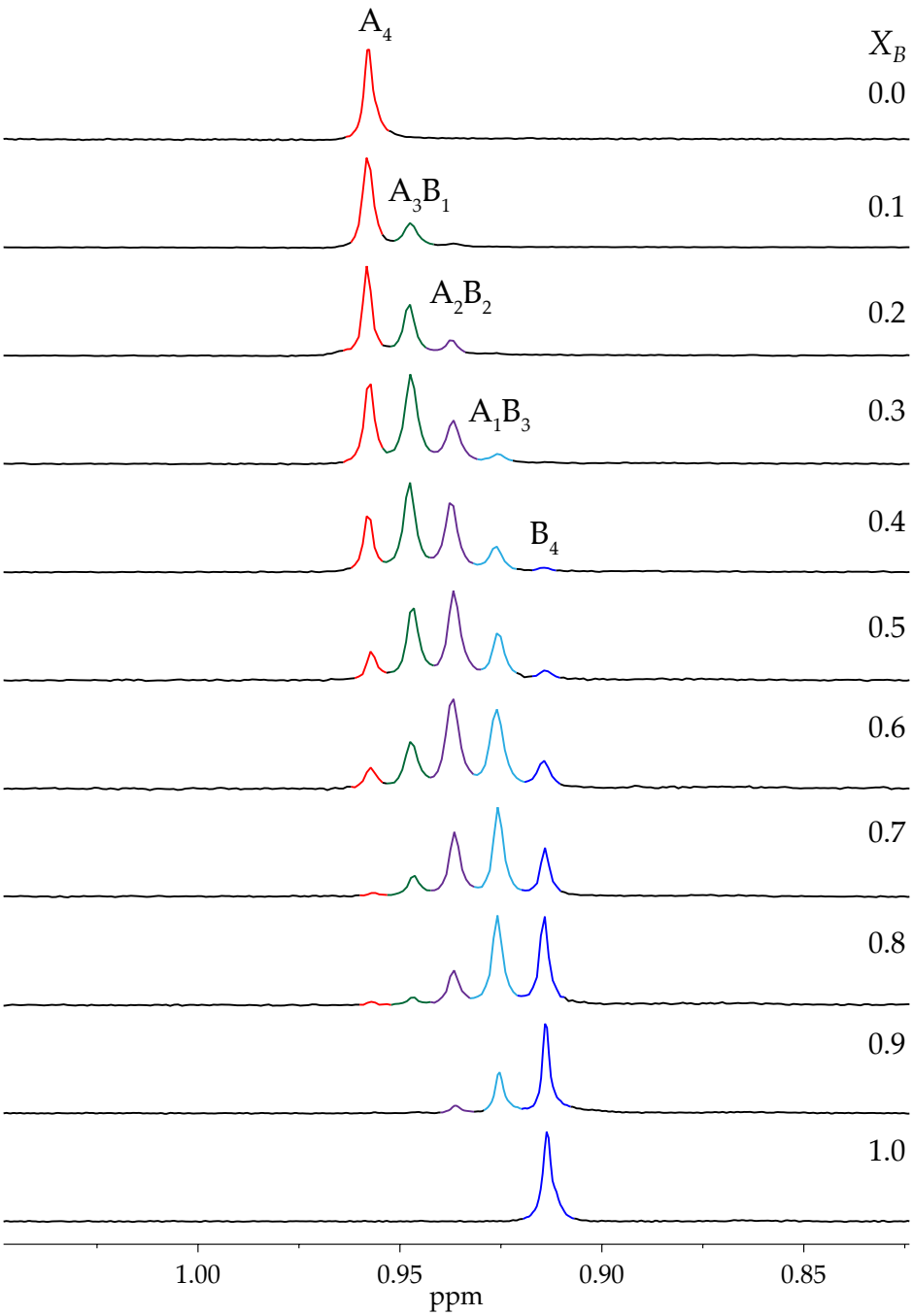

Figure A1.9. ^{6}Li NMR spectra for 0.10 M solutions of amino alkoxides [^{6}Li]**3a** (**A**) and [^{6}Li]**3b** (**B**) with varying mole fractions of **B** (X_B) in toluene at +60 °C.

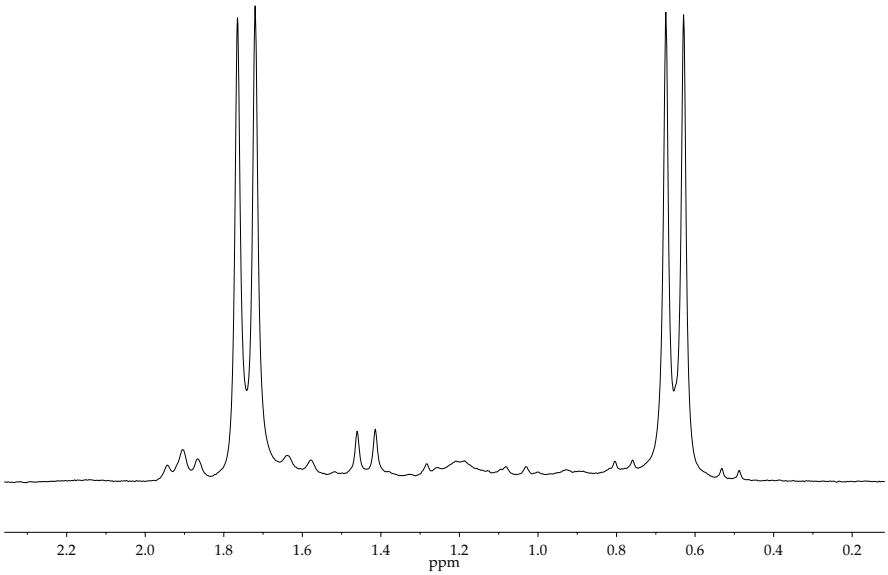

Figure A1.10. ^{6}Li NMR spectrum of **12b** formed by mixing [^{6}Li,^{15}N]LiHMDS (0.20 M) and **2b** (0.10 M) in d_8-toluene at -80 ºC. δ 1.74 (d, $^{2}J_{\text{Li-N}}$ = 4.0 Hz), δ 0.65 (d, $^{2}J_{\text{Li-N}}$ = 4.0 Hz).

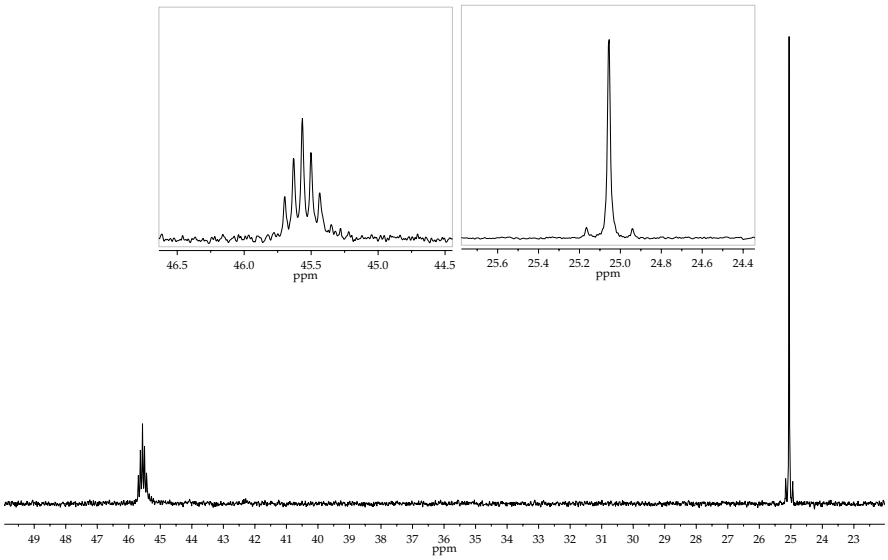

Figure A1.11. ^{15}N NMR spectrum of **12b** formed by mixing [^{6}Li,^{15}N]LiHMDS (0.20 M) and **2b** (0.10 M) in d_8-toluene at -80 ºC. The apparent pentet at δ 45.6 corresponds to the nitrogen in mixed aggregate **12b**, and the singlet at δ 25.1 to free [^{15}N]HMDS.

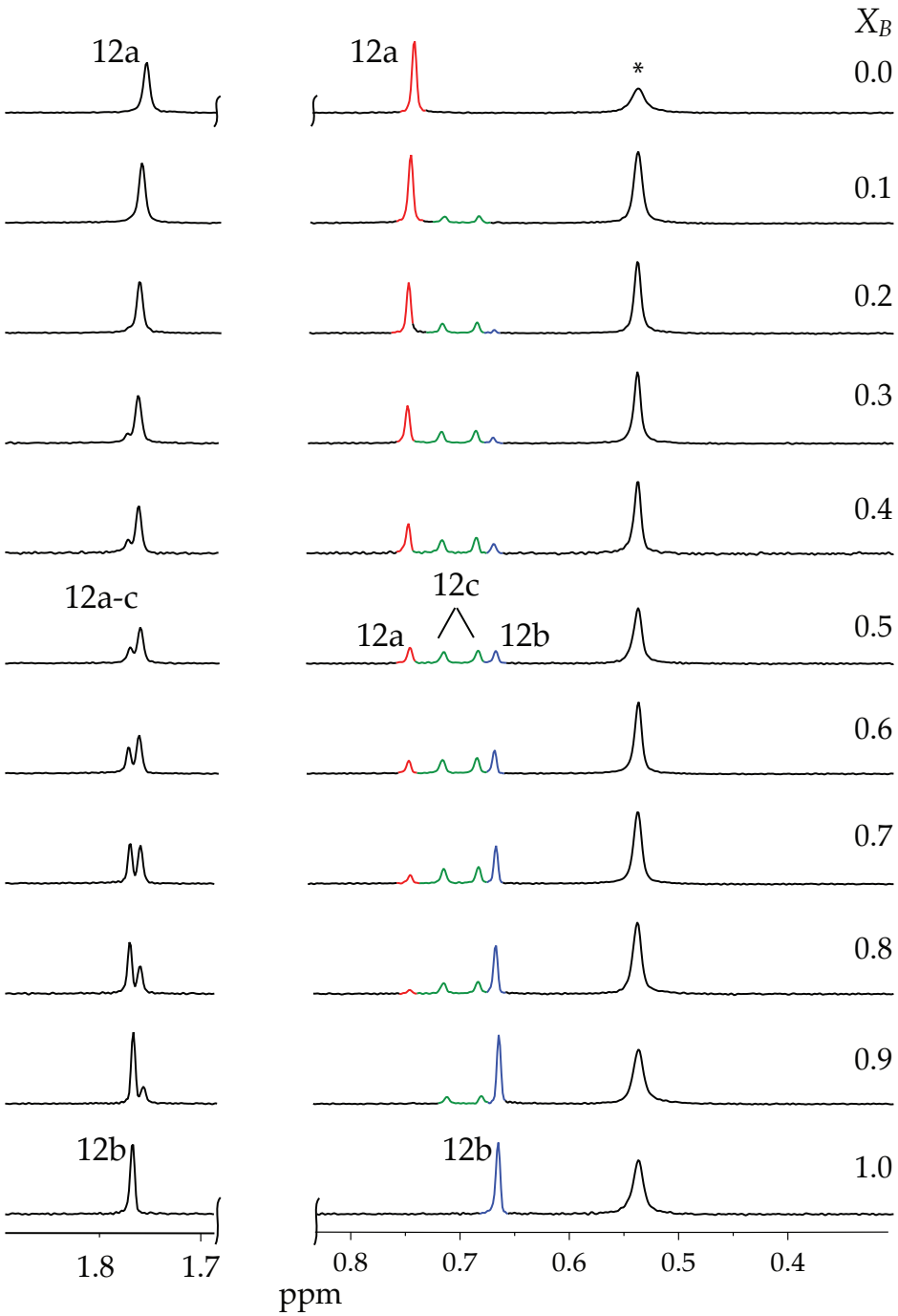

Figure A1.12. ^{6}Li NMR spectra of a mixture of [^{6}Li]**12a** and [^{6}Li]**12b** at 0.10 M total concentration with 0.20 M additional [^{6}Li]LiHMDS in toluene at -30 °C with varying measured mole fraction of **12b** (X_B). Asterisk (*) denotes excess [^{6}Li]LiHMDS.

AII.b. Job Plots (Method of Continuous Variations)

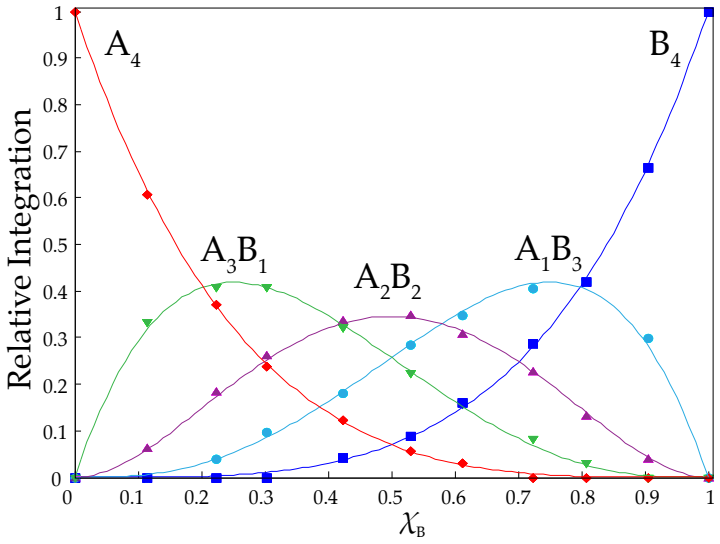

Figure A1.13. Job plot showing the relative integrals versus measured mole fractions of [^{6}Li]**2a** (X_B) for 0.10 M mixtures of amino alkoxides [^{6}Li]**2b** (**A**) and [^{6}Li]**2a** (**B**) in toluene at +60 °C corresponding to NMR data in figure A1.8.

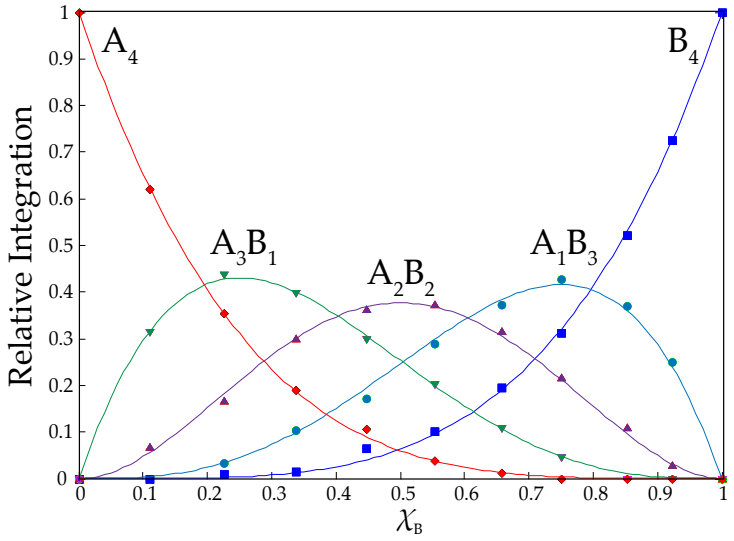

Figure A1.14. Job plot showing the relative integrals versus measured mole fractions of [^{6}Li]**3b** (X_B) for 0.10 M mixtures of amino alkoxides [^{6}Li]**3a** (**A**) and [^{6}Li]**3b** (**B**) in toluene at +80 °C corresponding to NMR data in figure A1.9.

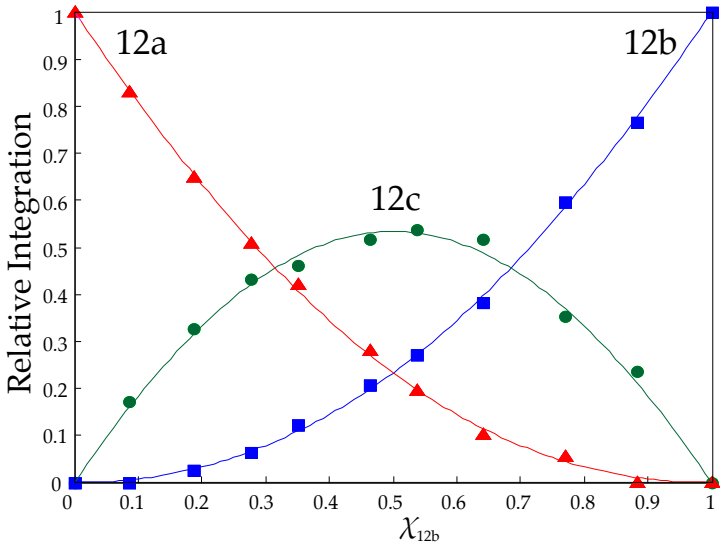

Figure A1.15. Job plot showing the relative integrals versus measured mole fractions of [^{6}Li]**12b** for 0.10 M mixtures of [^{6}Li]**12a** and [^{6}Li]**12b** with 0.20 M excess [^{6}Li]LiHMDS in toluene at -30 °C corresponding to NMR data in figure A1.12.

AII.c. X-Ray Crystal Structure Characterization

A solution of 0.30 M **2b** in toluene was concentrated under vacuum at room temperature in a dry NMR tube until solids begun to form. The tube was sealed under partial vacuum, then subjected to gentle heating until all solids redissolved. The solution was left at room temperature for 72 hours until needle-like crystals formed. The crystals were submitted for X-ray analysis to the Cornell X-ray Crystallography facility.

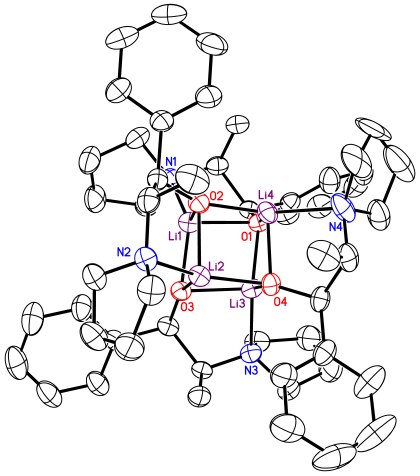

Figure A1.16. X-ray crystal structure of **2b**.

Table A1.1. Crystal data and structure refinement for lithium enolate **2b**.

Identification code	2b	
Empirical formula	C52 H72 Li4 N4 O4	
Formula weight	844.90	
Temperature	223(2) K	
Wavelength	0.71073 Å	
Crystal system	Monoclinic	
Space group	P2(1)	
Unit cell dimensions	a = 10.6188(7) Å	a= 90°.
	b = 21.8666(15) Å	b= 95.593(2)°.
	c = 21.4263(13) Å	g = 90°.
Volume	4951.4(6) $Å^3$	
Z	4	
Density (calculated)	1.133 Mg/m^3	
Absorption coefficient	0.070 mm^{-1}	
F(000)	1824	
Crystal size	0.50 x 0.25 x 0.03 mm^3	
Theta range for data collection	0.95 to 23.25°.	
Index ranges	-11<=h<=11, -23<=k<=22, -23<=l<=23	
Reflections collected	60393	
Independent reflections	6463 [R(int) = 0.0485]	
Completeness to theta = 23.25°	88.3 %	
Absorption correction	Semi-empirical from equivalents	
Max. and min. transmission	0.9983 and 0.9661	
Refinement method	Full-matrix least-squares on F^2	
Data / restraints / parameters	6463 / 15 / 1222	
Goodness-of-fit on F^2	1.051	
Final R indices [I>2sigma(I)]	R1 = 0.0339, wR2 = 0.0738	
R indices (all data)	R1 = 0.0491, wR2 = 0.0810	
Absolute structure parameter	0(10)	
Largest diff. peak and hole	0.109 and -0.165 $e.Å^{-3}$	

Table A1.2. Atomic coordinates (x 10^4) and equivalent isotropic displacement parameters ($Å^2$x 10^3) for **2b**. U(eq) is defined as one third of the trace of the orthogonalized U^{ij} tensor.

	x	y	z	U(eq)
Li(1)	5290(5)	9001(3)	5021(2)	41(1)
Li(2)	6724(5)	9942(3)	5067(2)	40(1)
Li(3)	5821(4)	9541(3)	6051(2)	38(1)
Li(4)	7494(5)	8932(3)	5583(2)	42(1)
O(1)	5867(2)	8668(1)	5883(1)	38(1)
O(2)	6915(2)	9121(1)	4739(1)	40(1)
O(3)	4914(2)	9820(1)	5256(1)	38(1)
O(4)	7486(2)	9775(1)	5895(1)	38(1)
N(1)	4092(2)	8258(1)	4793(1)	41(1)
N(2)	7406(2)	10232(1)	4173(1)	42(1)
N(3)	4728(2)	10107(1)	6548(1)	40(1)
N(4)	9319(2)	8874(2)	6158(2)	59(1)
C(1)	4567(3)	7872(2)	5334(2)	42(1)
C(2)	5751(3)	7519(2)	5207(2)	56(1)
C(3)	4831(3)	8288(2)	5929(1)	37(1)
C(4)	4880(3)	7893(2)	6509(2)	43(1)
C(5)	5962(4)	7605(2)	6761(2)	62(1)
C(6)	5950(5)	7201(2)	7256(2)	82(1)
C(7)	4820(6)	7092(2)	7517(2)	81(2)
C(8)	3762(5)	7385(2)	7292(2)	69(1)
C(9)	3777(4)	7776(2)	6787(2)	54(1)
C(10)	4045(3)	7953(2)	4177(2)	54(1)
C(11)	3220(4)	8367(2)	3752(2)	70(1)
C(12)	2223(4)	8581(2)	4161(2)	71(1)
C(13)	2765(3)	8445(2)	4828(2)	52(1)
C(14)	7837(3)	9652(2)	3905(2)	46(1)
C(15)	9229(3)	9513(2)	4100(2)	69(1)
C(16)	6971(3)	9129(2)	4096(2)	38(1)

C(17)	7363(3)	8511(2)	3851(2)	44(1)
C(18)	8114(4)	8110(2)	4217(2)	61(1)
C(19)	8415(4)	7540(2)	3998(2)	76(1)
C(20)	7964(5)	7346(2)	3414(2)	77(1)
C(21)	7228(4)	7742(2)	3036(2)	71(1)
C(22)	6938(3)	8314(2)	3252(2)	57(1)
C(23)	6291(3)	10484(2)	3804(2)	56(1)
C(24)	6143(4)	11123(2)	4054(2)	69(1)
C(25)	7490(4)	11312(2)	4277(2)	72(1)
C(26)	8299(3)	10748(2)	4181(2)	60(1)
C(27)	4161(3)	10503(2)	6032(2)	38(1)
C(28)	5049(3)	11016(2)	5893(2)	48(1)
C(29)	3834(3)	10102(2)	5443(2)	38(1)
C(30)	3086(3)	10453(2)	4907(2)	41(1)
C(31)	3183(3)	10275(2)	4299(2)	59(1)
C(32)	2512(4)	10566(3)	3798(2)	79(1)
C(33)	1732(4)	11052(2)	3897(3)	78(1)
C(34)	1611(4)	11228(2)	4490(2)	71(1)
C(35)	2276(3)	10935(2)	4996(2)	60(1)
C(36)	5317(3)	10447(2)	7097(2)	53(1)
C(37)	5523(4)	9963(2)	7605(2)	69(1)
C(38)	4523(4)	9480(2)	7429(2)	71(1)
C(39)	3801(3)	9715(2)	6829(2)	54(1)
C(40)	9626(3)	9519(2)	6307(2)	53(1)
C(41)	10271(3)	9833(2)	5791(2)	68(1)
C(42)	8368(3)	9857(2)	6408(1)	43(1)
C(43)	8631(3)	10519(2)	6576(2)	49(1)
C(44)	8459(3)	10979(2)	6138(2)	56(1)
C(45)	8685(4)	11590(2)	6298(3)	81(1)
C(46)	9089(5)	11737(3)	6910(4)	106(2)
C(47)	9285(6)	11289(4)	7350(3)	119(2)
C(48)	9051(4)	10684(3)	7184(2)	85(2)
C(49)	8910(20)	8604(8)	6803(10)	64(5)
C(50)	9501(10)	7955(6)	6779(10)	112(6)
C(51)	9932(11)	7863(5)	6177(7)	82(4)
C(52)	10345(10)	8507(5)	6053(7)	77(3)

C(49A)	9080(30)	8439(12)	6609(12)	62(5)
C(50A)	9091(16)	7795(5)	6344(8)	75(5)
C(51A)	10131(9)	7864(4)	5859(7)	57(3)
C(52A)	10392(8)	8539(4)	5802(6)	43(3)
Li(1')	2559(5)	9533(3)	909(3)	43(1)
Li(2')	572(5)	8924(3)	846(2)	42(1)
Li(3')	1766(5)	9062(3)	-135(3)	44(1)
Li(4')	587(4)	9943(3)	272(2)	40(1)
O(1')	2274(2)	9895(1)	54(1)	41(1)
O(2')	913(2)	9778(1)	1155(1)	42(1)
O(3')	2252(2)	8702(1)	689(1)	41(1)
O(4')	-64(2)	9132(1)	3(1)	39(1)
N(1')	4325(2)	10038(1)	1016(1)	48(1)
N(2')	-344(2)	8717(1)	1659(1)	44(1)
N(3')	2606(2)	8261(1)	-513(1)	45(1)
N(4')	-877(3)	10345(1)	-293(1)	49(1)
C(1')	4407(3)	10246(2)	357(2)	45(1)
C(2')	4981(3)	9775(2)	-47(2)	56(1)
C(3')	3056(3)	10406(2)	63(2)	38(1)
C(4')	3119(3)	10709(2)	-566(2)	43(1)
C(5')	2709(3)	10418(2)	-1119(2)	53(1)
C(6')	2744(4)	10703(2)	-1695(2)	66(1)
C(7')	3228(4)	11279(3)	-1723(2)	77(1)
C(8')	3665(4)	11573(2)	-1184(3)	78(1)
C(9')	3603(3)	11300(2)	-609(2)	61(1)
C(10')	4194(4)	10562(2)	1442(2)	61(1)
C(11')	4433(5)	10294(2)	2091(2)	79(1)
C(12')	5247(4)	9734(2)	2008(2)	72(1)
C(13')	5451(3)	9724(2)	1311(2)	62(1)
C(14')	-24(3)	9288(2)	2011(2)	45(1)
C(15')	1258(3)	9259(2)	2390(2)	61(1)
C(16')	-72(3)	9819(2)	1535(1)	39(1)
C(17')	-177(3)	10436(2)	1843(2)	43(1)
C(18')	686(4)	10895(2)	1783(2)	63(1)
C(19')	521(4)	11474(2)	2034(2)	81(1)
C(20')	-506(5)	11584(2)	2358(2)	77(1)

C(21')	-1390(5)	11135(3)	2409(2)	82(1)
C(22')	-1219(4)	10571(2)	2165(2)	69(1)
C(23')	-61(3)	8145(2)	2014(2)	58(1)
C(24')	-780(4)	7665(2)	1617(2)	72(1)
C(25')	-1993(4)	7992(2)	1353(2)	68(1)
C(26')	-1718(3)	8665(2)	1465(2)	58(1)
C(27')	3222(3)	7957(2)	51(2)	45(1)
C(28')	4593(3)	8152(2)	215(2)	59(1)
C(29')	2425(3)	8081(2)	607(2)	41(1)
C(30')	2970(3)	7753(2)	1198(2)	42(1)
C(31')	3571(3)	8072(2)	1694(2)	55(1)
C(32')	4057(4)	7776(2)	2233(2)	67(1)
C(33')	3942(4)	7156(3)	2290(2)	73(1)
C(34')	3353(4)	6829(2)	1803(2)	79(1)
C(35')	2874(4)	7131(2)	1263(2)	63(1)
C(36')	1496(4)	7910(2)	-793(2)	64(1)
C(37')	1209(4)	8154(2)	-1449(2)	73(1)
C(38')	2385(4)	8506(2)	-1588(2)	73(1)
C(39')	3359(4)	8327(2)	-1051(2)	66(1)
C(40')	-1311(3)	9817(2)	-694(2)	45(1)
C(41')	-494(4)	9718(2)	-1229(2)	65(1)
C(42')	-1291(3)	9247(2)	-268(2)	39(1)
C(45')	-2162(4)	7586(2)	-587(2)	66(1)
C(46')	-3027(4)	7611(2)	-1106(2)	67(1)
C(47')	-3364(3)	8170(2)	-1357(2)	67(1)
C(48')	-2814(3)	8702(2)	-1099(2)	55(1)
C(43')	-1903(3)	8685(2)	-590(2)	42(1)
C(44')	-1603(3)	8113(2)	-340(2)	52(1)
C(49')	-493(4)	10896(2)	-628(2)	65(1)
C(50')	-373(4)	11368(2)	-108(2)	79(1)
C(51')	-1434(4)	11211(2)	299(2)	75(1)
C(52')	-1877(3)	10582(2)	77(2)	59(1)

AI.d. DFT Computations

Geometries are optimized at the B3LYP level of theory using the 6-31G(d) basis set. Numbers above equilibrium arrows are ΔG_{MP2}. Energies are defined as follows: G is the sum of electronic and thermal free energies calculated at the B3LYP level of theory (T = 195 K). G_{MP2} is derived from an MP2 SP calculation corresponding to the DFT-optimized geometry and includes a thermal correction from the DFT calculation. [i.e. $G_{MP2} = (E_{HF} + E2 + \text{thermal correction})$]

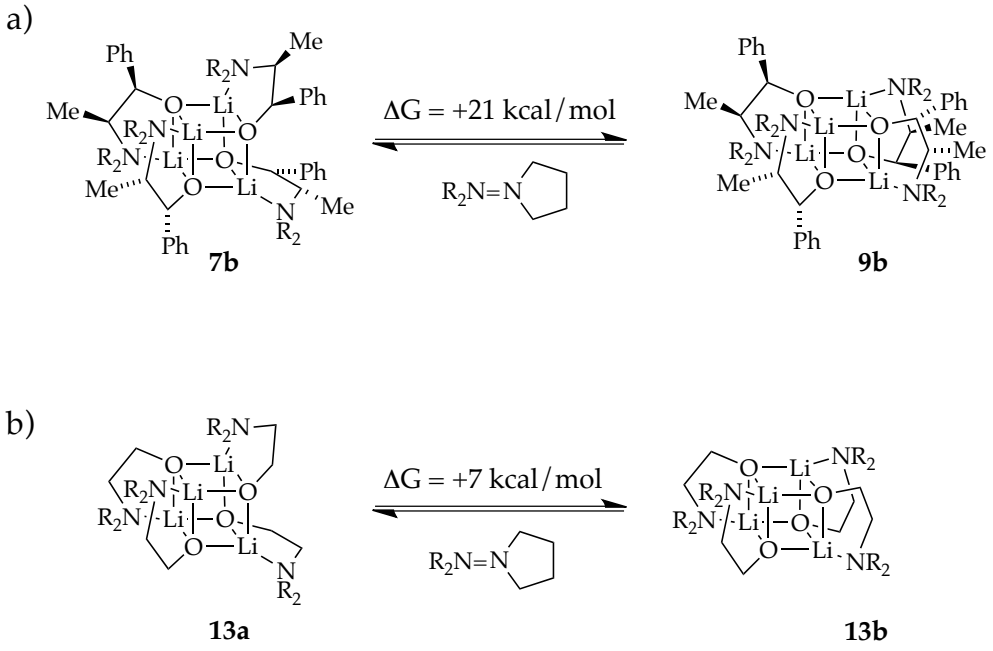

Figure A1.17.

Comparison of the relative free energies (ΔG_{MP2}, kcal/mol) at -78 °C of a) observed S_4 core pyrrolidinyl ephedrate **7b** and unobserved D_{2d} core structure **9b**, and b) analogous unsubstituted S_4 core **13a** and D_{2d} core **13b**.

Table A1.3. Optimized geometries, coordinates and energies for observed S_4 core tetramer **7b**.

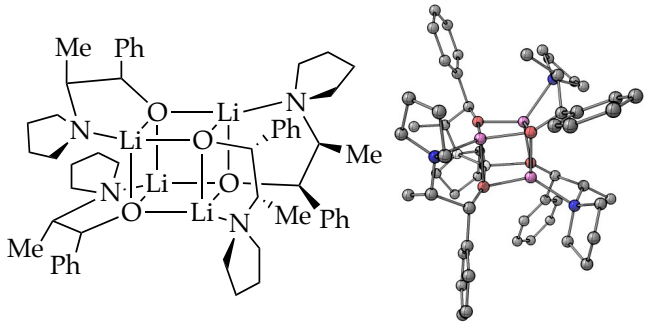

G = -2574.184593 Hartree
G_{MP2} = -2565.598563 Hartree

Atom	X	Y	Z	Atom	X	Y	Z
Li	0.841170	1.046029	-0.412403	H	4.343868	1.335696	-1.925817
Li	-1.042599	0.383821	1.210918	H	3.682964	1.346559	-0.294504
O	0.929614	0.289166	1.353827	C	2.700831	4.070609	-1.033620
Li	0.622382	-1.387823	0.422334	H	0.799794	3.410965	-1.923421
O	-1.343876	-1.360187	0.436360	H	2.143886	3.589491	-3.066918
Li	-1.094105	-0.371657	-1.191787	H	4.669047	3.506021	-0.196860
O	0.822351	-0.624707	-1.403988	H	4.624451	3.691718	-1.955584
C	1.684324	-0.546783	-2.489739	H	2.255273	3.988006	-0.034198
C	1.929813	0.955207	-2.919584	H	2.764463	5.133185	-1.288399
O	-1.069629	1.465685	-0.454728	N	2.253704	1.860422	-1.783194
C	-1.685766	2.168851	-1.481899	C	1.276449	-4.399412	1.638646
C	-3.010679	1.471939	-1.949113	C	0.698731	-4.136621	-0.640083
H	-3.479142	2.100043	-2.728892	C	2.586815	-4.514287	0.865852
C	-1.822427	-2.642969	0.209838	H	0.860804	-5.405894	1.832609
C	-1.046788	-3.709863	1.059538	H	1.386769	-3.891030	2.600330
H	-1.411345	-4.709608	0.753505	C	2.116411	-4.756973	-0.581424
C	1.293822	1.099762	2.419989	H	0.633271	-3.317998	-1.361762
C	0.445694	0.774651	3.700964	H	-0.043877	-4.898734	-0.927458
H	0.760621	1.462330	4.507512	H	3.144235	-3.574029	0.930531
C	-1.976509	0.412011	4.294408	H	3.229955	-5.312748	1.250015
C	-1.314060	2.484808	3.525270	H	2.793327	-4.312287	-1.314122
C	-3.293680	1.148174	3.991738	H	2.064380	-5.831309	-0.790216

H	-1.694076	0.564674	5.351874	N	0.400563	-3.622943	0.733581
H	-2.037460	-0.663456	4.114161	C	-3.822509	-0.755752	-2.752937
C	-2.848384	2.545950	3.480021	C	-2.103509	0.264593	-3.918496
H	-0.828729	3.071338	2.742859	C	-3.286339	-1.855090	-3.685314
H	-0.944693	2.862794	4.497092	H	-4.654940	-0.215950	-3.240530
H	-3.864267	0.619919	3.221324	H	-4.180397	-1.144234	-1.798962
H	-3.928547	1.205159	4.881242	C	-2.125229	-1.173775	-4.460805
H	-3.202002	2.719931	2.459533	H	-1.100371	0.696168	-3.898956
H	-3.229974	3.363160	4.099849	H	-2.739026	0.923347	-4.539622
N	-0.989237	1.046949	3.392300	H	-2.919572	-2.705793	-3.102573
C	3.658419	1.863868	-1.257177	H	-5.905160	-4.867521	-0.483983
C	1.877907	3.274944	-2.043486	H	-7.168878	-3.297929	0.979029
C	4.052323	3.344370	-1.086183	C	2.789967	1.073821	2.754596
N	-2.669667	0.153320	-2.555338	C	3.405323	2.203265	3.311608
H	0.933086	1.291685	-3.234128	C	3.576101	-0.064001	2.533005
H	1.072849	2.161305	2.185020	C	4.761658	2.198733	3.643186
H	-1.646907	-2.936634	-0.846730	H	2.813979	3.101728	3.481812
H	-1.035405	2.178203	-2.380628	C	4.932898	-0.075901	2.863647
H	1.214545	-0.981580	-3.396834	H	3.111457	-0.942219	2.095828
C	-1.945357	3.652278	-1.185587	C	5.532122	1.056052	3.419933
C	-2.302414	4.536408	-2.215807	H	5.217292	3.089092	4.069796
C	-1.814056	4.165375	0.106545	H	5.524013	-0.971845	2.687852
C	-2.539207	5.886145	-1.955631	H	6.589136	1.049211	3.672978
H	-2.387567	4.167419	-3.236551	C	0.700844	-0.653111	4.183241
C	-2.049122	5.516552	0.374971	H	0.105680	-0.908109	5.064534
H	-1.514437	3.482834	0.891533	H	0.489139	-1.374818	3.392024
C	-2.416718	6.382608	-0.655035	H	1.753847	-0.755872	4.459449
H	-2.813974	6.552963	-2.769461	H	-4.072434	-2.231083	-4.347237
H	-1.941447	5.892849	1.389844	H	-1.173554	-1.675497	-4.256660
H	-2.598449	7.434622	-0.450765	H	-2.273786	-1.187006	-5.545031
C	-3.999202	1.335459	-0.789151	C	2.855066	1.091562	-4.141241
H	-4.127956	2.310492	-0.309056	H	2.467772	0.491510	-4.972814
H	-4.983394	0.999445	-1.128456	H	2.909950	2.129671	-4.486871
H	-3.633196	0.627510	-0.042075	H	3.872275	0.744461	-3.938769
C	-1.329263	-3.554177	2.554199	C	2.982076	-1.343760	-2.299105

H	-1.033045	-2.565727	2.909707	C	3.655818	-1.373397	-1.071182
H	-2.401632	-3.669641	2.732983	C	3.531708	-2.070252	-3.365266
H	-0.814668	-4.310599	3.153402	C	4.856412	-2.070272	-0.923611
C	-3.332106	-2.808157	0.421603	H	3.236339	-0.835937	-0.227291
C	-4.056931	-1.932944	1.237574	C	4.726893	-2.779249	-3.222609
C	-4.021400	-3.863900	-0.192607	H	3.013488	-2.084122	-4.322191
C	-5.427890	-2.106425	1.440124	C	5.399689	-2.776202	-1.999611
H	-3.528938	-1.110404	1.708666	H	5.368810	-2.060043	0.035577
C	-5.391207	-4.044029	0.005991	H	5.129043	-3.336083	-4.065611
H	-3.478936	-4.551060	-0.839966	H	6.332091	-3.322815	-1.884097
C	-6.101243	-3.163708	0.825516				
H	-5.972177	-1.412802	2.076928				

Table A1.4. Optimized geometries, coordinates and energies at the B3LYP level of theory with 6-31G(d) basis set for unobserved D_{2d} core tetramer **9b**.

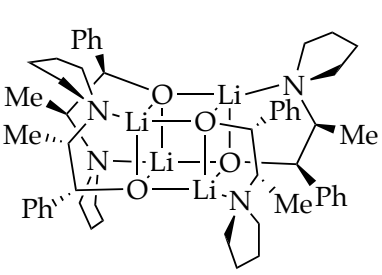

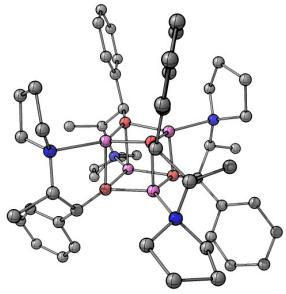

G = -2574.158243 Hartree
G_{MP2} = -2565.564775 Hartree

Atom	X	Y	Z	Atom	X	Y	Z
Li	0.653718	0.707339	-1.117836	C	1.491132	3.150891	-3.468372
Li	-0.653704	0.706364	1.118512	H	-0.322499	1.916048	-3.702389
O	1.265338	0.889929	0.690588	H	0.855514	1.767930	-5.022967
Li	1.136432	-1.099835	0.565175	H	3.151163	2.865308	-2.063061
O	-0.673091	-1.222092	1.290804	H	3.692583	3.092216	-3.725125
Li	-1.136607	-1.099181	-0.566151	H	0.998665	3.585026	-2.592267
O	0.672929	-1.220935	-1.291924	H	1.503107	3.919055	-4.247620
C	1.016268	-1.698751	-2.549296	N	1.408836	0.786243	-3.197718
C	0.936914	-0.561268	-3.638907	C	3.889570	-2.296403	1.150981
O	-1.265295	0.890715	-0.689734	C	2.874857	-1.611299	3.093064
C	-2.225425	1.128548	-1.654076	C	4.992695	-2.479328	2.214869
C	-3.469469	0.179847	-1.499737	H	4.253636	-2.074140	0.149765
H	-4.181527	0.420890	-2.305623	H	3.294626	-3.214975	1.074045
C	2.225548	1.126792	1.655091	C	4.274150	-2.122341	3.542284
C	3.469428	0.178012	1.499898	H	2.133946	-2.415246	3.179218
H	4.181578	0.418289	2.305931	H	2.515239	-0.769635	3.688106
C	-1.016424	-1.701049	2.547742	H	5.399987	-3.495437	2.210122
C	-0.936968	-0.564576	3.638392	H	5.827329	-1.794390	2.027323
H	0.145801	-0.412000	3.720942	H	4.177352	-2.985684	4.208543
C	-2.843330	1.112236	3.332416	H	4.821078	-1.351957	4.095543
C	-0.745604	1.887776	3.933063	N	2.983552	-1.236585	1.659469
C	-2.912186	2.635820	3.108648	C	-3.889958	-2.294794	-1.152816
H	-3.218331	0.862809	4.339288	C	-2.875134	-1.608258	-3.094339

H	-3.437244	0.562336	2.603589	C	-4.993082	-2.476756	-2.216877
C	-1.491072	3.147746	3.471227	H	-4.254028	-2.073269	-0.151438
H	0.322529	1.912637	3.704104	H	-3.295130	-3.213499	-1.076577
H	-0.855459	1.763381	5.024576	C	-4.274496	-2.118722	-3.543989
H	-3.151246	2.863518	2.065806	H	-2.134346	-2.412251	-3.181133
H	-3.692497	3.088888	3.728132	H	-2.515373	-0.766166	-3.688690
H	-0.998645	3.582608	2.595460	H	-5.400442	-3.492842	-2.212976
H	-1.502958	3.915243	4.251134	H	-5.827675	-1.791921	-2.028778
N	-1.408858	0.783352	3.198457	H	-4.177823	-2.981499	-4.211001
C	2.843322	1.115219	-3.331330	H	-4.821321	-1.347781	-4.096573
C	0.745638	1.891353	-3.931346	N	-2.983799	-1.234691	-1.660443
C	2.912199	2.638590	-3.106140	H	-0.145845	-0.408573	-3.721370
H	3.218350	0.866722	-4.338421	H	-0.231871	-2.398964	2.913144
H	3.437204	0.564638	-2.602994	H	1.822433	0.889143	2.661775
H	-1.822311	0.891669	-2.660942	H	2.489576	-1.207627	-5.075082
H	0.231688	-2.396283	-2.915365	C	-1.414350	-1.025652	5.026990
C	4.174803	0.401785	0.165173	H	-0.914861	-1.966866	5.284160
H	3.559178	0.033938	-0.658267	H	-1.159807	-0.298354	5.805832
H	4.344663	1.472476	0.018798	H	-2.489583	-1.212189	5.074057
H	5.148017	-0.097208	0.122730	C	-2.261422	-2.608093	2.478370
C	2.665664	2.596005	1.747309	C	-2.043059	-3.906268	1.983023
C	3.479550	3.046234	2.798343	C	-3.576090	-2.268572	2.822003
C	2.231418	3.531304	0.801501	C	-3.082658	-4.820706	1.827126
C	3.866291	4.383705	2.887974	H	-1.028953	-4.197997	1.716552
H	3.808887	2.345446	3.563610	C	-4.626691	-3.182066	2.674825
C	2.614719	4.872827	0.887042	H	-3.802037	-1.289703	3.224527
H	1.575727	3.188946	0.007708	C	-4.387707	-4.460723	2.174858
C	3.437626	5.303983	1.928043	H	-2.874189	-5.817994	1.446757
H	4.497773	4.709432	3.711226	H	-5.633957	-2.888379	2.961214
H	2.263743	5.582394	0.141247	H	-5.203055	-5.171330	2.066595
H	3.735396	6.347085	1.997760	C	-2.665282	2.597914	-1.745081
C	2.261218	-2.605922	-2.480729	C	-3.479063	3.049159	-2.795760
C	2.042769	-3.904569	-1.986660	C	-2.230891	3.532351	-0.798486
C	3.575922	-2.266122	-2.823948	C	-3.865569	4.386772	-2.884290
C	3.082319	-4.819202	-1.831585	H	-3.808504	2.349065	-3.561616

H	1.028633	-4.196516	-1.720542	C	-2.613957	4.874012	-0.882922
C	4.626476	-3.179803	-2.677592	H	-1.575275	3.189221	-0.004965
H	3.801936	-1.286871	-3.225503	C	-3.436764	5.306177	-1.923585
C	4.387405	-4.458936	-2.178884	H	-4.496973	4.713293	-3.707286
H	2.873784	-5.816850	-1.452199	H	-2.262875	5.582898	-0.136530
H	5.633772	-2.885880	-2.963632	H	-3.734350	6.349389	-1.992441
H	5.202717	-5.169682	-2.071262	C	-4.174901	0.402674	-0.164885
C	1.414347	-1.021095	-5.027901	H	-3.559330	0.034223	0.658323
H	0.914837	-1.962055	-5.285954	H	-4.344723	1.473268	-0.017753
H	1.159870	-0.293077	-5.806092	H	-5.148141	-0.096301	-0.122845

Table A1.5. Optimized geometries, coordinates and energies at the B3LYP level of theory with 6-31G(d) basis set for unsubstituted S_4 core tetramer **13a**.

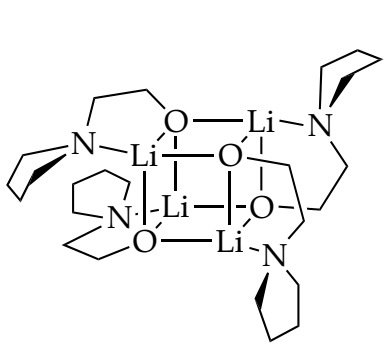

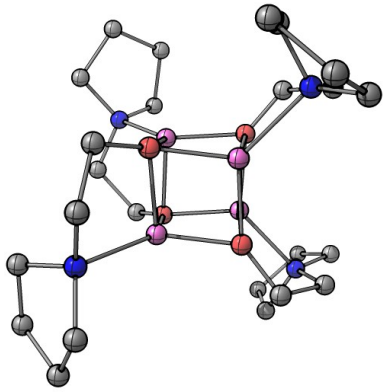

G = -1493.16961 Hartree
G_{MP2} = -1488.098718 Hartree

Atom	X	Y	Z	Atom	X	Y	Z
Li	0.066950	-0.694590	1.293791	H	-3.538680	0.230250	1.314494
Li	1.432836	-0.166526	-0.772256	H	2.620757	1.960899	2.050245
O	1.281372	0.755823	1.007120	H	3.263212	2.102795	-0.292531
Li	-0.214339	1.531845	0.127754	H	-3.066399	-0.946539	3.423497
O	0.063531	0.778220	-1.697593	H	-2.423976	1.154038	2.319981
Li	-1.052418	-0.588095	-0.968048	H	1.164017	-3.577028	-0.873196
O	-1.564328	0.270218	0.655001	H	0.139858	-2.512077	-2.821140
C	-2.491837	0.247761	1.681692	H	0.487390	1.689642	-3.520329
C	-2.334544	-0.985620	2.591790	H	1.246272	3.228057	-1.796359
O	0.443666	-1.721815	-0.262460	C	-0.573185	-0.105327	4.095505
C	0.223159	-3.006745	-0.727755	C	-0.732095	-2.406780	3.804027
C	-0.500830	-3.016924	-2.087420	C	0.708754	-0.671317	4.738244
H	-0.661833	-4.056528	-2.436622	H	-1.368553	0.020420	4.854180
C	-0.142763	1.794912	-2.613768	H	-0.414715	0.857901	3.604162
C	0.174295	3.184707	-2.028397	C	0.622937	-2.207391	4.502322
H	-0.040592	3.976333	-2.774110	H	-0.739995	-3.236175	3.089039
C	2.564431	1.032589	1.445683	H	-1.527863	-2.594497	4.549589
C	3.558418	1.215632	0.282639	H	1.596377	-0.254573	4.253282
H	4.580361	1.393275	0.673962	H	0.764733	-0.414192	5.800525
C	4.339752	0.309180	-1.867386	H	1.438475	-2.542530	3.853229

C	4.108093	-1.170569	-0.089987	H	0.686284	-2.783226	5.430696
C	4.439046	-1.080322	-2.517856	N	-0.965253	-1.130321	3.108749
H	5.346772	0.689000	-1.610328	C	-0.104989	4.668304	-0.086533
H	3.851594	1.057306	-2.500741	C	-2.002619	3.628281	-0.932489
C	4.326467	-2.070350	-1.322378	C	-1.176178	4.900447	0.992766
H	3.421549	-1.606134	0.640201	H	-0.077735	5.520101	-0.792140
H	5.068814	-0.964429	0.418369	H	0.904238	4.534931	0.316841
H	3.614613	-1.231573	-3.222398	C	-2.454375	4.226986	0.413339
H	5.372073	-1.196899	-3.077740	H	-2.488195	2.676405	-1.160972
H	3.477087	-2.746346	-1.457789	H	-2.210239	4.329857	-1.762397
H	5.221666	-2.689122	-1.206519	H	-0.882431	4.423248	1.933402
N	3.548751	0.076416	-0.647717	H	-1.315458	5.966375	1.197561
H	-2.668896	-2.972916	-0.252718	H	-2.811615	3.437494	1.081250
H	-2.938901	-4.017751	-1.665325	H	-3.276243	4.936481	0.276017
H	-3.814412	-0.450820	-3.042188	N	-0.547553	3.443280	-0.772886
H	-4.466878	-1.853965	-3.887498	C	-2.341414	-2.021525	-3.384776
H	-4.324838	-1.393436	-0.977196	C	-2.860062	-2.966336	-1.329110
H	-5.002970	-2.822439	-1.758807	C	-3.776075	-1.543488	-3.097657
N	-1.773974	-2.278966	-2.049896	H	-2.357883	-2.950693	-3.984976
H	-2.550875	-1.885225	2.001127	H	-1.730355	-1.286708	-3.918360
H	2.955578	0.231512	2.108119	C	-4.122257	-2.174187	-1.716942
H	-1.188168	1.808143	-2.987364				
H	-0.372613	-3.610488	-0.011362				

Table A1.6. Optimized geometries, coordinates and energies with 6-31G(d) basis set for unsubstituted D_{2d} core tetramer **13b**.

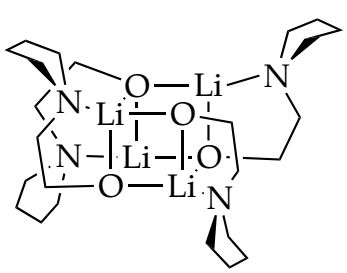

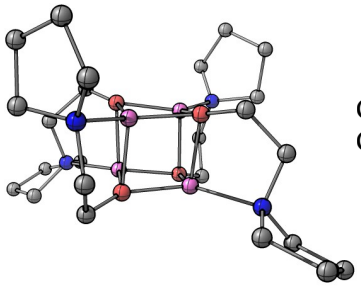

G = -1493.158199 Hartree
G_{MP2} = -1488.087406 Hartree

Atom	X	Y	Z	Atom	X	Y	Z
Li	0.035758	1.250456	0.793171	C	-3.692535	-0.430867	0.183822
Li	-0.035613	-1.250942	0.792414	H	-4.751687	-0.260469	0.450574
O	1.432165	-0.029686	0.963734	C	2.771796	-0.204505	1.246377
Li	1.253162	-0.032524	-1.038260	C	3.692682	0.430047	0.184082
O	-0.034228	-1.427976	-1.197798	H	4.751803	0.259288	0.450715
Li	-1.253199	0.032448	-1.038272	C	-0.120350	-2.774819	-1.497050
O	0.034116	1.427818	-1.197255	C	0.552774	-3.652906	-0.423501
C	0.119148	2.774659	-1.496758	H	1.622532	-3.410826	-0.402845
C	-0.553848	3.652362	-0.422818	C	-1.319977	-3.938934	1.171997
O	-1.432115	0.028977	0.963729	C	0.845300	-3.976901	2.002201
C	-2.771780	0.203178	1.246569	C	-1.493497	-3.829588	2.697843
H	-1.368733	-4.996014	0.847773	H	-0.367514	3.034027	-2.459425
H	-2.074100	-3.381832	0.610075	H	3.071370	0.244297	2.216524
C	-0.040530	-3.859316	3.255594	H	3.521958	1.512969	0.189220
H	1.797044	-3.442468	2.086188	H	-0.458300	4.726718	-0.679039
H	1.069633	-5.038409	1.785286	H	1.172585	3.110068	-1.606526
H	-1.986889	-2.888517	2.959851	H	-3.071193	-0.246467	2.216381
H	-2.111393	-4.644154	3.088296	H	-3.521619	-1.513762	0.188219
H	0.182025	-2.935443	3.798828	H	5.782749	0.437847	-3.443784
H	0.129132	-4.692546	3.944419	H	6.108245	0.922114	-1.781517
N	0.026174	-3.392073	0.926451	H	5.677088	-1.848754	-2.744699

C	1.319910	3.938778	1.171333	H	6.117790	-1.319814	-1.125364
C	-0.844842	3.976923	2.002935	N	3.371889	-0.044953	-1.186063
C	1.494386	3.830210	2.697145	C	-3.970864	-0.794532	-2.245868
H	1.368485	4.995694	0.846562	C	-3.945060	1.381001	-1.472226
H	2.073674	3.381387	0.609219	C	-5.438040	-0.326108	-2.410897
C	0.041757	3.859583	3.255787	H	-3.866088	-1.854328	-1.998089
H	-1.796565	3.442569	2.087642	H	-3.413024	-0.614486	-3.174309
H	-1.069253	5.038393	1.785904	C	-5.409390	1.153890	-1.942079
H	1.988392	2.889515	2.959349	H	-3.355370	1.839003	-2.275598
H	2.112135	4.645261	3.086816	H	-3.862727	2.026265	-0.594685
H	-0.180248	2.935636	3.799126	H	-5.782906	-0.435745	-3.443941
H	-0.127698	4.692752	3.944736	H	-6.108460	-0.921260	-1.782048
N	-0.026393	3.391803	0.926834	H	-5.677072	1.850286	-2.743038
C	3.970672	0.795426	-2.245399	H	-6.117540	1.320118	-1.124036
C	3.945241	-1.380636	-1.473238	N	-3.371864	0.045051	-1.186026
C	5.437910	0.327349	-2.410822	H	-1.623477	3.409764	-0.401562
H	3.865727	1.855044	-1.996932	H	0.365420	-3.034589	-2.460049
H	3.412801	0.615879	-3.173917	H	3.039106	-1.280478	1.335584
C	5.409478	-1.153009	-1.943150	H	-3.039420	1.278991	1.336637
H	3.355506	-1.838192	-2.276829	H	0.456554	-4.727208	-0.679685
H	3.863121	-2.026494	-0.596115	H	-1.174103	-3.109521	-1.605975

Table A1.7. Optimized geometries, coordinates and energies at the B3LYP level of theory with 6-31G(d) basis set for unsubstituted D_{2d} core tetramer **8a**.

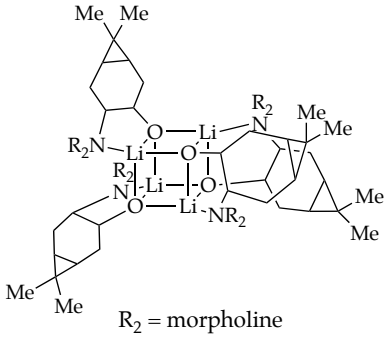

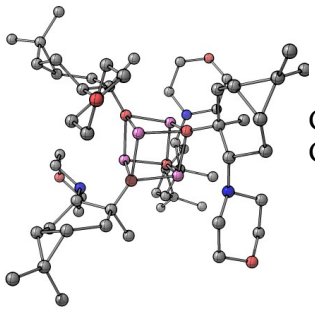

G = -3041.437536 Hartree
G_{MP2} = -2988.763774 Hartree

Atom	X	Y	Z	Atom	X	Y	Z
Li	-1.208837	0.631033	0.399523	H	7.603116	-1.796532	-1.870020
Li	-0.477234	-1.211903	-1.177998	O	-1.389289	-1.310039	0.525708
Li	0.477426	-1.212021	1.177841	C	-2.407886	-2.266672	0.634369
Li	1.208822	0.631198	-0.399541	C	-3.218566	-2.320873	-0.706116
O	0.466889	0.744722	1.408468	C	-3.393838	-1.851673	1.811068
C	-0.645963	2.765133	2.168884	H	-3.545913	-1.283525	-0.854999
H	-0.095304	3.216703	1.336363	C	-4.502026	-3.179968	-0.592615
C	-0.697006	3.835138	3.283791	H	-3.144919	-2.440542	2.704790
H	-1.414829	4.622782	3.026766	H	-3.104873	-0.824826	2.047916
H	-1.052842	3.399277	4.223503	C	-4.908557	-1.848342	1.586827
C	0.219407	1.512805	2.556190	H	-4.974824	-3.287985	-1.575414
C	1.594567	1.999111	3.190462	H	-4.255212	-4.196143	-0.267134
H	1.738814	1.491461	4.153323	C	-5.490916	-2.519620	0.356806
H	2.361072	1.594011	2.524432	C	-5.825167	-3.052126	1.738818
O	1.389525	-1.309773	-0.525929	C	-5.298874	-4.386212	2.233589
C	2.408139	-2.266373	-0.634688	C	-7.233718	-2.761617	2.238490
C	3.218729	-2.320757	0.705847	H	-5.336932	-4.425437	3.330056
C	3.394183	-1.851206	-1.811265	H	-5.913190	-5.213922	1.854910
H	3.546056	-1.283426	0.854888	H	-4.265319	-4.578506	1.941352
C	4.502215	-3.179810	0.592297	H	-7.938159	-3.535710	1.905727

H	3.145461	-2.440084	-2.705034
H	3.105121	-0.824389	-2.048125
C	4.908875	-1.847722	-1.586833
H	4.974916	-3.288051	1.575116
H	4.255471	-4.195914	0.266540
C	5.491161	-2.519191	-0.356874
C	5.825609	-3.051403	-1.738946
C	5.299455	-4.385443	-2.233994
C	7.234196	-2.760704	-2.238405
H	5.337790	-4.424561	-3.330454
H	5.913680	-5.213185	-1.855240
H	4.265824	-4.577761	-1.942035
H	7.938663	-3.534792	-1.905686
H	7.267123	-2.732606	-3.335746
C	-1.578639	4.260944	-4.647402
C	-2.523401	5.409181	-4.970959
H	-2.032636	6.159001	-5.605698
H	-3.412009	5.050515	-5.506890
H	-2.866308	5.917194	-4.062314
C	-2.236267	-4.057477	-2.220273
C	-2.971758	-1.956400	-3.105707
C	-1.443791	-4.279540	-3.504515
H	-3.219486	-4.534645	-2.355998
H	-1.732380	-4.560812	-1.394441
C	-2.182084	-2.264544	-4.375941
H	-4.014819	-2.281887	-3.264456
H	-2.979026	-0.873954	-2.938737
H	-1.390268	-5.349056	-3.730412
H	-0.416267	-3.894534	-3.395040
H	-2.686610	-1.831691	-5.245373
H	-1.172682	-1.830132	-4.308234
N	-2.378046	-2.613622	-1.918504
O	-2.078256	-3.659826	-4.612681
C	-0.493063	0.623066	3.602377
H	-1.348699	0.106849	3.160348
H	-7.266515	-2.733702	3.335839
H	-7.602763	-1.797415	1.870307
O	-0.466944	0.744840	-1.408457
C	-0.219434	1.513026	-2.556105
C	0.645736	2.765443	-2.168585
C	-1.594563	1.999179	-3.190582
H	0.095024	3.216750	-1.335960
C	0.696555	3.835658	-3.283303
H	-1.738352	1.491916	-4.153714
H	-2.361165	1.593573	-2.524964
C	-1.860999	3.496588	-3.360688
H	1.414266	4.623384	-3.026204
H	1.052394	3.400010	-4.223114
C	-0.684525	4.454721	-3.438600
H	1.614193	3.488026	0.205789
H	5.211698	1.923565	-2.577604
H	4.322683	0.988075	-1.347792
H	4.027685	3.882285	0.752068
H	3.625906	2.149179	0.639285
O	4.749281	2.963829	-0.901291
N	1.979117	2.414281	-1.568587
C	2.236306	-4.057569	2.219675
C	2.971859	-1.956646	3.105476
C	1.443900	-4.279851	3.503924
H	3.219511	-4.534809	2.355241
H	1.732335	-4.560721	1.393780
C	2.182212	-2.265012	4.375673
H	4.014920	-2.282156	3.264167
H	2.979140	-0.874171	2.938692
H	1.390383	-5.349407	3.729630
H	0.416370	-3.894824	3.394574
H	2.686757	-1.832301	5.245165
H	1.172800	-1.830610	4.308073
N	2.378141	-2.613662	1.918155
O	2.078418	-3.660338	4.612169

H	0.204197	-0.147484	3.944887
H	-0.828200	1.170426	4.492688
C	0.493287	0.623454	-3.602249
H	1.348992	0.107390	-3.160178
H	-0.203795	-0.147236	-3.944806
H	0.828362	1.170898	-4.492535
C	1.757266	-3.618800	-1.002113
H	0.946723	-3.851319	-0.309609
H	1.319685	-3.535968	-2.003585
H	2.451860	-4.466300	-1.015311
C	-1.756985	-3.619159	1.001511
H	-0.946523	-3.851563	0.308874
H	-1.319300	-3.536504	2.002950
H	-2.451589	-4.466653	1.014634
C	-3.083527	2.297479	2.549861
C	-2.379079	3.436169	0.573930
C	-4.397157	1.965123	1.847925
H	-3.225648	3.240956	3.100117
H	-2.854506	1.517858	3.276784
C	-3.719666	3.087020	-0.066319
H	-2.462485	4.434673	1.037845
H	-1.614399	3.487992	-0.205394
H	-5.211841	1.922570	2.577523
H	-4.322665	0.987427	1.347568
H	-4.027907	3.882103	-0.751691
H	-3.625926	2.149020	-0.639263
N	-1.979268	2.413863	1.568763
O	-4.749467	2.963220	0.901439
C	3.083344	2.298241	-2.549760
C	2.378849	3.436444	-0.573575
C	1.860640	3.496528	3.361116
H	2.729882	3.858794	2.814659
C	0.683963	4.454397	3.439305
H	0.802246	5.405838	2.920974
C	1.578075	4.260391	4.648072
C	2.522584	5.408719	4.972046
H	2.031637	6.158217	5.607025
H	3.411255	5.050064	5.507881
H	2.865402	5.917108	4.063582
C	1.086956	3.538191	5.889353
H	0.437189	2.688029	5.668491
H	1.936575	3.154533	6.469309
H	0.527869	4.222574	6.540776
C	-1.087399	3.539268	-5.888940
H	-0.528452	4.223983	-6.540132
H	-0.437465	2.689156	-5.668377
H	-1.936953	3.155646	-6.469015
H	-2.730297	3.858482	-2.814078
H	-0.802968	5.405958	-2.919932
H	6.299850	-1.988132	0.144258
H	5.381777	-0.909114	-1.870563
H	-5.381513	-0.909835	1.870799
H	-6.299714	-1.988545	-0.144135
C	4.397043	1.965879	-1.847960
H	3.225339	3.241866	-3.099791
H	2.854377	1.518779	-3.276866
C	3.719506	3.087314	0.066539
H	2.462118	4.435048	-1.037299

REFERENCES

1. (a) *Ions and Ion Pairs in Organic Reactions*; Szwarc, M., Ed.; Wiley: New York, 1972; Vols. 1 and 2. (b) Wardell, J. L. In *Comprehensive Organometallic Chemistry*; Wilkinson, G., Stone, F. G. A., Abels, F. W., Eds.; Pergamon: New York, 1982; Vol. 1, Chapter 2. (c) Wakefield, B. J. *The Chemistry of Organolithium Compounds*; Pergamon Press: New York, 1974. (d) Brown, T. L. *Pure Appl. Chem.* **1970**, *23*, 447.

2. Seebach, D. *Angew. Chem., Int. Ed. Engl.* **1988**, *27*, 1624. Seebach, D. In *Proceedings of the Robert A. Welch Foundation Conferences on Chemistry and Biochemistry*; Wiley: New York, 1984.

3. (a) Grabowski, E. J. J. "Reflections on Process Research". In *Chemical Process Research: The Art of Practical Organic Synthesis*; Abdel-Magid, A. F.; Ragan, J. A., Eds. American Chemical Society, Washington D.C.: USA 2004; pp 1-21. (b) Thompson, A. S.; Corley, E. G.; Huntington, M. F.; Grabowski, E. J. J. *Tetrahedron Lett.* **1995**, *36*, 8937. (c) Huffman, M. A.; Yasuda, N.; DeCamp, A. E.; Grabowski, E. J. J. *J. Org. Chem.* **1995**, *60*, 1590. (d) Tan, L.; Chen, C.-Y.; Tillyer, R. D.; Grabowski, E. J. J.; Reider, P. J. *Angew. Chem., Int. Ed. Engl.* **1999**, *38*, 711. (e) Pierce, M. E.; Parsons, R. L., Jr.; Radesca, L. A.; Lo, Y. S.; Silverman, S.; Moore, J. R.; Islam, Q.; Choudhury, A.; Fortunak, J. M. D.; Nguyen, D.; Luo, C.; Morgan, S. J.; Davis, W. P.; Confalone, P. N.; Chen, C. Y.; Tillyer R. D.; Frey, L.; Tan, L. S.; Xu, F.; Zhao, D.; Thompson, A. S.; Corley, E. G.; Grabowski, E. J. J.; Reamer, R.; Reider, P. J. *J. Org. Chem.* **1998**, *63*, 8536.

4. (a) Ye, M.; Logaraj, S.; Jackman, L. M.; Hillegass, K.; Hirsh, K.; Bollinger, A. M.; Grosz, A. L.; Mani, V. *Tetrahedron* **1994**, *50*, 6109. (b) Rochet, P.; Vatele, J. M.; Gore, J. *Synlett* **1993**, 105. (c) Vijn, R. J.; Speckamp, W. N.; De Jong, B. S.; Hiemstra, H. *Angew. Chem.* **1984**, *96*, 165. (d) Dieter, R. K.; Datar, R. *Can. J. Chem.* **1993**, *71*, 814. (e) Boireau, G.; Abenhaim, D.; Henry-Basch, E. *Tetrahedron* **1979**, *35*, 1457. (f) Boireau, G.; Abenhaim, D.; Bourdais, J.; Henry-Basch, E. *Tetrahedron Lett.* **1976**, *17*, 4781. (g) Zweig, J. S.; Luche, J. L.; Barreiro, E.; Crabbe, P. *Tetrahedron Lett.* **1975**, *16*, 2355. (h) Vadecard, J.; Plaquevent, J.-C.; Duhamel, L.; Duhamel, P.

J. Org. Chem. **1994**, *59*, 2285. (i) Malmvik, A. C.; Obenius, U.; Henriksson, U. *J. Chem. Soc., Perkin Trans. 2* **1986**, 1899. (j) Gerlach, U.; Haubenreich, T.; Huenig, S. *Chem. Ber.* **1994**, *127*, 1969. (k) Kumamoto, T.; Aoki, S.; Nakajima, M.; Koga, K. *Tetrahedron: Asymmetry* **1994**, *5*, 1431. (l) Fehr, C.; Stempf, I.; Galindo, J. *Angew. Chem., Int. Ed. Engl.* **1993**, *32*, 1042. (m) Milne, D.; Murphy, P. J. *J. Chem. Soc., Chem. Commun.* **1993**, 884. (n) Mukaiyama, T.; Soai, K.; Sato, T.; Shimizu, H.; Suzuki, K. *J. Am. Chem. Soc*. **1979**, *101*, 1455. (o) Schön, M.; Naef, R. *Tetrahedron: Asymmetry* **1999**, *10*, 169. (p) Gärtner, P.; Letschnig, M.; Knollmüller, M. *Monatsh. Chem.* **2000**, *131*, 867. (q) Knollmüller, M.; Ferencic, M.; Gärtner, P. *Tetrahedron: Asymmetry* **1999**, *10*, 3969. (r) Scott, M. S.; Lucas, A. C.; Luckhurst, C. A.; Prodger, J. C.; Dixon, D. *J. Org. Biomol. Chem*. **2006**, *4*, 1313. (s) Riant, O.; Hannedouche, *J. Org. Biomol. Chem*. **2007**, *5*, 873. (t) Khartabil, H. K.; Gros, P. C.; Fort, Y.; Ruiz-Lopez, M. F. *J. Am. Chem. Soc.* **2010**, *132*, 2410. (u) Coldham, I.; Raimbault, S.; Whittaker, D. T. E.; Chovatia, P. T.; Leonori, D.; Patel, J. J.; Sheikh, N. S. *Chem. Eur. J.* **2010**, *16*, 4082. (v) Coldham, I.; Dufour, S.; Haxell, T. F. N.; Howard, S.; Vennall, G. P. *Angew. Chem. Int. Ed.* **2002**, *41*, 3887. (w) Gros, P.; Fort, Y. *Eur. J. Org. Chem.* **2002**, 3375. (x) Gros, P.; Fort, Y.; Caubère, P. *J. Chem. Soc., Perkin Trans. 1,* **1997**, 3071.

5. Parsons, R. L., Jr. *Curr. Opin. Drug Discovery Dev.* **2000**, *3*, 783. Kauffman, G. S.; Harris, G. D.; Dorow, R. L.; Stone, B. R. P.; Parsons, R. L.; Pesti, J. A.; Magnus, N. A.; Fortunak, J. M.; Confalone, P. N.; Nugent, W. A. *Org. Lett.* **2000**, *2*, 3119.

6. Thompson, A.; Corley, E. G.; Huntington, M. F.; Grabowski, E. J. J.; Remenar, J. F.; Collum, D. B. *J. Am. Chem. Soc*. **1998**, *120*, 2028. Xu, F.; Reamer, R. A.; Tillyer, R.; Cummins, J. M.; Grabowski, E. J. J.; Reider, P. J.; Collum, D. B.; Huffman, J. C. *J. Am. Chem. Soc.* **2000**, *122*, 11212.

7. Parsons, R. L., Jr.; Fortunak, J. M.; Dorow, R. L.; Harris, G. D.; Kauffman, G. S.; Nugent, W. A.; Winemiller, M. D.; Briggs, T. F.; Xiang, B.; Collum, D. B. *J. Am. Chem. Soc.* **2001**, *123*, 9135.

8. For extensive leading references to solution structural studies of enolates and related O-lithiated species see: McNeil, A. J.; Toombes, G. E. S.; Gruner, S. M.; Lobkovsky, E.; Collum, D. B.; Chandramouli, S. V.; Vanasse, B. J.; Ayers, T. A. *J. Am. Chem. Soc.* **2004**, *126*, 16559.

9. (a) Arnett, E. M.; Nichols, M. A.; McPhail, A. T. *J. Am. Chem. Soc.* **1990**, *112*, 7059. (b) Nichols, M. A.; McPhail, A. T.; Arnett, E. M. *J. Am. Chem. Soc.* **1991**, *113*, 6222.

10. Streitwieser, A. *J. Org. Chem.* **2009**, *74*, 4433 and references cited therein.

11. Diffusion-ordered NMR spectroscopy (DOSY) shows considerable potential to examine the structures of LiX salts: Li, D.; Keresztes, I.; Hopson, R.; Williard, P. G. *Acc. Chem. Res.* **2009**, *42*, 270.

12. (a) Liou, L. R.; McNeil, A. J.; Ramírez, A.; Toombes, G. E. S.; Gruver, J. M.; Collum, D. B. *J. Am. Chem. Soc.* **2008**, *130*, 4859. (b) De Vries, T. S.; Goswami, A.; Liou, L. R.; Gruver, J. M.; Jayne, E.; Collum, D. B. *J. Am. Chem. Soc.* **2009**, *131*, 13142. (c) Tomasevich, L. L.; Collum, D. B. *J. Org. Chem.* **2013**, *78*, 7498 and references cited therein.

13. Renny, J. S.; Tomasevich, L. L.; Tallmadge, E. H.; Collum, D. B. *Angew. Chem., Int. Ed.* **2013**, *52*, early view.

14. (a) Herberich, G. E.; Spaniol, T. P.; Fischer, A. *Chem. Ber.* **1994**, *127*, 1619. (b) Armstrong, D. R.; Davies, R. P.; Raithby, P. R.; Snaith, R.; Wheatley, A. E. H. *New J. Chem.* **1999**, *23*, 499. (c) Strohmann, C.; Seibel, T.; Schildbach, D. *J. Am. Chem. Soc.* **2004**, *126*, 9876. (d) Iwasaki, M.; Narita, T.; Umino, Y. *J. Organomet. Chem.* **2011**, *696*, 2763. (e) Al-Masri, H. T.; Sieler, J.; Hey-Hawkins, E. *Appl. Organometal. Chem.* **2003**, 17, 63. (f) Morris, J. J.; MacDougall, D. J.; Noll, B. C.; Henderson, K. W. *Dalton Trans*. **2008**, 3429. (g) van der Schaaf, P. A.; Jastrezebski, J. T. B. H.; Hogerheide, M. P.; Smeets, W. J. J.; Spek, A. L.; Boersma, J.; van Koten, G. *Inorg. Chem*. **1993**, 32, 4111. (h) Khartabil, H. K.; Gros, P. C.; Fort, Y.; Ruiz-Lopez, M. F. *J.*

Org. Chem. **2008**, 73, 9393. (i) Khartabil, H. K.; Martins-Costa, M. T. C.; Gros, P. C.; Fort, Y.; Ruiz-Lopez, M. F. *J. Phys. Chem. B* **2009**, *113*, 6459.

15. (a) Arvidsson, P. I.; Ahlberg, P.; Hilmersson, G. *Chem. Eur. J.* **1999**, *5*, 1348. (b) Bauer, W. *J. Am. Chem. Soc.* **1996**, *118*, 5450. (c) Bauer, W.; Griesinger, C. *J. Am. Chem. Soc.* **1993**, *115*, 10871. (d) DeLong, G. T.; Pannell, D. K.; Clarke, M. T.; Thomas, R. D. *J. Am. Chem. Soc.* **1993**, *115*, 7013. (e)Thomas, R. D.; Clarke, M. T.; Jensen, R. M.; Young, T. C. *Organometallics* **1986**, *5*, 1851. (f) Bates, T. F.; Clarke, M. T.; Thomas, R. D. *J. Am. Chem. Soc.* **1988**, *110*, 5109. (g) Fraenkel, G.; Hsu, H.; Su, B. M. In *Lithium: Current Applications in Science, Medicine, and Technology*; Bach, R. O., Ed.; Wiley: New York, 1985; pp 273-289. (h) Heinzer, J.; Oth, J. F. M.; Seebach, D. *Helv. Chim. Acta* **1985**, *68*, 1848. (i) Fraenkel, G.; Henrichs, M.; Hewitt, J. M.; Su, B. M.; Geckle, M. J. *J. Am. Chem. Soc.* **1980**, *102*, 3345. (j) Lucht, B. L.; Collum, D. B. *J. Am. Chem. Soc.* **1996**, *118*, 3529. (k) Knorr, R.; Menke, T.; Ferchland, K.; Mahlstäubl, J.; Stephenson, D. S. *J. Am. Chem. Soc.* **2008**, *130*, 14179.

16. Mulvey, R. E. *Chem. Soc. Rev.* **1991**, *20*, 167.

17. Hall, P. L.; Gilchrist, J. H.; Harrison, A. T.; Fuller, D. J.; Collum, D. B. *J. Am. Chem. Soc.* **1991**, *113*, 9575.

18. Fedyunina, I. V.; Plemenkov, V. V; Bikbulatova, S.; Nikitina, L. E.; Litvinov, I. A.; Kataeva, O. N. *Chem. Nat. Compds.* **1992**, *28*, 173.

19. Romesberg, F. E.; Bernstein, M. P.; Gilchrist, J. H.; Harrison, A. T.; Fuller, D. J.; Collum, D. B. *J. Am. Chem. Soc.* **1993**, *115*, 3475. An improvement based on a dissolving metal protocol will be reported.

20. (a) Jackman, L. M.; DeBrosse, C. W. *J. Am. Chem. Soc.* **1983**, *105*, 4177. (b) Reich, H. J.; Kulicke, K. J. *J. Am. Chem. Soc.* **1996**, *118*, 273. (c) Deana, R. K.; Recklinga, A. M.; Chena, H.; Daweab, L. N.; Schneiderac, C. M.; Kozak, C. M. *Dalton Trans.* **2013**, *42*, 3504. (d) Reed, D.; Barr, D.; Mulvey, R. E.; Snaith, R. *J Chem. Soc., Dalton Trans.* **1986**, 557. (e) MacDougall, D. J.; Noll, B. C.; Kennedy, A.

R.; Henderson, K. W. *J. Chem. Soc. Dalton Trans.* **2006**, *15*, 1875. (f) Boyle, T. J.; Pedrotty, D. M.; Alam. T. M.; Vick, S. C.; Rodriguez, M. A. *Inorg. Chem.* **2000**, *39*, 5133.

21. (a) Weingarten, H.; Van Wazer, J. R. *J. Am. Chem. Soc.* **1965**, *87*, 724. (b) Goralski, P.; Legoff, D.; Chabanel, M. *J. Organomet. Chem.* **1993**, *456*, 1. (c) Desjardins, S.; Flinois, K.; Oulyadi, H.; Davoust, D.; Giessner-Prettre, C.; Parisel, O.; Maddaluno, J. *Organometallics* **2003**, *22*, 4090. (d) Günther, H. *J. Braz. Chem. Soc.* **1999**, *10*, 241. (e) Kissling R. M.; Gagne, M. R. *J. Org. Chem.* **2001**, *66*, 9005.

22. After surveying a subset of the community, we have chosen to refer to $(LiX)_n$ and $(LiX)_m(LiX')_n$ as a "homoaggregate" and "heteroaggregate", respectively, and reserve the term "mixed aggregate" for $(LiX)_m(LiY)_n$.

23. Measuring the mole fraction within only the ensemble of interest rather than the overall mole fraction of lithium alkoxides added to the samples eliminates the distorting effects of impurities.

24. Frisch, M. J.; Trucks, G.; W.; Schlegel, H. B.; Scuseria, G. E.; Robb, M. A.; Cheeseman, J. R.; Montgomery, Jr., J. A.; Vreven, T.; Kudin, K. N.; Burant, J. C.; Millam, J. M.; Iyengar, S. S.; Tomasi, J.; Barone, V.; Mennucci, B.;Cossi, M.; Scalmani, G.; Rega, N.; Petersson, G. A.; Nakatsuji, H.; Hada, M.; Ehara, M.; Toyota, K.; Fukuda, R.; Hasegawa, J.; Ishida, M.; Nakajima, T.; Honda, Y.; Kitao, O.; Nakai, H.; Klene, M.; Li, X.; Knox, J. E.; Hratchian, H. P.; Cross, J. B.; Bakken, V.; Adamo, C.; Jaramillo, J.; Gomperts, R.; Stratmann, R. E.; Yazyev, O.; Austin, A. J.; Cammi, R.; Pomelli, C.; Ochterski, J. W.; Ayala, P. Y.; Morokuma, K.; Voth, G. A.; Salvador, P.; Dannenberg, J. J.; Zakrzewski, V. G.; Dapprich, S.; Daniels, A. D.;Strain, M. C.; Farkas, O.; Malick, D. K.; Rabuck, A. D.; Raghavachari, K.; Foresman, J. B.; Ortiz, J. V.; Cui, Q.; Baboul, A. G.; Clifford, S.; Cioslowski, J.; Stefanov, B. B.; Liu, G.; Liashenko, A.; Piskorz, P.; Komaromi, I.; Martin, R. L.; Fox, D. J.; Keith, T.; Al-Laham, M. A.; Peng, C. Y.; Nanayakkara, A.; Challacombe, M.; Gill, P. M. W.; Johnson, B.; Chen, W.; Wong, M. W.; Gonzalez,

C.; and Pople, J. A.; Gaussian, Inc., Wallingford CT, 2004. *GaussianVersion 3.09*; revision A.1; Gaussian, Inc.: Wallingford, CT, 2009. Gaussian 03, Revision B.04.

25. When the chemical bonds broken in the reactant are the same as the type of bonds formed the reaction is isodesmic.

26. Although homo- and heterosolvated dimeric enolates coordinated by *N,N,N',N'*-tetraalkyldiamines fail resolve (unpublished), the corresponding mixed diamine solvates of *n*-BuLi and PhLi resolve well: (a) Hoffmann, D.; Collum, D. B. *J. Am. Chem. Soc.* **1998**, *120*, 5810. (b) Rutherford, J. L.; Hoffmann, D.; Collum, D. B. *J. Am. Chem. Soc.* **2002**, *124*, 264.

27. Casy, B. M.; Flowers, R. A. *J. Am. Chem. Soc.* **2011**, *133*, 11492.

28. For examples of reactions that are fast relative to the rates of aggregate-aggregate exchanges see: (a) McGarrity, J. F.; Ogle, C. A. *J. Am. Chem. Soc.* **1985**, *107*, 1810. (b) Jones, A. C.; Sanders, A. W.; Bevan, M. J.; Reich, H. J. *J. Am. Chem. Soc.* **2007**, *129*, 3492. (c) Thompson, A.; Corley, E. G.; Huntington, M. F.; Grabowski, E. J. J.; Remenar, J. F.; Collum, D. B. *J. Am. Chem. Soc*. **1998**, *120*, 2028. (d) Jones, A. C.; Sanders, A. W.; Sikorski, W. H.; Jansen, K. L.; Reich, H. J. *J. Am. Chem. Soc.* **2008**, *130*, 6060. (e) Reich, H. J. *J. Org. Chem.* **2012**, *77*, 5471.

29. Lucht, B. L.; Collum, D. B. *Acc. Chem. Res.* **1999**, *32*, 1035.

CHAPTER II

Azaaldol Condensation of a Lithium Enolate Solvated by *N,N,N′,N′*-Tetramethylethylenediamine: Dimer-Based 1,2-Addition to Imines

Abstract

The lithium enolate of *tert*-amylacetate solvated by *N,N,N′,N′*-tetramethylethylenediamine (TMEDA) is shown to be a doubly-chelated dimer. Adding the dimeric enolate to 4-fluorobenzaldehyde-*N*-phenylimine affords an N-lithiated β-amino ester shown to be monomeric using ^{6}Li and ^{15}N NMR spectroscopies. Rate studies using ^{19}F NMR spectroscopy reveal reaction orders consistent with a transition structure of stoichiometry $[(ROLi)_2(TMEDA)_2(imine)]^{‡}$. Density functional theory computations explore several possible dimer-based transition structures with monodentate and bidentate coordination of TMEDA. Supporting rate studies using *N,N,N′,N′*-tetramethylcyclohexanediamine showing analogous rates and rate law suggest that TMEDA is fully chelated.

---

*Reprinted with permission from De Vries, T. S.; Bruneau, A. M.; Liou, L. R.; Subramanian, H.; Collum, D. B. *J. Am. Chem. Soc.* **2013**, *135*, 4103. Copyright 2013 American Chemical Society.

Introduction

Lithium enolates are of undeniable importance to synthetic chemists[1] yet pose particularly onerous mechanistic challenges owing to complex aggregation phenomena. Solid-state structural studies initiated by Seebach with significant contributions by Williard have grown into a considerable body of work.[2] Much less is known about the structures of enolates in solution[3] and how solvation and aggregation influence reactivity.[4,5,6,7,8] The seminal spectroscopic and mechanistic studies were those of Jackman and coworkers.[4] The preponderance of progress in untangling the contributions of equilibrating aggregates and monomers to enolate reactivity comes from Streitwieser and coworkers.[6] Most recently, Reich and coworkers have focused on measuring relative reactivities of aggregates and monomers under *nonequilibrium* conditions.[7]

The present study of 1,2-additions of metal enolates to imines—so-called azaaldol condensations—dovetails a long-standing program aimed at understanding 1,2-additions[9] and lithiations[10] of imines with an emergent interest in structures and reactivities of lithium enolates.[1,2,11,12,13] Azaaldol condensations are of particular importance in the synthesis of biologically and medicinally significant β-amino esters, β-lactams, and 1,3-amino alcohols.[14,15,16] The flexibility of imines that synthetic chemists find appealing[16]—the capacity to vary the substituents on the imine moiety—has proven to be equally important in untangling organolithium structure-reactivity relationships.

Herein we describe rate and mechanistic studies of the azaaldol addition of *tert*-amyl acetate **2** (*t*-Am = $C(CH_3)_2Et$) to imine **1** (eq 1) mediated by *N,N,N′,N′*-tetramethylethylenediamine (TMEDA).[8] The reaction is clean,

proceeds at tractable rates without complicating lactamization,[17] and is readily monitored with ^{19}F NMR spectroscopy.[18] A combination of structural, rate, and computational studies revealed an enolate dimer-based mechanism.

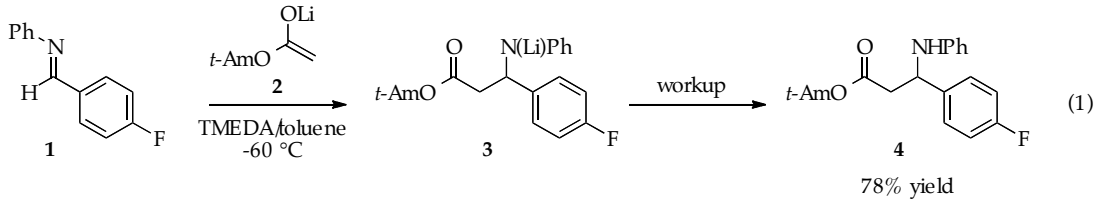

Results.

Solution Structures. Previous studies of TMEDA-solvated enolates using the method of continuous variation (the method of Job) have shown enolate **2** to be doubly chelated dimer **2a**.[19] Adduct [^{6}Li,^{15}N]**3** prepared from [^{15}N]**1** and [^{6}Li]LDA.[20] was shown using ^{6}Li and ^{15}N NMR spectroscopies[21,22,23] to be monomer **3a**. The ^{6}Li spectrum shows a 1:1 ^{6}Li doublet (J = 6.6 Hz) and 1:1:1 ^{15}N triplet J = 6.9 Hz).[24] No mixed aggregates are formed. Treatment of β-amino ester **4** with 1.0 equiv of [^{6}Li]LDA in the presence of TMEDA regenerates **3a**.

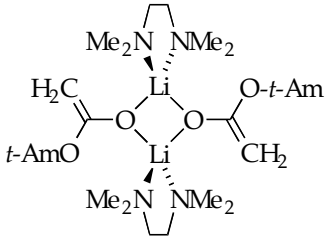

2a

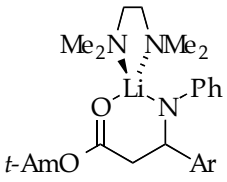

3a

Kinetics. Adding 1.0 equiv of imine **1** to enolate **2** in 0.65 M TMEDA/toluene at -60 °C and monitoring with in situ IR spectroscopy revealed an overall second-order decay (Figure 1), offering no evidence of autocatalysis or other mixed aggregation effects.[25] To conduct detailed rate studies under pseudo-first-order we turned to ^{19}F NMR spectroscopy. Injecting imine **1** (resulting in 0.005 M **1**) into a solution of enolate **2** and TMEDA afforded clean first-order decays and affiliated values of k_{obsd} (Figure 1 inset.) A standard control experiment confirmed the absence of autocatalysis: sequential injections of imine **1** (0.005 M) into a solution of enolate and TMEDA afforded indistinguishable values of k_{obsd} (within 10%). Monitoring k_{obsd} versus enolate concentration[26] showed a first-order dependence consistent with a dimer-based addition (Figure 2). An analogous plot of k_{obsd} versus TMEDA concentration revealed a zeroth-order dependence (Figure 3). The idealized rate law[27] described by eq 2 implicates the transition structure of stoichiometry shown in equation 3.[28]

$$-d[\text{imine}]/dt = k[\text{imine}][\text{TMEDA}]^0[\text{enolate}] \qquad (2)$$

$$(\text{ROLi})_2(\text{TMEDA})_2 + \text{imine} \longrightarrow [(\text{ROLi})_2(\text{TMEDA})_2(\text{imine})]^{\ddagger} \qquad (3)$$

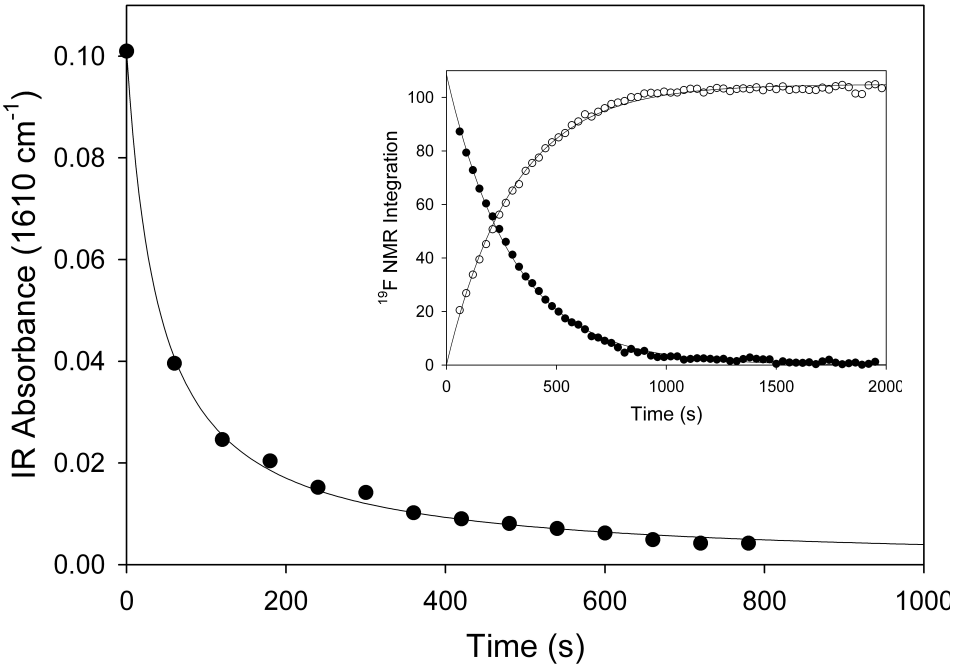

Figure 2.1. Curve fitting for the condensation of the lithium enolate of *tert*-amyl acetate enolate **2** (0.10 M)[26] with equimolar imine **1** (0.10 M) in 0.65 M TMEDA/toluene at -60 °C. The curve depicts an unweighted least-squares fit to the second-order function: $y = [A]_0/(1+[A]_0 \cdot k \cdot t)$ ($[A]_0 = 0.101 \pm 0.001$ M, $k = 0.24 \pm 0.01$ M^{-1} s^{-1}). The inset shows the loss of **1** and formation of **3** using lithium enolate **2** (0.10 M), imine **1**, (0.005 M), and 0.55 M TMEDA/toluene at -60 °C (pseudo-first-order conditions). Imine **1** is represented by the symbol • and the product **3** by o. The curves depict unweighted least-squares fits to $y_{S2} = y_0 \cdot e^{-b \cdot t}$ ($y_0 = 108.6 \pm 0.1$, $b = 3.32 \pm 0.03 \times 10^{-3}$ s^{-1}) and $y_{S3} = y_0 \cdot (1 - e^{-b \cdot t})$ ($y_0 = 104.9 \pm 0.1$, $b = 3.28 \pm 0.03 \times 10^{-3}$ s^{-1}).

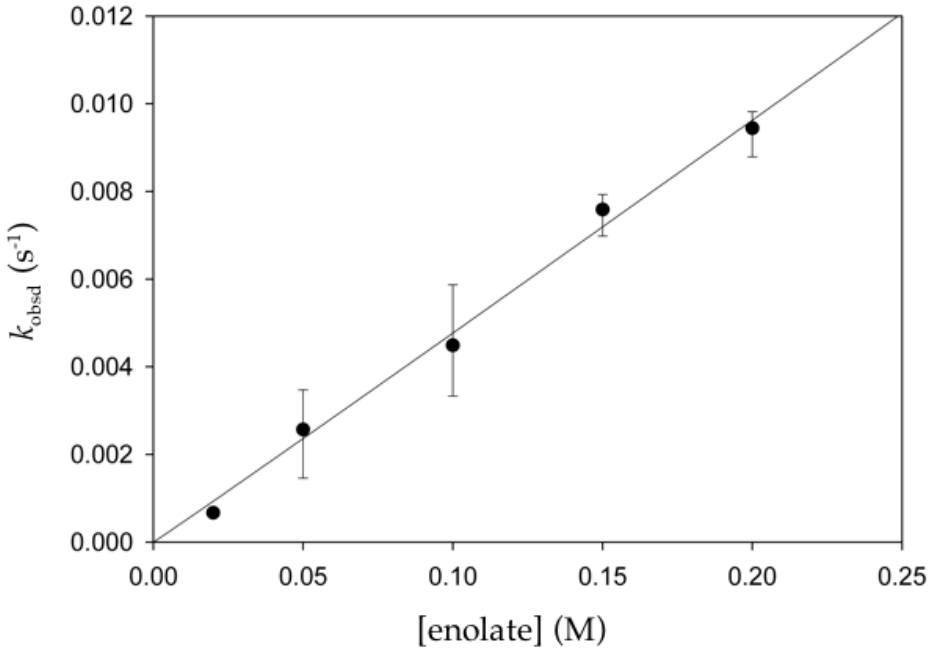

Figure 2.2. Plot of k_{obsd} versus concentration of enolate 2 for the condensation of **1** (0.005 M) with **2** in 0.60 M TMEDA / toluene at -60 °C**. The curve depicts the unweighted least-squares fit to $k_{obsd} = k\cdot[2]^b$ (k = 0.049 ± 0.007, b = 1.01 ± 0.08).**

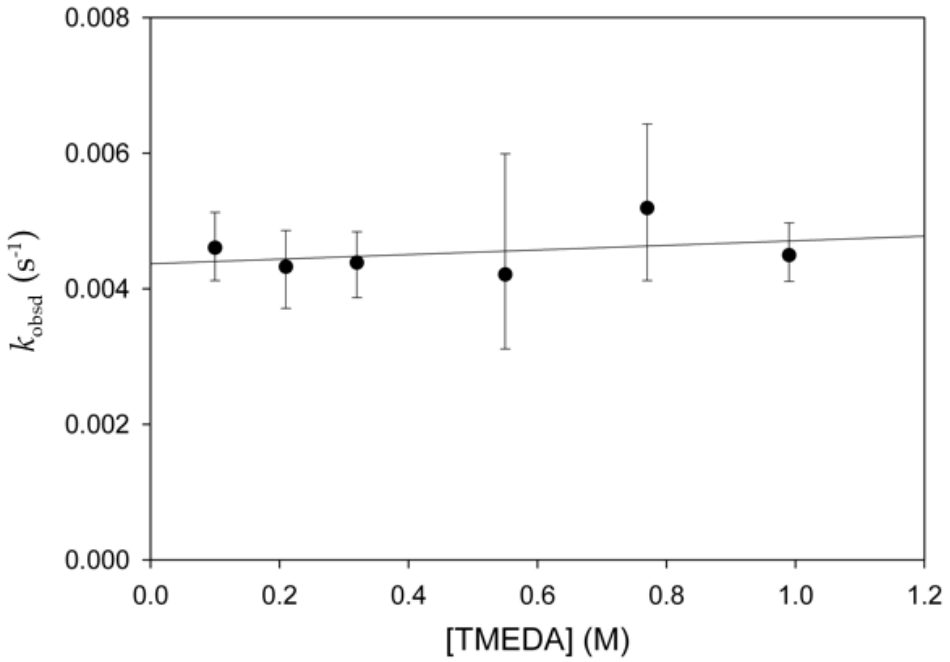

Figure 2.3. Plot of k_{obsd} versus free TMEDA concentration[26] in toluene cosolvent for the condensation of lithium enolate **2** (0.10 M) with imine **1** (0.005 M) at -60 °C. **The curve depicts the an unweighted least-squares fit to $k_{obsd} = k + k'\cdot[TMEDA]_{free}$ (k = 0.0044 ± 0.0003, k' = 0.0003 ± 0.0005).**

Computations. Density functional theory (DFT) computations at the B3LYP/6-31G(d) level[29] evaluated dimer-based pathways including cyclic dimers, open dimers,[30] and triple ions.[31,32,33,34] We modeled the *tert*-amyl group with a methyl. The reported energies correspond to the calculated free energies of activation at -60 °C and to fully balanced equilibria. Intrinsic reaction coordinate (IRC) calculations were performed to confirm the validity of the structures.[35] Figure 4 shows the computed structures in order of increasing free energy. A number of configurations were calculated including open and closed dimers with combinations of mono- and bidentate TMEDA ligands (**5a**-**5f**).[36] Structure **5g** manifests an imine nitrogen bridging two lithiums. The structure of

the lowest energy form, **5a**, is an open dimer with both mono- and bidentate TMEDA. Triple ion **5h** with an $(\eta^2\text{-TMEDA})_2Li^+$ counterion is energetically ridiculous;[37] DFT routinely fails with such fully ionized forms.[38] We do, however, believe that **5h** is worthy of further consideration.

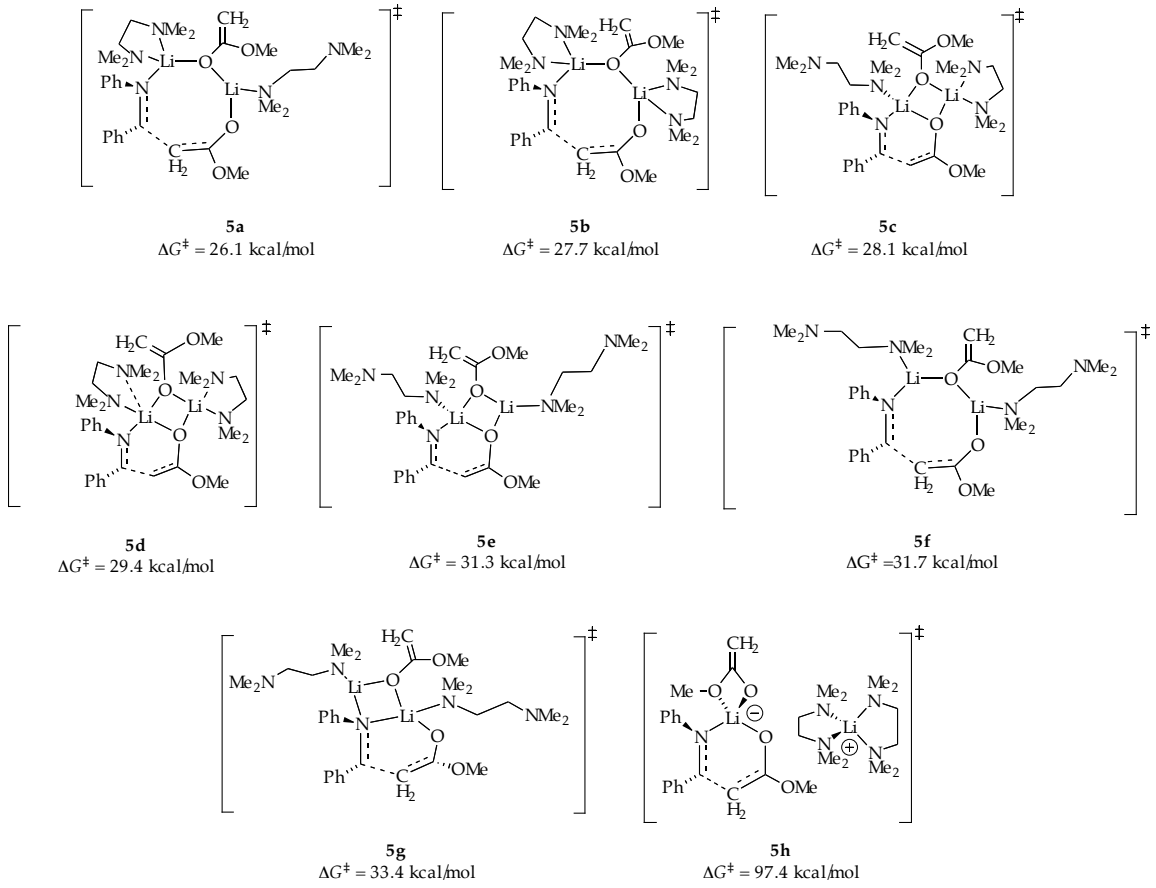

Figure 2.4. DFT Computed transition structures of stoichiometry $[(ROLi)_2(TMEDA)_2(imine)]^‡$.

Kinetics Revisited: Enolate-TMCDA. To resolve the ambiguity about whether TMEDA is functioning as a mono- or bidentate ligand we investigated *N,N,N′,N′*-tetramethylcyclohexane-diamine (TMCDA).[39] The notion was simple:

TMCDA is a surrogate of TMEDA but is more strongly chelating[40] and displays no tendency to bind as a monodentate ligand.[41] Cursory examination of azaaldol condensation of enolate **2** revealed rates that were nearly indistinguishable ($k_{TMCDA}/k_{TMEDA} = 0.9$)[42] and provided an analogous rate law (supporting information). Computations offered transition structures **7a** and **7b**. The $(\eta^2\text{-TMCDA})_2Li^+$ counterion in **7b** has crystallographic support.[43] Despite considerable effort, we found no closed dimer analogous to **5d**.

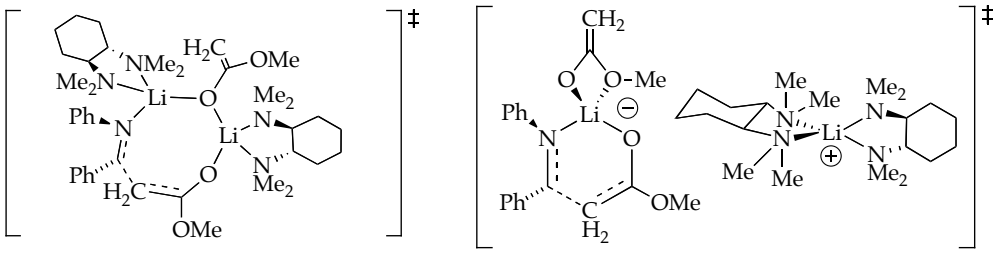

7a
$\Delta G^{\ddagger} = 9.6$ kcal/mol

7b
$\Delta G^{\ddagger} = 105.1$ kcal/mol

Discussion.

Using a combination of ^{6}Li and ^{15}N NMR spectroscopies we have shown that *tert*-amyl acetate **2** is disolvated dimer **2a** in the presence of TMEDA. Rate studies using ^{19}F NMR spectroscopy revealed that there is no autocatalysis and that the addition of **2a** to fluorinated imine **1** is first order in imine, first order in enolate dimer **2a**, and zeroth order in TMEDA. The rate law (eq 2) is consistent with reaction via a *bis*-TMEDA-solvated enolate dimer as depicted generically in eq 3.

The experimentally elusive details of the dimer-based transition structure were examined using DFT computations, revealing a number of viable

candidates (Figure 4). The two most viable pathways are summarized in Scheme 1. Dimer-based transition structure **5a**, containing both η^1- and η^2-bound TMEDA ligands, was predicted to be the lowest energy form. We would be reckless, however, to distinguish them using calculated $\Delta G^{\ddagger}$'s alone. For example, we found doubly chelating structure **5b** is very plausible. Consequently, we investigated TMCDA as a strongly chelating surrogate for TMEDA. We know of no evidence, experimental or computational, that TMCDA can coordinate as a monodentate ligand. The basal assumption, therefore, is that the rates and mechanisms using TMCDA and TMEDA diverge only if TMEDA is functioning as a non-chelating ligand somewhere along the reaction coordinate. Experimentally indistinguishable rates and rate laws for the two diamines cast the deciding vote for **5b** as the most logical transition structure. We hasten to add, however, that despite the enormous computed barrier for triple ion **5h**—DFT is notoriously incapable of modeling ionization energies[38]—triple ion **5h** has considerable appeal. Triple ions, including those derived from lithium enolates,[32] are well precedented[31,32] The $(\eta^2$-TMEDA$)_2Li^+$ counterion is well precedented[37] and the $(\eta^2$-TMCDA$)_2Li^+$ cation has been documented as well.[43] The bidentate interaction of the ester enolate in **5h** also has structural precedent.[44]

Scheme 1

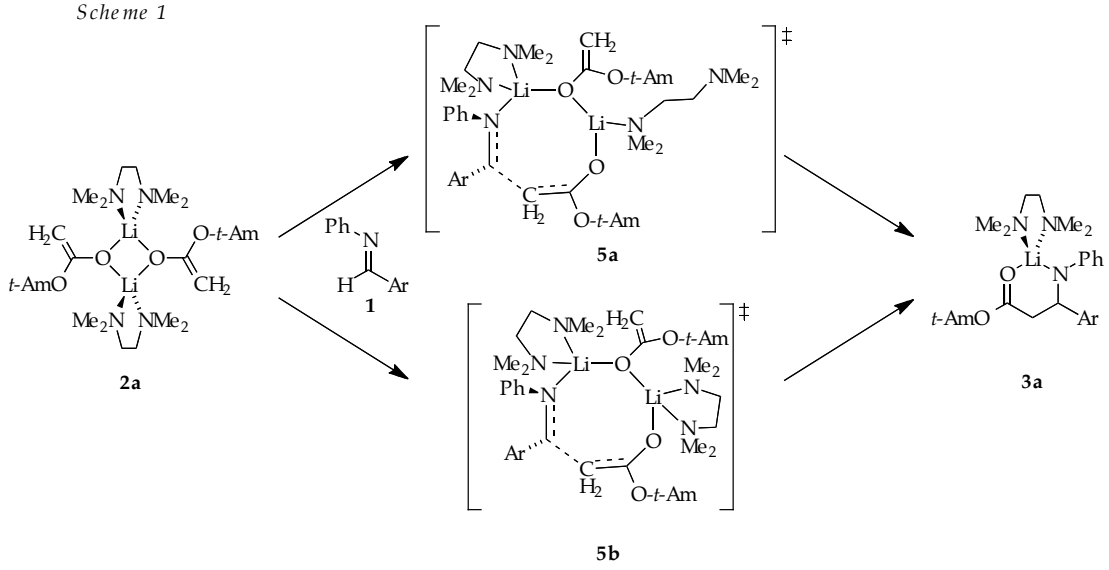

Conclusion.

The azaaldol addition of a disolvated dimeric lithium enolate to an aryl imine occurs through a transition structure consisting of a disolvated dimeric enolate. Although details of the transition structure are unclear, calculations slightly favor an open dimer (1.6 kcal/mol) with only one of the two TMEDA molecules chelating.

The dimer-based reaction is interesting in light of dominant beliefs in the earlier days of organolithium chemistry that monomers are the central fleeting intermediate. Streitwieser has wrestled with this question for a number of years and concludes that monomers are often key intermediates. Similarly, Reich has found that in non-equilibrating mixtures of monomers and dimers the monomers are almost always more reactive. That is not to say, however, that when dimers or tetramers are the observable form in solution the most favorable pathway necessarily proceeds via energetically costly deaggregations.[45]A number of

groups have endorsed the notion of aggregate-based enolate reactivity. Enolates are a very broad class of intermediate. Throw into the debate the huge roles of solvent, temperature, concentration, and choice of electrophile, and considerable mechanistic variation is to be expected.

Experimental.

Reagents and Solvents. TMEDA, TMCDA, and toluene were distilled from solutions containing sodium benzophenone ketyl. The toluene stills contained approximately 1% tetraglyme to dissolve the ketyl. LDA, [^{6}Li]LDA, and [^{6}Li,^{15}N]LDA were prepared as described previously.[23] Solutions of LDA were titrated for active base using a literature method.[46] Air- and moisture-sensitive materials were manipulated under argon using standard glovebox, vacuum line, and syringe techniques. Imine **1** was prepared using a literature procedure.[47]

NMR Techniques. All NMR samples were prepared using stock solutions and sealed under partial vacuum. Standard ^{6}Li, ^{13}C, ^{15}N, and ^{19}F NMR spectra were recorded on a 500 MHz spectrometer at 73.57, 125.79, 50.66, and 470.35 MHz (respectively). The ^{6}Li, ^{13}C, and ^{15}N resonances are referenced to 0.30 M [^{6}Li]LiCl/MeOH at –90 °C (0.0 ppm), the CH_2O resonance of THF at –90 °C (67.57 ppm), and neat Me_2NEt at –90 °C (25.7 ppm), respectively.

Kinetics. Samples for NMR kinetics were prepared from stock solutions at room temperature: (1) *tert*-amyl acetate in toluene, (2) imine **1** and fluorobenzene internal standard in toluene, and (3) LDA/TMEDA in toluene. The NMR tube was capped with a septum, evacuated, flushed several times with argon, flame dried, put under argon, cooled in dry ice/acetone bath, and charged sequentially

with the LDA/TMEDA and *tert*-amyl acetate stock solutions with agitation. The stock solutions were prepared to give final concentrations of 0.005 M each of **1** and fluorobenzene standard, 0.11 M LDA, and 0.10 M *tert*-amyl acetate upon completion of the imine injection. The tube was vortexed for approximately 10 s at room temperature and placed in a -78 °C bath. A length of 25 μm ID flexible capillary tubing was inserted directly into the solution of LDA at -78 °C at the curved portion of the tube. The NMR tube was then inserted into the pre-cooled NMR probe and equilibrated at -60 C, and 400 μL LDA stock and 100 μL ester stock were added sequentially via syringe through the septum.A collection array at 30 s intervals was initiated, and a 100 μL stock solution of imine was injected into the tube giving 10 s to thermally equilibrate before spectral acquisition. The loss of **1** (δ -107.4 ppm) and formation of **3** (δ -117.2 ppm) were monitored relative to a fluorobenzene internal standard (0.007 M, δ -112.96 ppm). The decay of **1** was followed to beyond five half-lives. In processing, the integral area was normalized relative to the fluorobenzene standard. The rate constant was obtained by fitting the decay for each run to the first-order function, $f(x) = ae^{bx}$.

Aminoester 4. Lithium diisopropylamide (218 mg, 2.04 mmol) was dissolved in toluene (16.0 mL) and TMEDA (2.0 mL, 13.3 mmol) in a 50 mL round-bottom flask and cooled to -60 °C. To this mixture was added *tert*-amyl acetate (330 μL, 2.22 mmol), with stirring for 5 min to ensure full enolization. Then imine **1** (307 mg, 1.53 mmol) dissolved in toluene (2.5 mL) was added. After 2 h, the reaction was quenched with methanol (4 mL), allowed to warm to room temperature, and acidified with saturated aq. NH_4Cl (4 mL). The organic layer was washed with water (8 mL), dried over Na_2SO_4, and via rotary evaporation.

The resulting yellowish oil was recrystallized from hot methanol (3.5 mL), yielding 399 mg of white needles (78% yield) with mp=89-90.5 °C. 2-Methyl-2-butyl 3-(4-fluorophenyl)-3- phenylamino-propanoate (**4**): analytical thin layer chromatography (TLC) on K6F silica gel 60 Å, 4:1 hexanes/EtOAc, Rf=0.39. IR (neat, cm^{-1}) 3380, 2975, 2922, 1703, 1603, 1507; ^{1}H NMR: δ 7.34 (1H, **A**A'BB'Y, $J_{A\text{-}A'}$=2.2 Hz, $J_{A\text{-}B}$=8.7 Hz, $J_{A\text{-}X}$=5.0 Hz), 7.34 (1H, A**A'**BB'Y, $J_{A\text{-}A'}$=2.2 Hz, $J_{A'\text{-}B'}$=8.7 Hz, $J_{A'\text{-}X}$=5.0 Hz), 7.09 (2H, dd, *J*=8.2, 7.3 Hz), 6.99 (1H, AA'**B**B'Y, $J_{B\text{-}B'}$=2.5 Hz, $J_{A\text{-}B}$=8.7 Hz, $J_{B\text{-}X}$=8.7 Hz), 6.99 (1H, AA'B**B'**Y, $J_{A'\text{-}B'}$=8.7 Hz, $J_{B'\text{-}B}$=2.5 Hz, $J_{B'\text{-}X}$=8.7 Hz), 6.67 (1H, t, 7.3 Hz), 6.52 (2H, d, 8.2 Hz), 4.75 (1H, AB**M**X, $J_{A\text{-}M}$=5.8 Hz, $J_{B\text{-}M}$=7.2 Hz, $J_{M\text{-}X}$=6.1 Hz), 4.61 (1H, ABM**X**, $J_{M\text{-}X}$=6.1 Hz), 2.71 (1H, **A**BMX, $J_{A\text{-}B}$=14.6 Hz, $J_{A\text{-}M}$=5.8 Hz), 2.69 (1H, A**B**MX, $J_{A\text{-}B}$=14.6 Hz, $J_{B\text{-}M}$=7.2 Hz), 1.70 (2H, q, *J*=7.5 Hz), 1.34 (6H, s), 0.78 (3H, t, *J*=7.5 Hz); ^{13}C NMR: δ 170.4, 162.2 (d, $J_{C\text{-}F}$=245 Hz), 146.9, 138.1 (d, $J_{C\text{-}F}$=3 Hz), 129.3, 128.1 (d, $J_{C\text{-}F}$=8 Hz), 117.9, 116.7 (d, $J_{C\text{-}F}$=21 Hz), 113.7, 84.1, 54.7, 44.2, 33.6, 25.6, 25.6, 8.3; ^{19}F NMR: δ - 115.6. Molecular ion calculated for C20H24FNO2: 329.1791; EIMS found m/z=329.1793. ^{1}H NMR ABMX and AA'BB'Y couplings were identified using spin simulation in MestReNova 7.1.1.

Aminoester [^{15}N]4. Prepared as above using **[^{15}N]S2**, made from commercially available ^{15}N-aniline. ^{1}H NMR**: δ 7.34 (2H, app dd), 7.10 (2H, dd, *J* = 8.3, 7.3 Hz), 6.99 (2H, app t), 6.67 (1H, t, *J* = 7.3 Hz), 6.52 (2H, d, *J* = 7.8 Hz), 4.75 (1H, app q), 4.61 (1H, app d), 2.75-2.65 (2H, app m), 1.70 (2H, q, *J* = 7.5 Hz), 1.34 (6H, s), 0.78 (3H, t, *J* = 7.5 Hz); ^{13}C NMR: δ 170.4, 162.2 (d, $J_{C\text{-}F}$ = 245 Hz), 146.9 (d, $J_{C\text{-}N}$ = 13 Hz), 138.1 (d, $J_{C\text{-}F}$ = 3 Hz), 129.4, 128.1 (dd, $J_{C\text{-}F}$ = 8, 1 Hz), 118.0, 115.7 (d, $J_{C\text{-}F}$ = 21 Hz), 113.7 (d, $J_{C\text{-}N}$ = 2 Hz), 84.1, 54.7 (d, $J_{C\text{-}N}$ = 10 Hz), 44.2, 33.6, 25.6, 25.6, 8.3; ^{19}F NMR: δ -115.6; ^{15}N NMR: δ 73.2. Molecular ion calculated for

$C_{20}H_{24}F^{15}NO_2$: 330.1761; EIMS found m/z = 330.1759.

Azaaldol adduct [^{6}Li,^{15}N]3. Individual stock solutions of substrate **[^{15}N]S2** (0.22 M in toluene) and [^{6}Li]LiHMDS (0.20 M in TMEDA/toluene) were prepared at room temperature. An NMR tube was flame-dried under vacuum and allowed to come to room temperature. It was then backfilled with argon and placed in a -78 °C dry ice/ acetone bath. Base (300 μL of stock solution) and substrate (300 μL of stock solution) were added sequentially via syringe. The tube was sealed under partial vacuum, vortexed for approximately 10 s at room temperature, and cooled to -78 °C. ^{6}Li NMR spectra were recorded at -60 °C on a 500 MHz spectrometer with and without broadband ^{15}N decoupling. Chemical shifts are reported relative to a 0.30 M ^{6}LiCl/MeOH standard at the reported probe temperature. ^{15}N NMR spectra were recorded using the INEPT pulse sequence at -60 °C on a 500 MHz spectrometer with and without broadband ^{6}Li decoupling. ^{6}Li NMR: δ 1.54 ($J_{Li\text{-}N}$ = 6.6 Hz); ^{19}F NMR: δ -117.1; ^{15}N NMR: δ 123.9 (t, $J_{Li\text{-}N}$ = 6.6 Hz).

APPENDIX II:

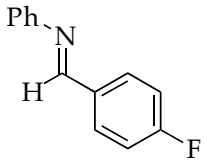

1

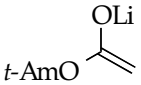

2

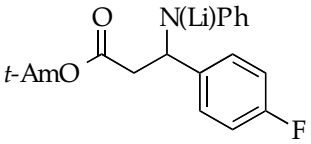

3

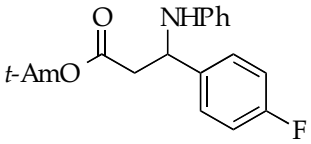

4

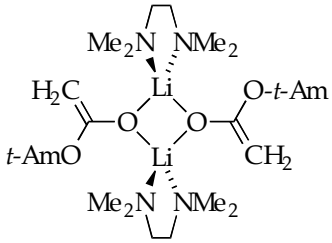

2a

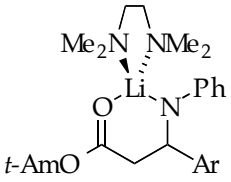

3a

AII.a NMR Spectroscopic Studies

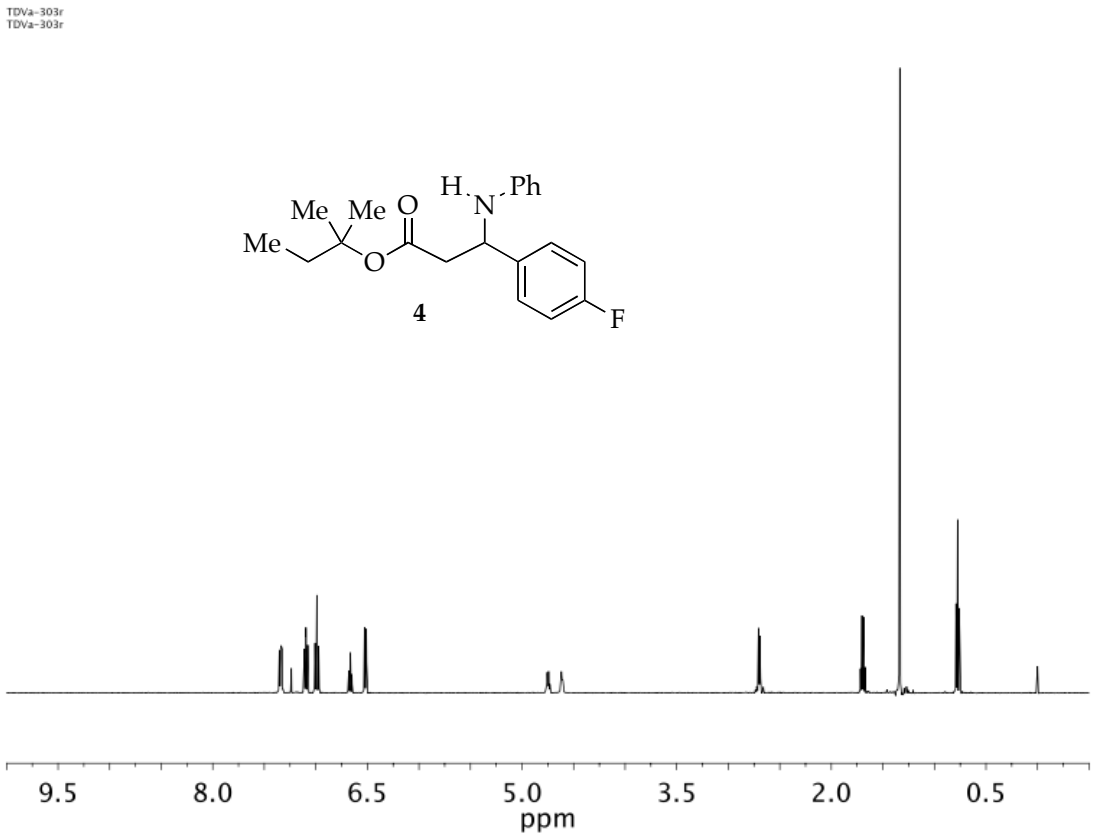

Figure A2.1. ^{1}H NMR spectrum of **4** in $CDCl_3$.

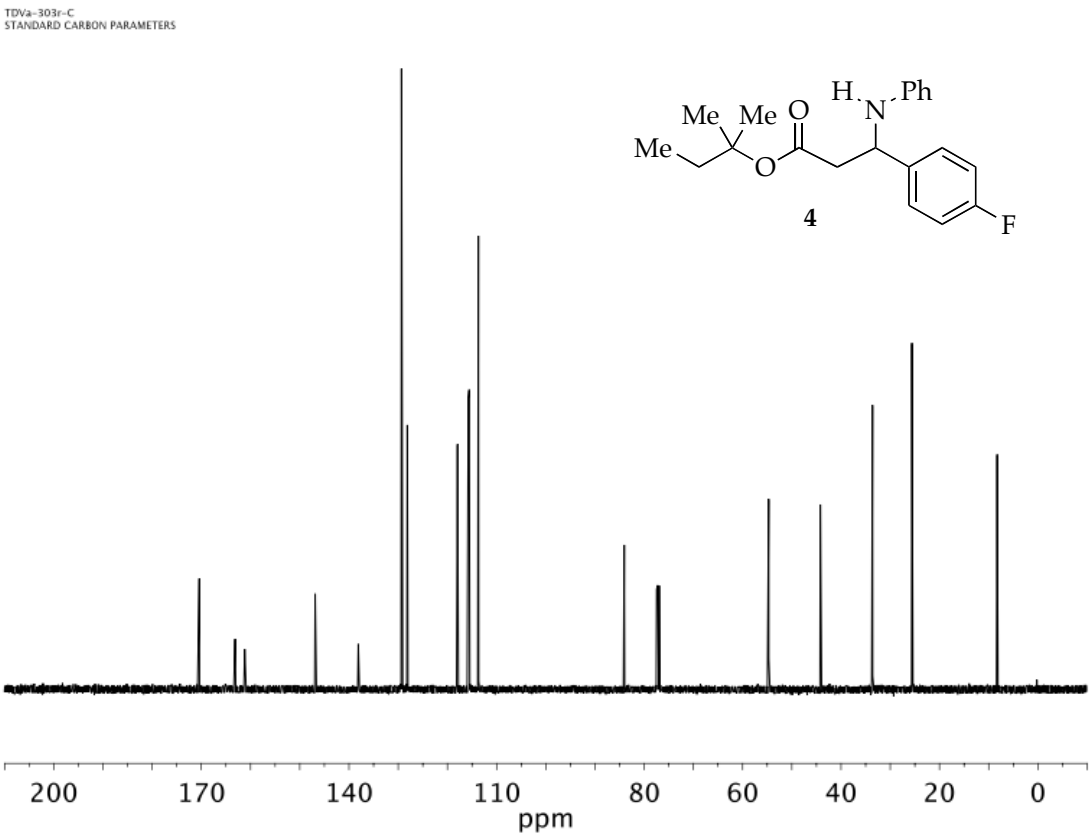

Figure A2.2. ^{13}C NMR spectrum of **4** in $CDCl_3$.

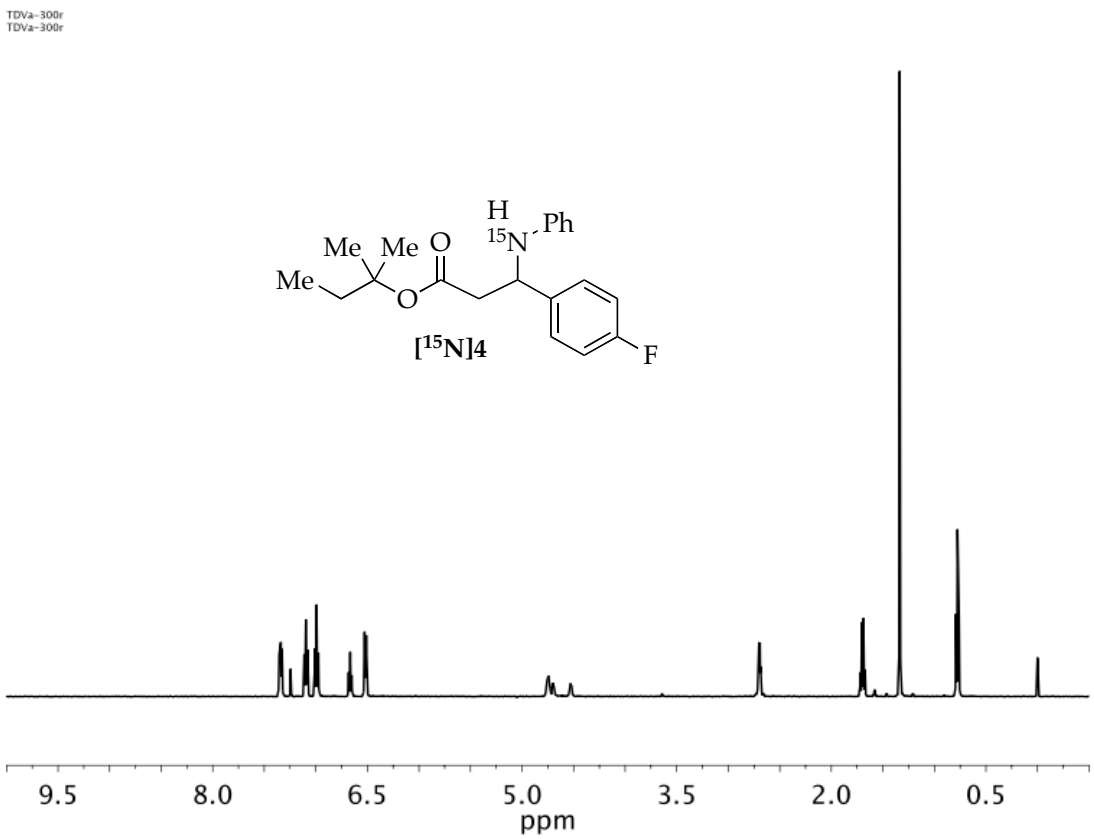

Figure A2.3. ^{1}H NMR spectrum of [^{15}N]**4** in $CDCl_3$.

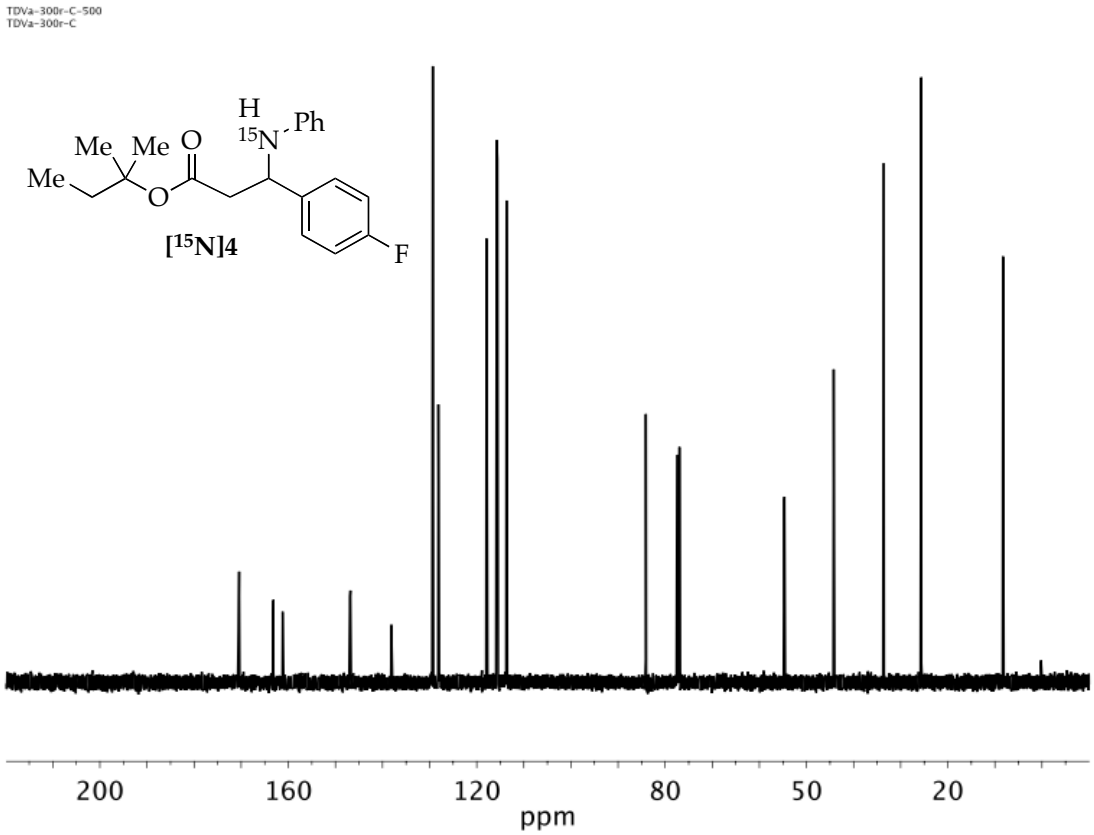

Figure A2.4. ^{13}C NMR spectrum of [^{15}N]**4** in $CDCl_3$.

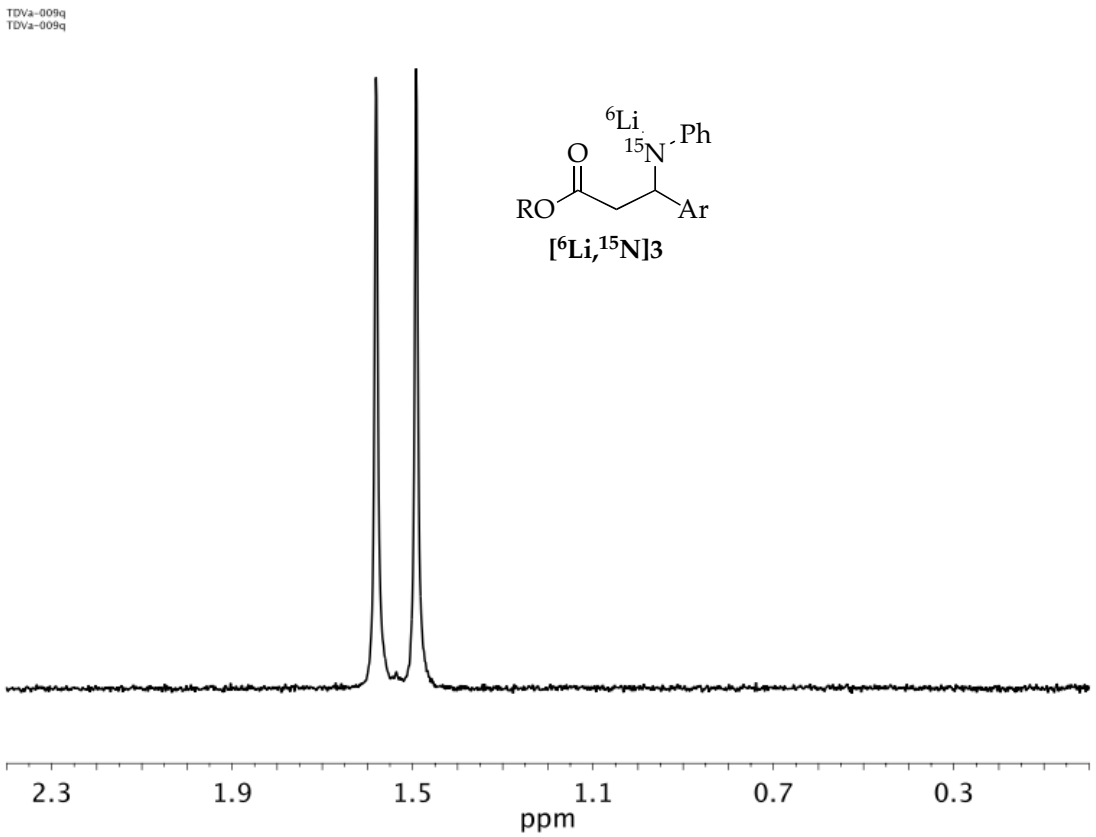

Figure A2.5. ^{6}Li NMR spectrum of a 0.10 M solution of [^{6}Li,^{15}N]**3** in 0.60 M TMEDA/toluene at -60 °C.

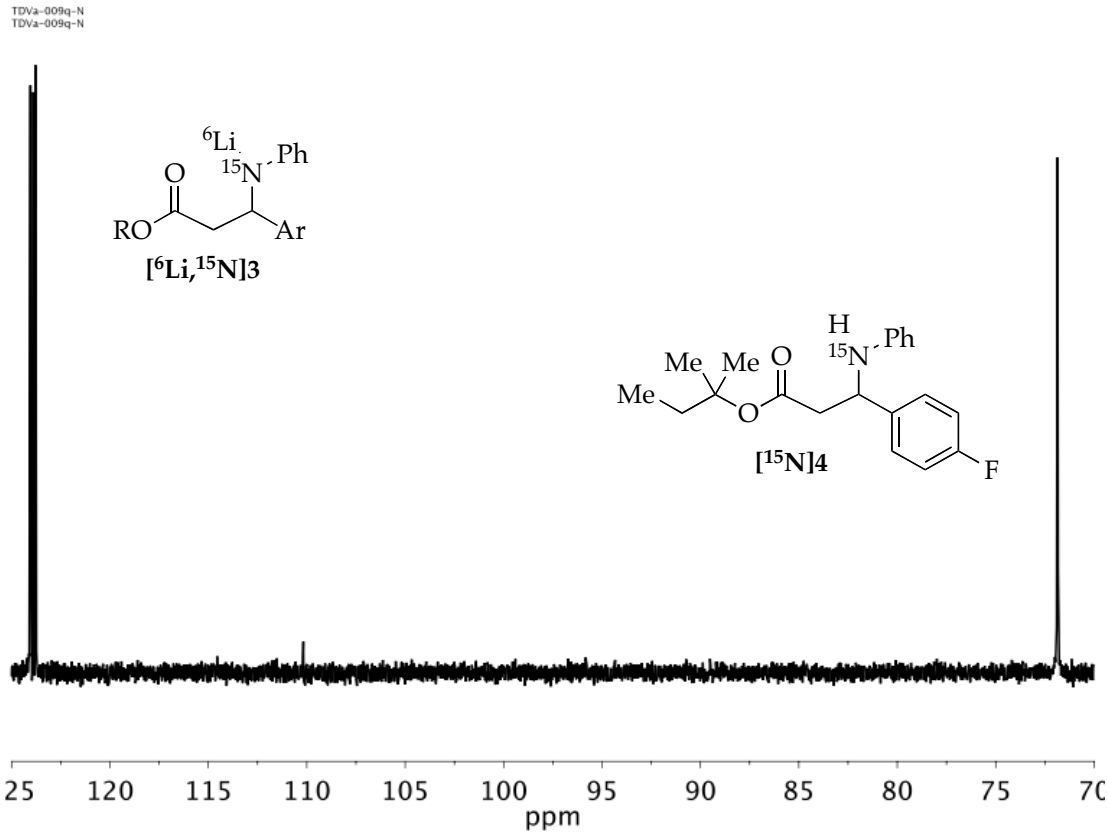

Figure A2.6. ^{15}N NMR spectrum of a 0.10 M solution of [^{6}Li,^{15}N]**3** in 0.60 M TMEDA/toluene at -60 °C generated from adduct [^{15}N]**4** and LiHMDS.

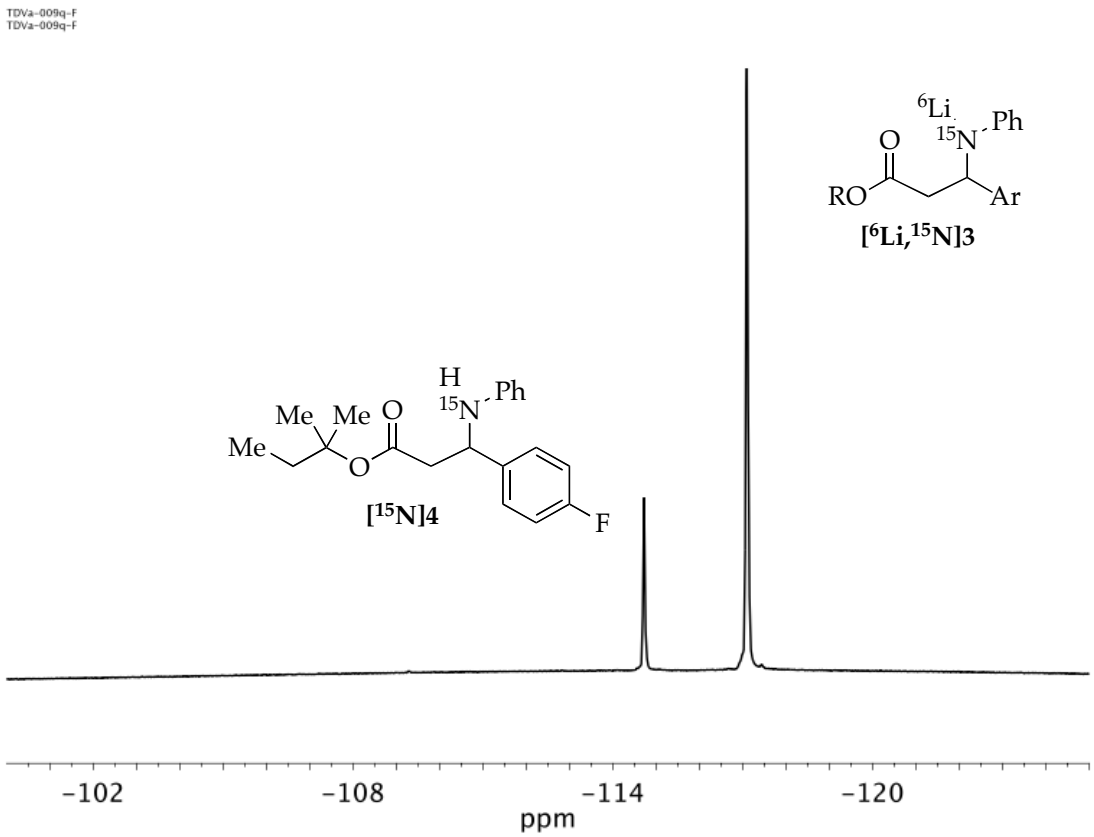

Figure A2.7. ^{19}F NMR spectrum of a 0.10 M solution of [^{6}Li,^{15}N]**3** in 0.60 M TMEDA/toluene at -60 °C generated from adduct [^{15}N]**4** and LiHMDS.

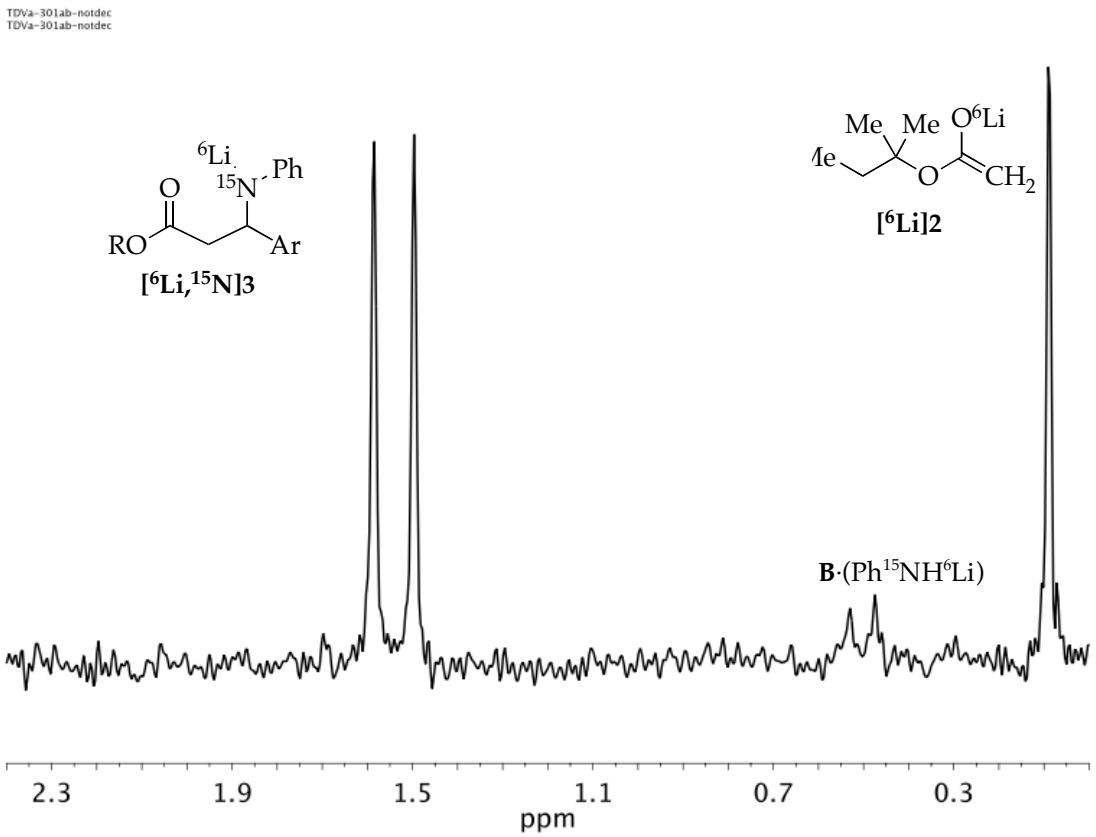

Figure A2.8. ^{6}Li NMR spectrum of a solution of 0.050 M [^{6}Li,^{15}N]**3** and 0.050 M enolate [^{6}Li]**2** prepared using [^{6}Li]LDA in 0.60 M TMEDA/toluene at -60 °C.

AII.b NMR and IR Kinetic Studies

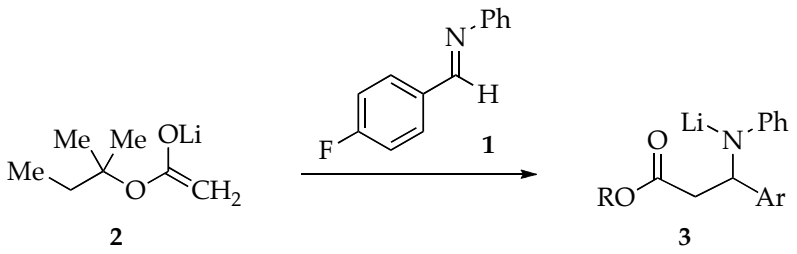

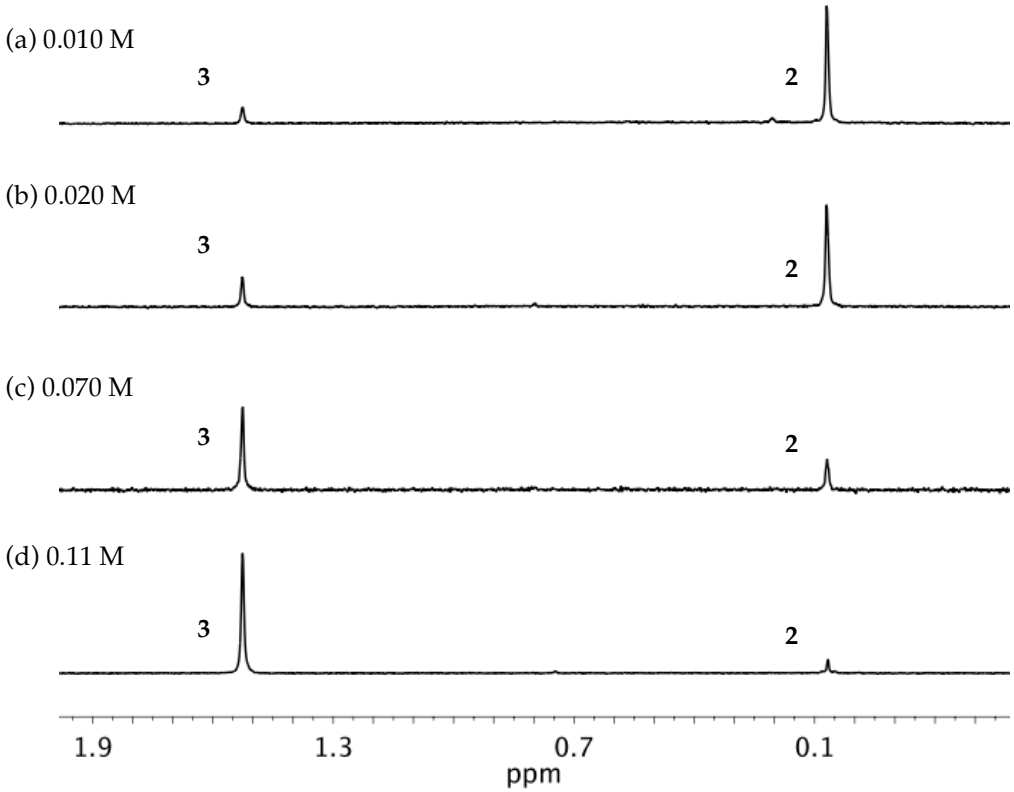

Figure A2.9. Representative ^{6}Li NMR spectroscopic analysis of the condensation of the lithium enolate of *tert*-amyl acetate (**2**, 0.10 M) with the following concentrations of *N*-(4-fluorobenzylidene)-aniline (**1**): (a) 0.010 M, (b) 0.020 M, (c) 0.070 M, (d) 0.11 M) in 0.55 M TMEDA / toluene at -60 °C.

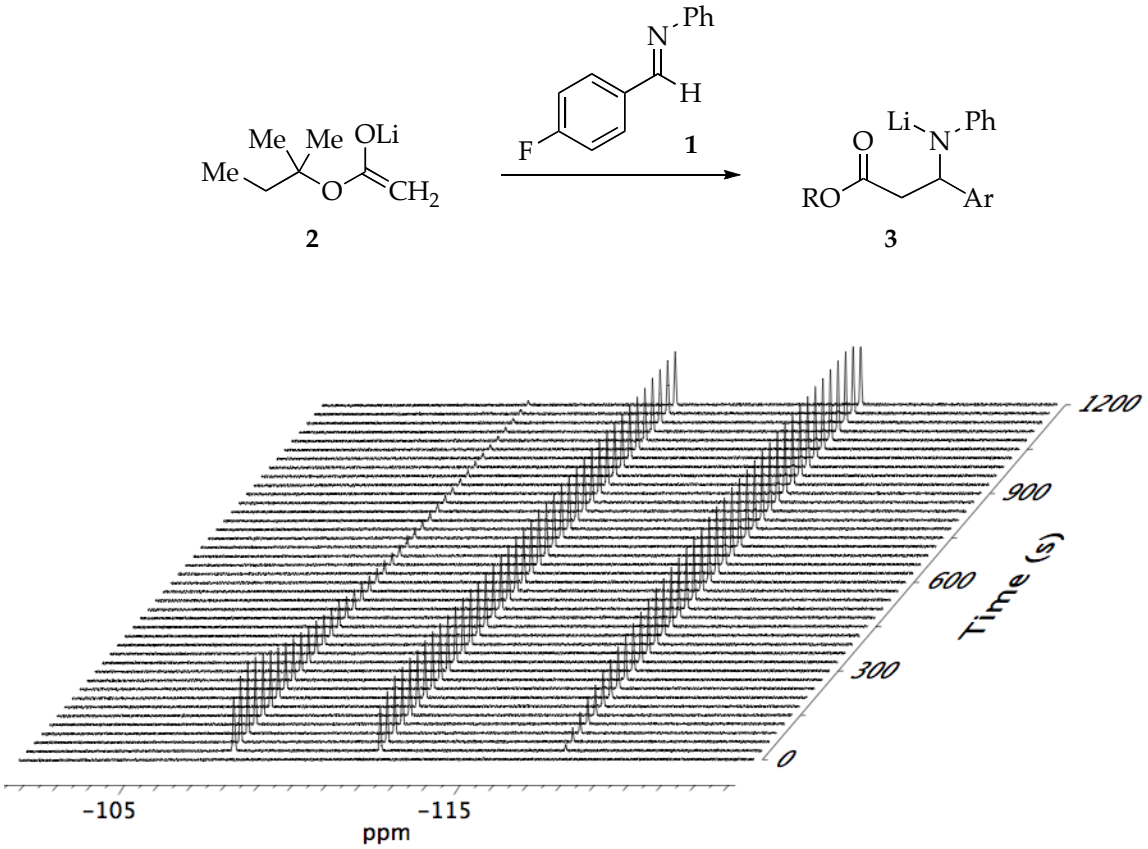

Figure A2.10. Representative ^{19}F NMR spectroscopic analysis of the condensation of the lithium enolate of *tert*-amyl acetate (**2**, 0.10 M) with *N*-(4-fluorobenzylidene)-aniline (**1**, 0.005 M) in 0.55 M TMEDA / toluene at -60 °C. The resonances correspond to **1** (δ -107.4 ppm), **2** (δ -117.2 ppm) and internal standard (fluorobenzene, 0.007 M, δ -112.96 ppm).

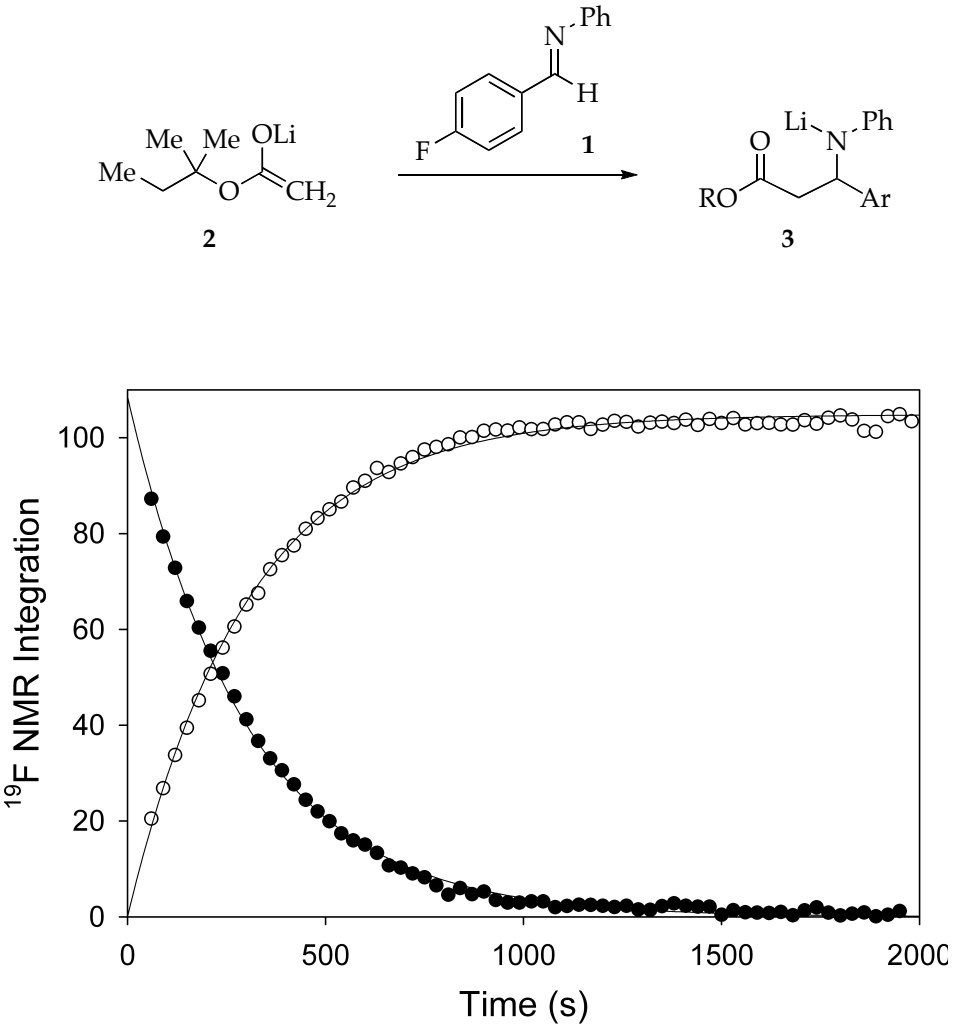

Figure A2.11. Representative curve fitting for the condensation of the lithium enolate of *tert*-amyl acetate (**2**, 0.10 M) with *N*-(4-fluorobenzylidene)aniline (**1**, 0.005 M) in 0.55 M TMEDA / toluene at -60 °C. Imine **1** is represented by the symbol • and product **3** by o. The curves depict unweighted least-squares fits to $y_1 = y_0 \cdot e^{-b \cdot t}$ ($y_0 = 108.6 \pm 0.1$, $b = 3.32 \pm 0.03 \times 10^{-3}$ s^{-1}) and $y_{s3} = y_0 \cdot (1 - e^{-b \cdot t})$ ($y_0 = 104.9 \pm 0.1$, $b = 3.28 \pm 0.03 \times 10^{-3}$ s^{-1}).

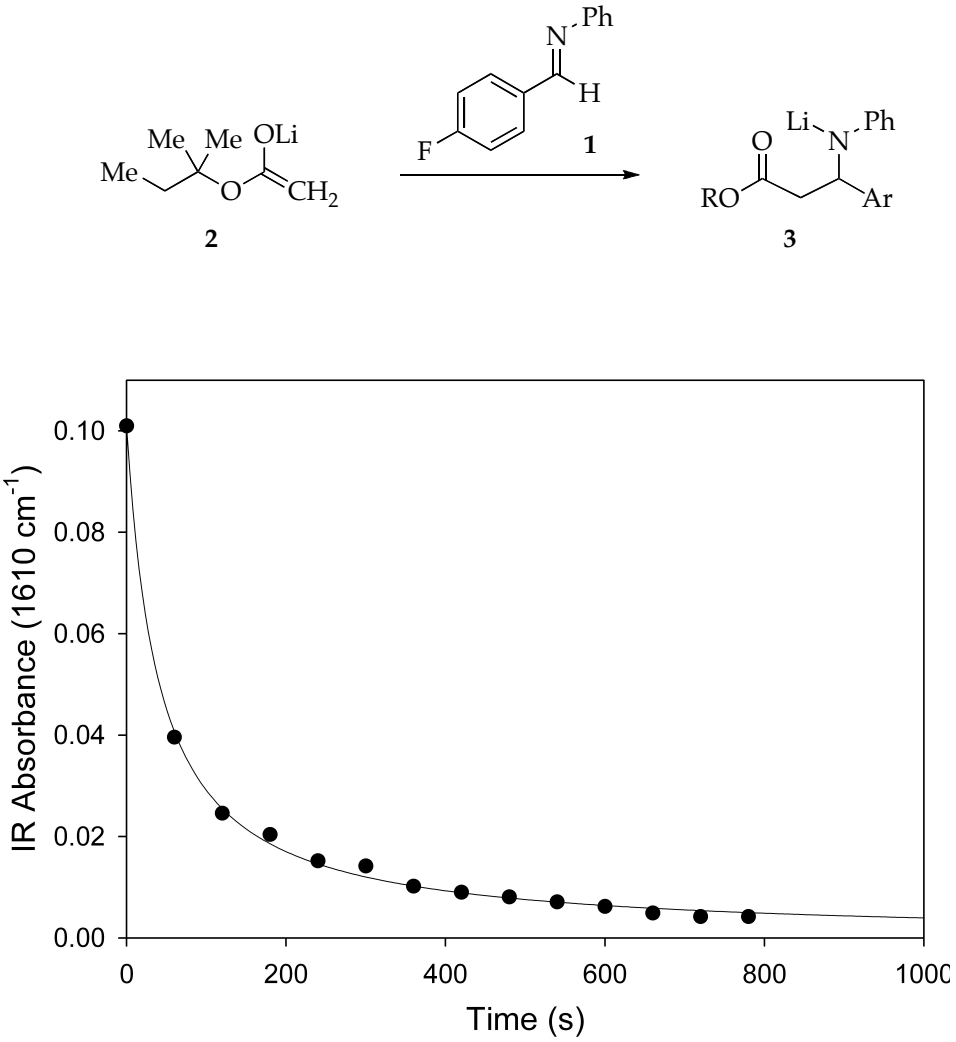

Figure A2.12. Condensation of the lithium enolate of *tert*-amyl acetate (**2**, 0.10 M) with stoichiometric *N*-(4-fluorobenzylidene)aniline (**1**, 0.10 M) in 0.65 M TMEDA / toluene at -60 ºC. The curve depicts and unweighted least-squares fit to $y = [A]_0 / (1+[A]_0 \cdot k \cdot t)$ ($[A]_0 = 0.101 \pm 0.001$ M, $k = 0.24 \pm 0.01$ M^{-1} s^{-1}).

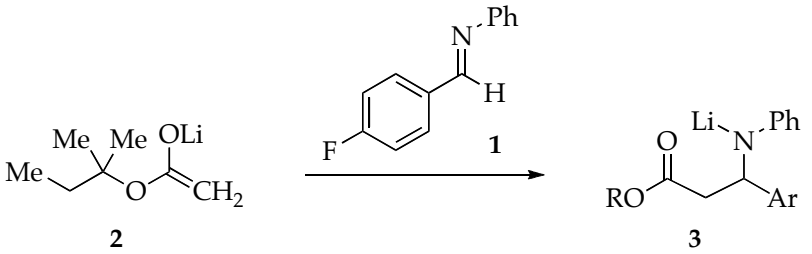

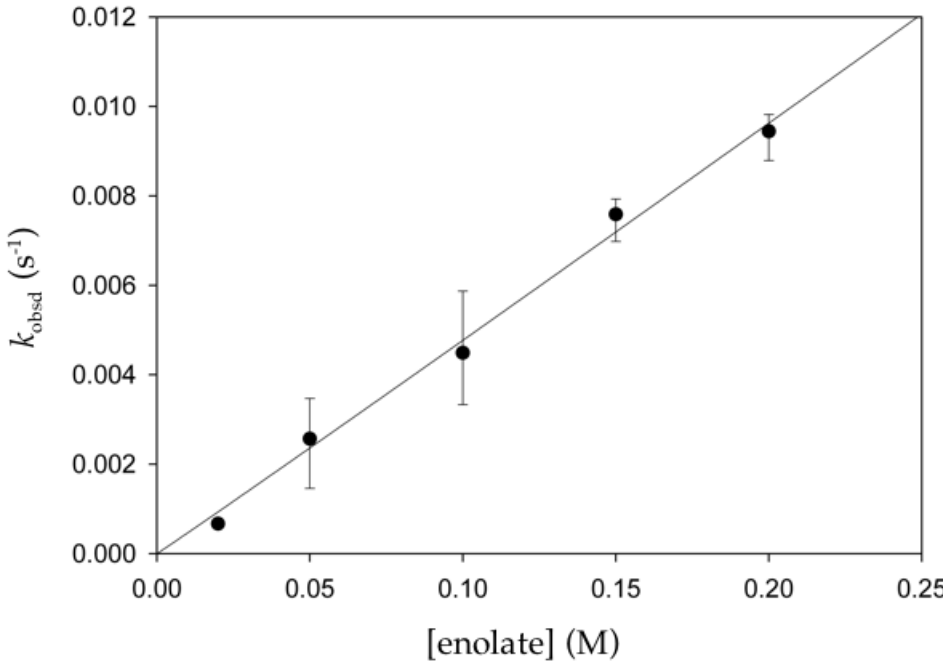

Figure A2.13. Plot of k_{obsd} versus [2] for the condensation of enolate **2** with *N*-(4-fluorobenzylidene)aniline (**1**, 0.005 M) in 0.60 M TMEDA / toluene at -60 °C**. The curve depicts the result of an unweighted least-squares fit to $k_{obsd} = k\cdot[2]^b$ (k = 0.049 ± 0.007, b = 1.01 ± 0.08).**

[**2**] (N)	k_{obsd} 1 x 10^3 (s^{-1})	k_{obsd} 2 x 10^3 (s^{-1})	k_{obsd} avg x 10^3 (s^{-1})
0.020[a]	0.69 ± 0.01	0.65 ± 0.05	0.67
0.050[a]	3.40 ± 0.07	1.7 ± 0.3	2.6
0.10	3.36 ± 0.03	5.6 ± 0.2	4.5
0.15	7.87 ± 0.06	7.3 ± 0.3	7.6
0.20	9.7 ± 0.1	9.2 ± 0.4	9.4

[a] $[\mathbf{1}]_{init}$ = 0.001 M.

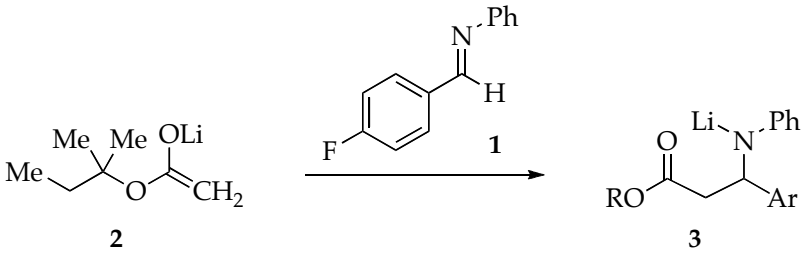

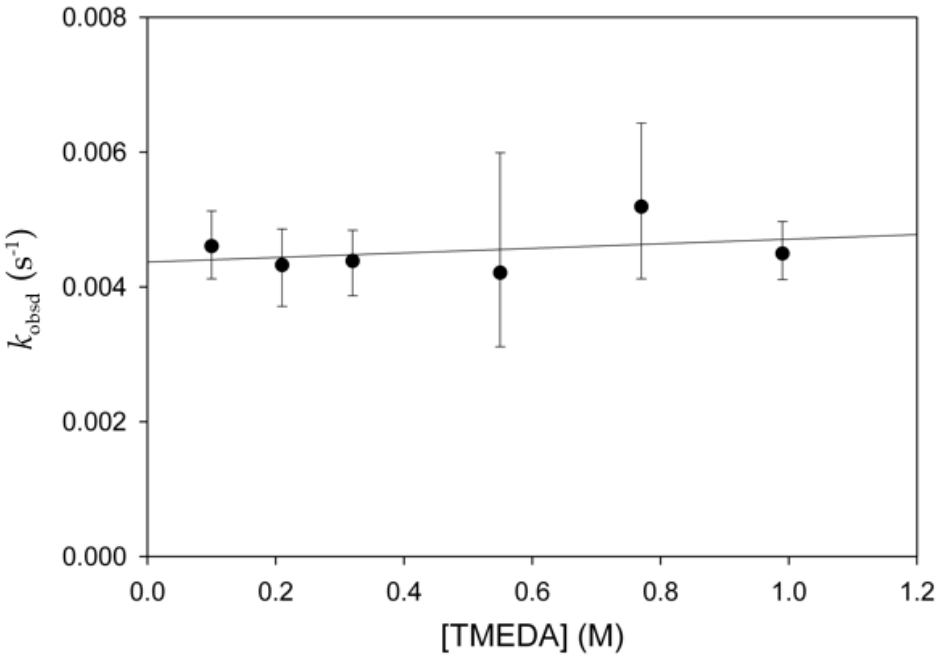

Figure A2.14. Plot of k_{obsd} versus excess [TMEDA] in toluene cosolvent for the condensation of the lithium enolate of *tert*-amyl acetate (**2**, 0.10 M) with *N*-(4-fluorobenzylidene)aniline (**1**, 0.005 M) at -60 °C**. The curve depicts the result of an unweighted least-squares fit to $k_{obsd} = k + k' \cdot [TMEDA]_{free}$ (k = 0.0044 ± 0.3, k' = 0.3 ± 0.5).**

$[TMEDA]_{free}$ (M)	k_{obsd} 1 x 10^3 (s^{-1})	k_{obsd} 2 x 10^3 (s^{-1})	k_{obsd} avg x 10^3 (s^{-1})
0.10	4.18 ± 0.06	5.0 ± 0.1	4.6
0.21	4.80 ± 0.06	3.9 ± 0.1	4.3
0.32	4.80 ± 0.04	4.0 ± 0.1	4.4
0.55	3.36 ± 0.03	3.2 ± 0.1	
0.55	5.7 ± 0.3	4.6 ± 0.1	4.2
0.77	4.2 ± 0.1	6.2 ± 0.3	5.2
0.99	4.16 ± 0.05	4.8 ± 0.1	4.5

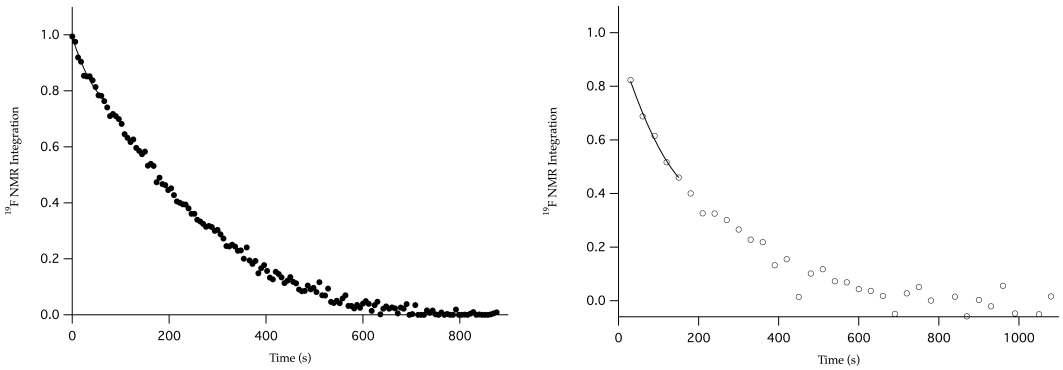

Figure A2.15. Initial rate curve fitting for the condensation of the lithium enolate of *tert*-amyl acetate (**2**, 0.10 M) with *N*-(4-fluorobenzylidene)aniline (**1**, 0.005 M) in 0.70 M TMCDA / toluene at -60 °C (left) and in 0.70 M TMEDA / toluene at -60 °C (right). The curves depict unweighted least-squares fits to $y_1 = y_0 + bx + cx^2$; $y_0 = 0.95543 \pm 0.0299$ M, $b = -0.0048636 \pm 0.00076$ M^{-1} s^{-1}, $c = 1.0381e^{-5} \pm 4.14e^{-6}$ (left); $y_0 = 0.99133 \pm 0.0106$ M, $b = -0.0053595 \pm 0.000743$ M^{-1} s^{-1}, $c = 3.0665e^{-5} \pm 1.09e^{-5}$ (right) where $b = k_{obsd}$. $(k_{TMCDA} / k_{TMEDA}) = (-0.0048636 / -0.0053595) = 0.91$.

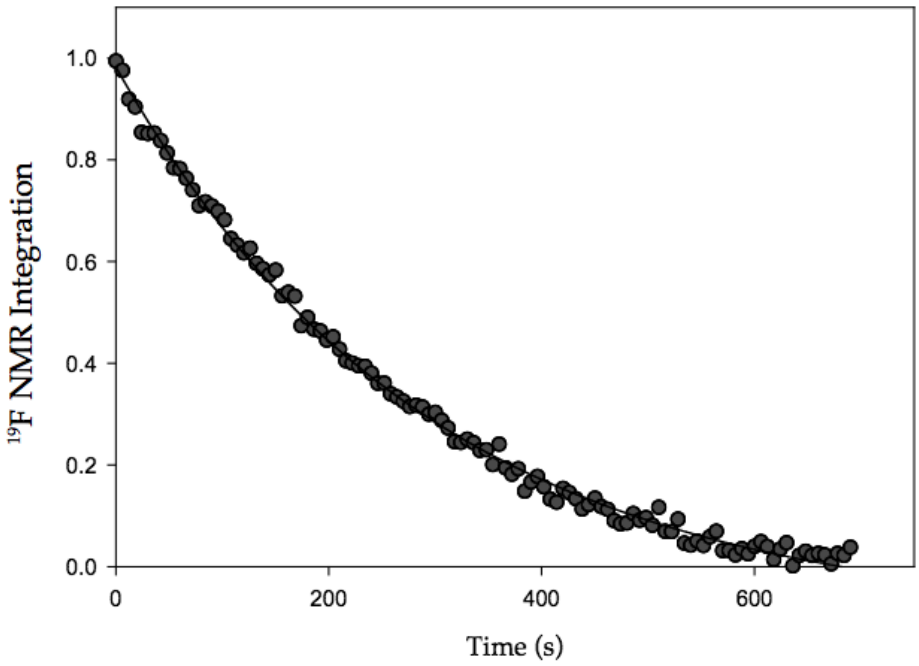

Figure A2.16. Representative curve fitting for the condensation of the lithium enolate of *tert*-amyl acetate (**2**, 0.10 M) with *N*-(4-fluorobenzylidene)aniline (**1**, 0.005 M) with 7 equiv TMCDA at -60 °C. Imine **1** is represented by the symbol •. The curve depicts unweighted least-squares fits to $y_1 = y_0 \cdot (1+e^{-b \cdot t})$; $y_0 = 1.0$ M, $b = 3.4 \times 10^{-3}$ s^{-1}.

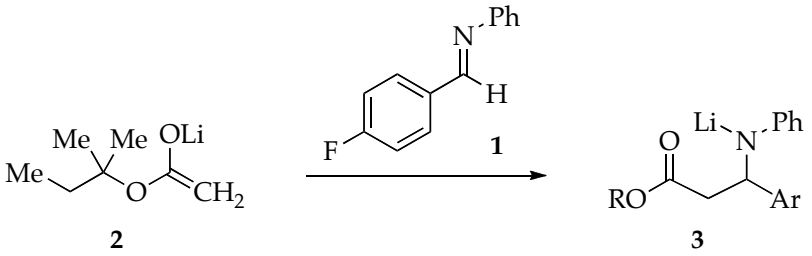

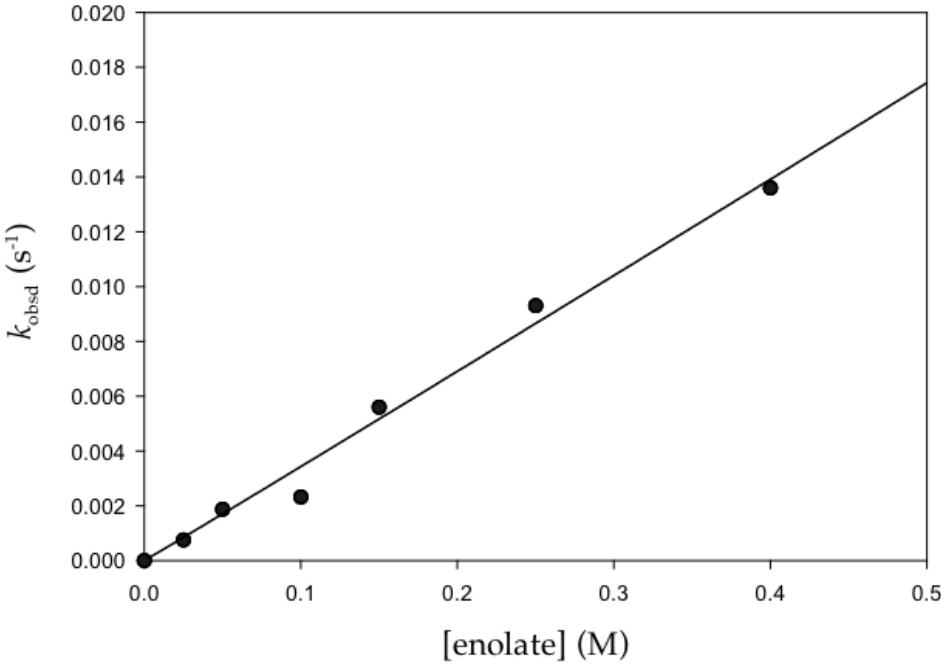

Figure A2.17. Plot of k_{obsd} versus [2] for the condensation of enolate **2** with *N*-(4-fluorobenzylidene)aniline (**1**, 0.005 M) in 7 equiv TMCDA/toluene at -60 °C**. The curve depicts the result of an unweighted least-squares fit to $k_{obsd} = k\cdot[2]^b$; b = 1.01.**

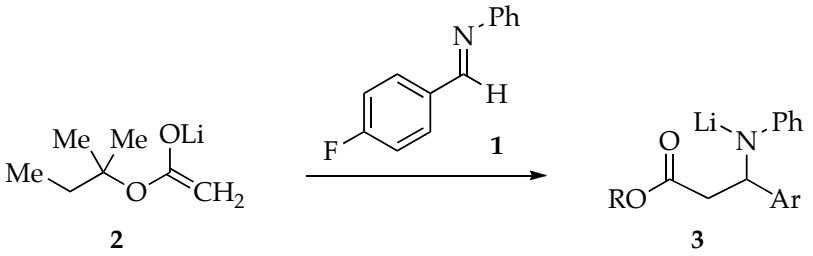

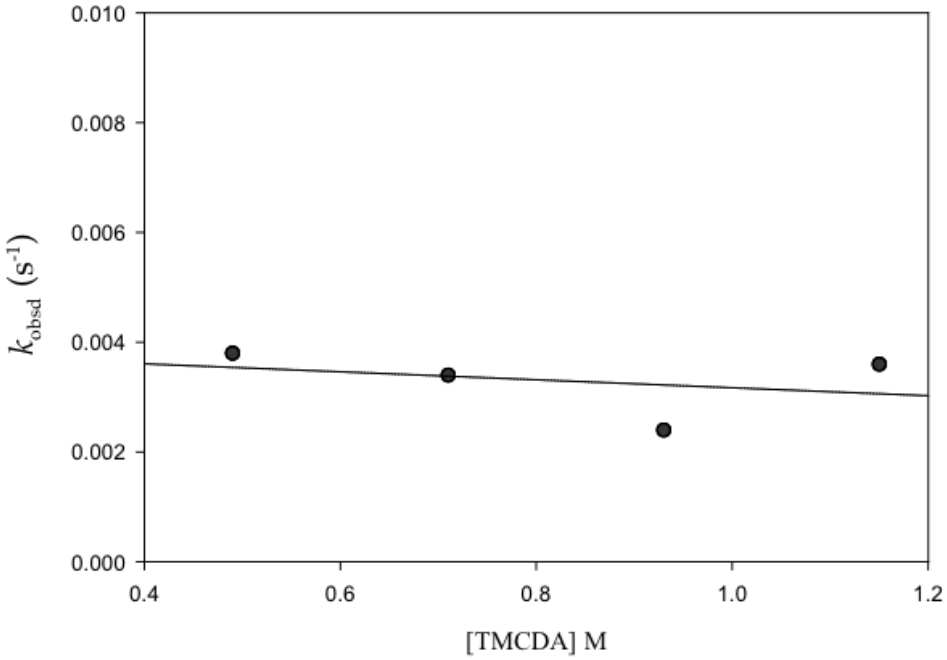

Figure A2.18. Plot of k_{obsd} versus [TMCDA] in toluene cosolvent for the condensation of the lithium enolate of *tert*-amyl acetate (**2**, 0.10 M) with *N*-(4-fluorobenzylidene)aniline (**1**, 0.005 M) at -60 ºC **showing a zero-order dependency on [TMCDA].**

AII.c DFT Computations

Table A2.1: DFT Optimized geometry, coordinates, and MP2 corrected energy for imine **1**.

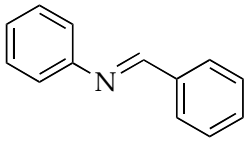

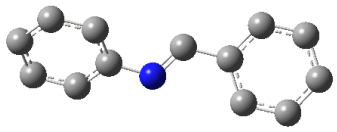

1
G = -554.7569897
(-60 °C)

Atom	X	Y	Z	Atom	X	Y	Z
C	0.401497	0.403579	-0.169238	H	0.095103	1.404539	-0.510148
N	-0.456713	-0.503666	0.115513	C	1.849830	0.181027	-0.082378
C	-1.832073	-0.214580	0.068027	C	2.728064	1.219922	-0.426913
C	-2.695626	-1.228360	-0.379684	C	4.108208	1.036109	-0.352880
C	-4.068399	-1.007563	-0.447704	C	4.624318	-0.191253	0.065761
C	-4.607288	0.215864	-0.039052	C	3.755773	-1.233762	0.410433
C	-3.759028	1.216412	0.439297	C	2.379297	-1.051601	0.338961
C	-2.381414	1.008509	0.492809	H	1.690868	-1.848009	0.602599
H	-1.729703	1.777881	0.897430	H	4.158372	-2.189196	0.736249
H	-4.171807	2.162086	0.781442	H	5.699605	-0.337749	0.123990
H	-5.680399	0.381405	-0.077523	H	4.778854	1.847696	-0.621603
H	-4.722393	-1.796406	-0.810126	H	2.322945	2.175220	-0.753984
H	-2.263401	-2.177633	-0.681557				

Table A2.2: DFT Optimized geometry, coordinates, and MP2 corrected energy for ground state dimer of lithium enolate **2**.

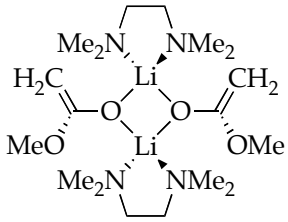

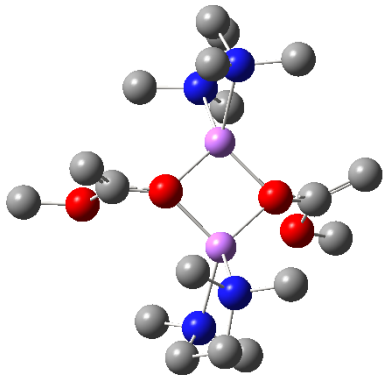

2
G = -1241.537100
(-60 °C)

Atom	X	Y	Z	Atom	X	Y	Z
C	0.225739	4.291968	-1.490664	C	-2.803888	-0.975202	-2.102770
O	0.300275	2.958600	-1.019421	H	-2.935270	-1.883451	-1.508943
C	-0.253160	2.672353	0.233120	H	-3.594874	-0.941031	-2.874115
O	-0.084969	1.422097	0.541140	H	-1.826932	-1.046359	-2.586590
Li	-1.271903	-0.019384	0.238451	H	-4.964850	0.072159	-1.053090
O	0.080946	-1.306950	-0.003128	H	-4.171872	1.310862	-0.077833
Li	1.273392	0.155506	0.246022	H	-3.967060	-1.710500	0.388391
C	0.081443	-2.520899	-0.460156	H	-5.003784	-0.606666	1.295094
C	-0.112700	-3.664480	0.250352	C	-2.634305	-1.612418	2.486104
H	-0.097876	-4.652508	-0.188230	H	-2.405893	-2.475151	1.854466
H	-0.263244	-3.590755	1.319959	H	-1.761820	-1.413895	3.116001
O	0.319164	-2.537706	-1.838521	H	-3.487842	-1.858940	3.143537
C	0.348592	-3.791793	-2.496844	C	-3.093929	0.752815	2.478818
H	0.546206	-3.582851	-3.551681	H	-2.210791	0.900186	3.106218
H	1.142203	-4.438973	-2.099610	H	-3.201244	1.645191	1.857953
H	-0.610735	-4.318476	-2.404364	H	-3.981549	0.659627	3.131316
C	-0.884740	3.619711	0.976143	N	2.688312	-0.314029	1.874981
H	-0.986110	4.651533	0.670029	C	4.017509	-0.159257	1.260684
H	-1.252096	3.346044	1.957159	C	3.999510	-0.475274	-0.239298
H	0.726099	4.990757	-0.806786	N	3.045137	0.368386	-0.976714
H	0.731198	4.308099	-2.460225	C	2.779199	-0.179056	-2.313972
H	-0.815309	4.617744	-1.621268	H	2.073135	0.477627	-2.830637

N	-2.898243	-0.439517	1.645067	H	3.230584	0.309061	3.858613
C	-4.043752	-0.680289	0.750937	C	2.416070	-1.711402	2.233991
C	-4.069331	0.282872	-0.439631	H	1.394022	-1.794276	2.610215
N	-2.835187	0.212269	-1.238721	H	2.481828	-2.357309	1.356035
C	-2.648206	1.428353	-2.039790	H	3.116730	-2.079319	3.006079
H	-1.689354	1.372532	-2.561482	H	3.698405	-0.251480	-2.923779
H	-3.452410	1.563748	-2.785773	H	2.315387	-1.164446	-2.227009
H	-2.620498	2.299706	-1.379498	C	3.500507	1.759497	-1.088896
H	4.343193	0.874123	1.413850	H	3.682485	2.187549	-0.099953
H	4.770657	-0.798792	1.754903	H	4.429567	1.842681	-1.682249
C	2.523065	0.553378	3.045329	H	2.711644	2.350971	-1.557294
H	2.665227	1.598876	2.756369	H	5.025323	-0.375653	-0.642033
H	1.504216	0.448361	3.429122	H	3.699640	-1.518317	-0.389889

Table A2.3: DFT Optimized geometry, coordinates, and MP2 corrected energy for TMEDA dichleated open dimer transition structure **5a**.

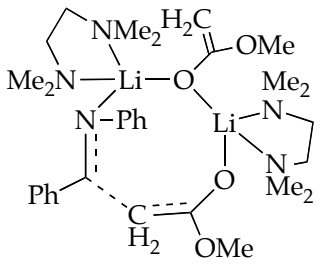

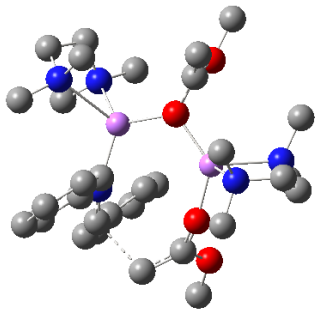

5a
G = -1796.284042
(-60 °C)

Atom	X	Y	Z	Atom	X	Y	Z
C	-0.820237	4.901310	0.962154	H	2.305937	1.966373	2.228094
O	-1.353819	3.618846	0.649713	N	2.484331	-0.718293	-2.319942
C	-0.984327	2.517143	1.391500	C	2.725818	-2.146459	-2.598819
O	-1.560698	1.460861	1.051331	C	3.369795	-2.901360	-1.438294
Li	-2.007465	-0.054322	0.042895	N	2.559965	-2.886434	-0.210122
O	-0.711084	-1.146583	-0.911199	C	3.421164	-3.031398	0.969977
Li	1.158889	-0.818042	-0.517848	H	2.809376	-3.026103	1.873680
N	1.449803	0.374706	1.158906	H	4.004773	-3.970600	0.945297
C	1.471696	-0.445685	2.302725	H	4.117938	-2.189820	1.027477
C	0.514606	-1.478423	2.405686	C	1.563318	-3.964606	-0.226039
C	0.495612	-2.341912	3.500533	H	2.040583	-4.961947	-0.275442
C	1.430200	-2.207860	4.531265	H	0.964330	-3.911815	0.686754
C	2.388912	-1.195999	4.441671	H	0.881897	-3.855044	-1.072881
C	2.413509	-0.330401	3.348984	H	3.578484	-3.936163	-1.766523
H	3.192671	0.424636	3.292362	H	4.342707	-2.455442	-1.212045
H	3.134541	-1.084390	5.225878	H	1.758761	-2.596612	-2.850808
H	1.414214	-2.880405	5.384472	H	3.376806	-2.263057	-3.487239
H	-0.258349	-3.125011	3.550970	C	3.730575	0.002831	-2.021458
H	-0.214240	-1.583672	1.607282	H	3.508960	1.066870	-1.919080
C	1.726883	1.666423	1.351893	H	4.484757	-0.126463	-2.819530
C	1.940680	2.572377	0.191504	H	4.157433	-0.337255	-1.075283
C	1.163125	2.495274	-0.975124	C	1.836189	-0.111681	-3.493747

C	1.376939	3.385303	-2.028256	H	1.674347	0.951579	-3.306141
C	2.379821	4.355619	-1.946618	H	2.459723	-0.213931	-4.401041
C	3.163455	4.436899	-0.793809	H	0.866756	-0.585096	-3.658948
C	2.939344	3.556653	0.265710	C	-1.203466	-1.972176	-1.792448
H	3.547569	3.629003	1.165166	C	-1.681013	-3.225935	-1.567065
H	3.948136	5.185532	-0.717869	H	-2.085326	-3.861356	-2.342714
H	2.544228	5.044597	-2.770958	H	-1.638818	-3.624241	-0.562040
H	0.750084	3.326394	-2.914710	O	-1.198782	-1.412085	-3.072621
H	0.370899	1.756189	-1.036644	C	-1.653634	-2.206916	-4.155616
H	-1.524167	-1.602157	-5.056946	H	-5.770270	0.923512	-0.346627
H	-1.070114	-3.132260	-4.249445	H	-4.448823	1.472750	0.697402
H	-2.713739	-2.470697	-4.045831	C	-3.537597	1.994158	-1.587020
N	-3.786106	0.635394	-1.085164	H	-2.809108	1.945009	-2.402489
C	-4.757154	0.669844	0.020821	H	-4.459244	2.466355	-1.974811
C	-4.831182	-0.651328	0.789449	H	-3.115995	2.610069	-0.790765
N	-3.563040	-1.000214	1.456218	C	-4.235667	-0.222283	-2.187325
C	-3.431857	-0.301330	2.743111	H	-5.207232	0.108971	-2.599146
H	-2.463425	-0.542557	3.188654	H	-3.484735	-0.194203	-2.979394
H	-4.233716	-0.594520	3.445781	H	-4.324717	-1.260669	-1.859896
H	-3.459796	0.778312	2.591868	C	0.044976	2.593120	2.354382
C	-3.475694	-2.448603	1.671671	H	0.400561	3.559417	2.695247
H	-2.524272	-2.684189	2.158213	H	0.022121	1.817068	3.110975
H	-4.292130	-2.828880	2.312949	H	0.260393	4.940525	0.789757
H	-3.505706	-2.966432	0.709687	H	-1.317093	5.603420	0.288637
H	-5.083634	-1.462004	0.099456	H	-1.036536	5.181932	2.000382
H	-5.660414	-0.594469	1.518227				

Table A2.4: DFT Optimized geometry, coordinates, and MP2 corrected energy for TMEDA monochleated open dimer transition structure **5b**.

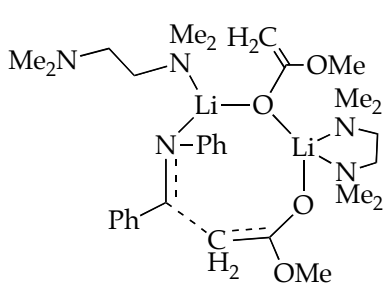

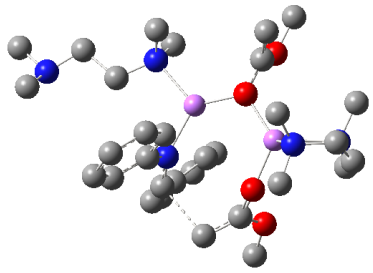

5b
G = -1796.271055
(-60 °C)

Atom	X	Y	Z	Atom	X	Y	Z
C	1.777519	4.368765	-1.567035	C	-1.221948	-0.841642	-2.146086
O	2.137676	3.064398	-1.127635	C	-2.125845	-0.779605	-3.229578
C	1.652533	1.957719	-1.797806	C	-2.328020	-1.881582	-4.059506
O	2.087913	0.866459	-1.358473	C	-1.648463	-3.081124	-3.837482
Li	2.532703	-0.323298	0.003748	C	-0.758518	-3.163021	-2.763359
O	1.138490	-0.939824	1.180018	C	-0.547454	-2.064645	-1.932415
Li	-0.555985	-0.483629	0.594987	H	0.165719	-2.129120	-1.113512
N	-2.281004	-1.048467	1.694784	H	-0.219596	-4.088444	-2.572770
C	-2.216370	-0.312675	2.967298	H	-1.813092	-3.937010	-4.485981
H	-2.353479	0.756307	2.775233	H	-3.034016	-1.802835	-4.883171
H	-2.977329	-0.639994	3.694775	H	-2.695542	0.126902	-3.410796
H	-1.227922	-0.454577	3.414157	C	-1.170071	1.453040	-1.608024
C	-2.150613	-2.498559	1.918653	C	-1.258986	2.525239	-0.586975
H	-1.169818	-2.711950	2.356456	C	-0.539200	2.481868	0.620330
H	-2.927917	-2.898841	2.589457	C	-0.690629	3.488750	1.573588
H	-2.220213	-3.019623	0.957939	C	-1.560590	4.557817	1.342816
C	-3.465336	-0.695385	0.880510	C	-2.272746	4.617473	0.143056
H	-3.431992	0.382923	0.693818	C	-2.119965	3.611945	-0.811536
H	-3.335688	-1.189322	-0.087065	H	-2.682137	3.660244	-1.741727
C	-4.843887	-1.037470	1.475762	H	-2.951936	5.444370	-0.048271
N	-5.933649	-0.500464	0.657484	H	-1.677234	5.339968	2.088312
C	-6.092035	-1.210136	-0.607658	H	-0.115678	3.441915	2.494852

H	-6.900940	-0.747121	-1.183035	H	0.181766	1.688546	0.795470
H	-5.180813	-1.145325	-1.208096	H	-1.700131	1.684462	-2.532175
H	-6.339717	-2.282565	-0.472388	C	1.387108	-1.483128	2.341732
C	-7.190512	-0.484983	1.394718	C	1.621896	-2.798280	2.590534
H	-7.970429	-0.021627	0.780215	H	1.826161	-3.192401	3.576388
H	-7.542912	-1.495359	1.684853	H	1.590301	-3.496780	1.763989
H	-7.079660	0.110789	2.307232	O	1.373507	-0.522934	3.350695
H	-4.948627	-2.131516	1.619039	C	1.615145	-0.948856	4.682416
H	-4.928773	-0.579744	2.467993	H	1.558441	-0.053538	5.306300
N	-0.996463	0.196693	-1.228799	H	0.861822	-1.674805	5.015877
H	2.609701	-1.402338	4.784994	C	4.493918	1.772536	0.995030
N	3.792988	-1.855288	-1.065855	H	5.499803	2.133476	1.278305
C	3.353992	-3.246441	-0.913268	H	4.204184	2.201941	0.034296
H	3.287835	-3.496750	0.148907	H	3.778374	2.122346	1.745050
H	4.036327	-3.961006	-1.409220	C	4.680994	-0.266621	2.252224
H	2.360360	-3.361336	-1.356453	H	5.697340	-0.034204	2.620948
C	3.785713	-1.482484	-2.487543	H	3.947493	0.141929	2.951165
H	4.066348	-0.434854	-2.606699	H	4.547950	-1.350797	2.238390
H	4.475438	-2.114485	-3.076749	H	6.429977	-0.103180	0.271290
H	2.773660	-1.591499	-2.884324	C	0.673646	2.084360	-2.795692
C	5.123120	-1.657504	-0.463240	H	0.430225	3.049131	-3.224729
H	5.183989	-2.286268	0.430440	H	0.552081	1.227929	-3.447903
H	5.925567	-2.000398	-1.141897	H	0.704183	4.551938	-1.448739
C	5.385085	-0.198636	-0.081007	H	2.332205	5.063576	-0.931928
H	5.289157	0.435564	-0.968335	H	2.061939	4.529941	-2.614536
N	4.435204	0.306239	0.923608				

Table A2.5: DFT Optimized geometry, coordinates, and MP2 corrected energy for TMEDA unchleated open dimer transition structure **5c**.

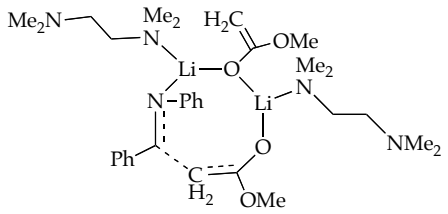

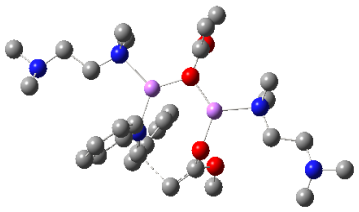

5c
G = -1796.254494
(-60 °C)

Atom	X	Y	Z	Atom	X	Y	Z
C	-2.524718	-2.642382	2.435494	C	1.759408	-1.626556	-1.579551
O	-2.442079	-1.731727	1.339731	C	2.686996	-2.673175	-1.783023
C	-1.672640	-2.048717	0.239169	C	3.153303	-2.983240	-3.060063
O	-1.752737	-1.218347	-0.695149	C	2.723774	-2.259862	-4.175419
Li	-1.907580	0.611585	-0.597665	C	1.812181	-1.217311	-3.992151
O	-0.434576	1.734850	-0.387983	C	1.335900	-0.907698	-2.719534
Li	1.159014	0.767335	-0.269159	H	0.591143	-0.124944	-2.593794
N	3.012282	1.797240	-0.157710	H	1.455135	-0.649019	-4.847898
C	3.003629	2.483631	1.143486	H	3.092444	-2.504521	-5.167624
H	3.021233	1.739717	1.946471	H	3.869618	-3.792878	-3.181704
H	3.858399	3.166173	1.279040	H	3.069204	-3.227904	-0.930659
H	2.082507	3.066276	1.237436	C	1.091783	-2.139704	0.619279
C	3.023205	2.768790	-1.264657	C	0.973663	-1.718956	2.044180
H	2.114350	3.377641	-1.219119	C	0.443305	-0.475423	2.428549
H	3.895683	3.441448	-1.235591	C	0.374400	-0.116488	3.775387
H	3.033708	2.229296	-2.217625	C	0.830946	-0.989002	4.766246
C	4.085820	0.783518	-0.268748	C	1.356369	-2.229290	4.397705
H	3.946954	0.063446	0.544395	C	1.424366	-2.587678	3.051217
H	3.910294	0.244269	-1.203921	H	1.839850	-3.553594	2.771164
C	5.535648	1.299900	-0.212702	H	1.719763	-2.916353	5.157793
N	6.496424	0.203105	-0.079283	H	0.777376	-0.705866	5.814181
C	6.580313	-0.624561	-1.278573	H	-0.044421	0.849110	4.046938
H	7.305508	-1.428228	-1.111300	H	0.053012	0.211109	1.683353
H	5.616491	-1.090474	-1.499762	H	1.561447	-3.119891	0.511797

H	6.903120	-0.055249	-2.173766	C	-0.542157	3.018153	-0.144815
C	7.813986	0.701136	0.293573	C	-0.586314	4.013515	-1.065581
H	8.494376	-0.143314	0.449908	H	-0.674333	5.060015	-0.808237
H	8.266462	1.364314	-0.471124	H	-0.528985	3.751885	-2.115031
H	7.747988	1.262045	1.232377	O	-0.608139	3.251334	1.224167
H	5.759986	1.927701	-1.098543	C	-0.738111	4.593799	1.667841
H	5.656023	1.941439	0.667763	H	-0.776493	4.553673	2.758847
N	1.294578	-1.213141	-0.321845	H	0.118259	5.205141	1.354760
H	-1.658619	5.054038	1.286055	C	-8.472497	-0.235282	-1.475620
N	-3.887594	1.331672	-0.504692	H	-8.970667	-0.073591	-0.498398
C	-3.988767	1.684529	0.921585	H	-8.553652	0.691259	-2.054527
H	-3.864638	0.778598	1.523191	H	-9.024118	-1.017714	-2.008400
H	-4.951026	2.154271	1.181622	C	-6.950376	-1.902190	-0.667074
H	-3.184540	2.381238	1.179633	H	-7.300823	-1.863777	0.384486
C	-4.063090	2.516135	-1.358242	H	-7.546988	-2.654004	-1.194560
H	-4.010197	2.214527	-2.409804	H	-5.912064	-2.244137	-0.668293
H	-5.024403	3.030046	-1.193395	H	-6.549238	0.553921	0.348848
H	-3.252485	3.225679	-1.163815	C	-0.765445	-3.129327	0.256140
C	-4.771200	0.204061	-0.880343	H	-0.841281	-3.896696	1.018817
H	-4.572185	-0.037919	-1.930652	H	-0.468437	-3.479479	-0.726245
H	-4.445697	-0.654091	-0.286684	H	-1.563703	-2.743306	2.948833
C	-6.285405	0.438719	-0.722176	H	-3.257550	-2.215342	3.123516
H	-6.557472	1.378456	-1.216326	H	-2.870553	-3.628254	2.102561
N	-7.072756	-0.621175	-1.353915				

Table A2.6: DFT Optimized geometry, coordinates, and MP2 corrected energy for TMEDA dichleated closed dimer transition structure **5d**.

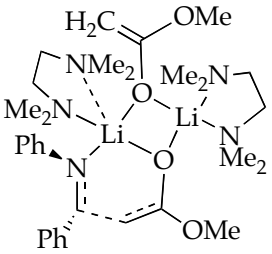

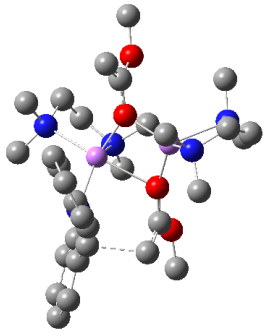

5d
G = -1796.279143
(-60 °C)

Atom	X	Y	Z	Atom	X	Y	Z
C	-2.688979	-0.758387	-3.567899	N	-1.234385	-1.476098	1.085363
O	-1.637032	-0.174186	-2.798865	C	-0.295681	-2.322623	1.695437
C	-0.898049	-0.956613	-1.952535	C	0.474027	-1.793509	2.757003
O	0.033073	-0.345279	-1.370319	C	1.393002	-2.564242	3.460041
Li	1.850090	-0.122591	-0.885426	C	1.601401	-3.907326	3.127402
O	1.547261	0.847057	0.698286	C	0.873120	-4.448750	2.068447
Li	-0.324437	0.463193	0.817734	C	-0.051375	-3.678905	1.359096
N	-1.135045	2.060380	2.379443	H	-0.591345	-4.154807	0.548082
C	-0.846892	3.419786	1.875138	H	1.020732	-5.488631	1.783787
C	-1.681875	3.877370	0.676164	H	2.314427	-4.513540	3.679190
N	-1.587930	3.019391	-0.503640	H	1.948607	-2.111661	4.278116
C	-2.662869	3.303612	-1.449530	H	0.325413	-0.756473	3.032371
H	-2.588968	4.318209	-1.889164	C	-2.117909	-2.060773	0.260545
H	-2.630503	2.571400	-2.261848	C	-3.429605	-1.425751	-0.058627
H	-3.634393	3.224162	-0.951460	C	-3.636344	-0.041398	-0.146520
C	-0.298138	3.145380	-1.183663	C	-4.905595	0.465119	-0.432549
H	0.524286	2.904146	-0.509167	C	-5.989374	-0.390626	-0.639646
H	-0.271849	2.431467	-2.010544	C	-5.794302	-1.770366	-0.561268
H	-0.144483	4.168153	-1.584852	C	-4.527742	-2.276436	-0.273880
H	-2.736717	3.930527	0.967209	H	-4.383191	-3.352820	-0.206272
H	-1.377290	4.919333	0.446888	H	-6.627132	-2.451894	-0.715362
H	-1.018104	4.162657	2.679499	H	-6.973965	0.014208	-0.858747

H	0.218933	3.452446	1.631250	H	-5.051403	1.539871	-0.496094
C	-0.321654	1.840633	3.586178	H	-2.807873	0.645220	-0.008153
H	0.743272	1.862987	3.339687	H	-2.241003	-3.143871	0.340945
H	-0.525621	2.604680	4.359463	C	2.458093	1.490249	1.368406
H	-0.559770	0.862586	4.013051	C	3.261224	0.998523	2.347951
C	-2.550058	1.891511	2.733615	H	3.995698	1.594358	2.871968
H	-3.184358	1.993747	1.852665	H	3.134429	-0.033371	2.648205
H	-2.699309	0.884436	3.132241	O	2.529945	2.824544	0.951720
H	-2.877353	2.625326	3.493985	C	3.474911	3.675017	1.578619
H	3.361907	4.657948	1.113791	N	3.051334	0.729920	-2.531269
H	3.289437	3.759116	2.657479	C	2.219292	1.263159	-3.616140
H	4.501800	3.316472	1.426928	H	2.822425	1.594816	-4.480714
N	3.297446	-1.797133	-0.987245	H	1.508887	0.501281	-3.948813
C	3.825155	-2.174523	0.333847	H	1.648016	2.117692	-3.246108
H	4.240108	-1.291674	0.827377	C	3.908819	1.794223	-1.990846
H	4.608731	-2.950000	0.257926	H	4.578828	2.213594	-2.763518
H	3.013168	-2.560171	0.953843	H	3.282944	2.590333	-1.582556
C	2.638753	-2.954627	-1.606756	H	4.519826	1.412496	-1.169447
H	2.168256	-2.672712	-2.552929	H	4.686279	-0.100435	-3.634632
H	3.350945	-3.777518	-1.800515	C	-1.266750	-2.288695	-1.651877
H	1.859491	-3.321248	-0.934401	H	-2.008943	-2.797089	-2.257312
C	4.373930	-1.268977	-1.842807	H	-0.449235	-2.912430	-1.311381
H	5.028874	-0.659074	-1.212942	H	-3.503974	-1.111132	-2.929330
H	4.999880	-2.084120	-2.250207	H	-3.057237	0.038485	-4.217256
C	3.840152	-0.422416	-2.999517	H	-2.315677	-1.585265	-4.183862
H	3.189088	-1.034167	-3.633385				

Table A2.7: DFT Optimized geometry, coordinates, and MP2 corrected energy for TMEDA monochleated closed dimer transition structure **5e**.

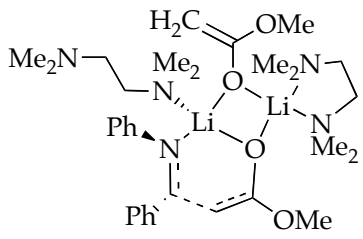

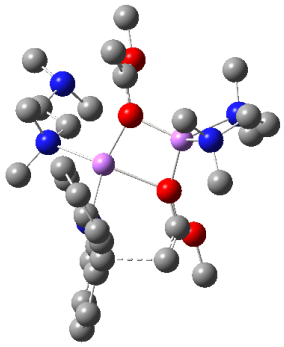

5e
G = -1796.271617
(-60 °C)

Atom	X	Y	Z	Atom	X	Y	Z
C	-0.054394	2.864835	-3.675036	H	3.916193	0.629920	2.760115
O	-0.133009	1.663046	-2.908641	N	-0.305213	2.068371	1.244723
C	-0.893578	1.626279	-1.772921	C	-1.417248	1.951633	2.088300
O	-0.888392	0.512773	-1.188878	C	-1.387903	0.929027	3.066421
Li	-1.685410	-1.149413	-0.805039	C	-2.444698	0.717338	3.944360
O	-0.573956	-1.618811	0.615148	C	-3.587885	1.522233	3.889486
Li	0.232053	0.079492	0.773301	C	-3.640985	2.540046	2.937248
N	2.304694	-0.357519	1.731752	C	-2.584433	2.755295	2.050225
C	3.015297	-1.077765	0.651518	H	-2.675785	3.563712	1.333369
C	4.448190	-1.556159	0.962688	H	-4.517695	3.181757	2.877967
N	4.932963	-2.528671	-0.019911	H	-4.413947	1.361412	4.576533
C	5.103535	-1.953038	-1.348305	H	-2.372093	-0.078824	4.681530
H	5.828406	-1.113103	-1.368129	H	-0.504220	0.301542	3.132750
H	5.466434	-2.725956	-2.034466	C	-0.254657	3.132787	0.429122
H	4.148132	-1.589525	-1.736514	C	1.026908	3.528155	-0.226961
C	6.168815	-3.154560	0.430870	C	1.972358	2.605074	-0.698261
H	6.006763	-3.641112	1.398992	C	3.145619	3.034023	-1.318681
H	6.476686	-3.922316	-0.287948	C	3.403479	4.397638	-1.478735
H	7.008363	-2.439125	0.544442	C	2.472383	5.328629	-1.015080
H	5.136541	-0.690504	1.044831	C	1.297778	4.895261	-0.399612
H	4.456136	-2.057435	1.937063	H	0.577928	5.627218	-0.039086
H	2.407345	-1.946118	0.379892	H	2.661346	6.393207	-1.127771

H	3.033156	-0.405616	-0.215309	H	4.319895	4.729849	-1.959187
C	2.019021	-1.215474	2.890460	H	3.859992	2.299153	-1.681543
H	1.449727	-2.094784	2.583324	H	1.780411	1.543500	-0.595808
H	2.930265	-1.542999	3.419441	H	-0.838896	4.016803	0.701457
H	1.414252	-0.651938	3.608488	C	-0.407658	-2.848280	1.007665
C	3.006774	0.854399	2.177553	C	-1.054536	-3.475394	2.024669
H	3.287928	1.463746	1.316189	H	-0.872502	-4.504121	2.303813
H	2.332547	1.448622	2.801357	H	-1.764608	-2.907333	2.612312
O	0.558451	-3.490265	0.229619	H	-3.554655	-1.158869	-3.278570
C	0.920411	-4.819023	0.567442	N	-2.016752	-2.365487	-2.557494
H	1.731432	-5.097307	-0.109820	C	-1.194094	-1.889214	-3.676761
H	1.273492	-4.887158	1.604500	H	-1.426946	-2.416781	-4.619362
H	0.078578	-5.512873	0.437505	H	-1.340667	-0.815538	-3.818698
N	-3.858881	-1.191192	-0.545372	H	-0.139128	-2.051636	-3.439270
C	-4.231567	-1.587489	0.821063	C	-1.714687	-3.776383	-2.279736
H	-3.740873	-2.531035	1.074912	H	-1.935252	-4.422661	-3.148728
H	-5.324273	-1.702603	0.936668	H	-0.659000	-3.868489	-2.016029
H	-3.884916	-0.826438	1.525161	H	-2.294275	-4.131416	-1.424098
C	-4.414204	0.132625	-0.852608	H	-3.849258	-2.880537	-3.539141
H	-4.084709	0.469613	-1.839549	C	-1.494282	2.785455	-1.229340
H	-5.519395	0.129594	-0.834824	H	-1.528486	3.701199	-1.809807
H	-4.056202	0.852619	-0.112187	H	-2.373734	2.593936	-0.626265
C	-4.283637	-2.201044	-1.530674	H	0.442715	3.663163	-3.115751
H	-4.175526	-3.186001	-1.066246	H	0.541650	2.614569	-4.554849
H	-5.352945	-2.091369	-1.787524	H	-1.049366	3.199131	-3.992473
C	-3.450011	-2.146147	-2.815099				

Table A2.8: DFT Optimized geometry, coordinates, and MP2 corrected energy for TMEDA unchleated closed dimer transition structure **5f**.

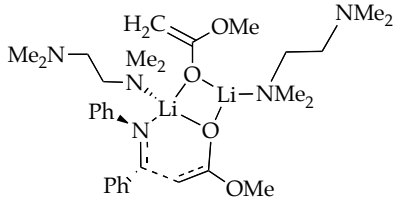

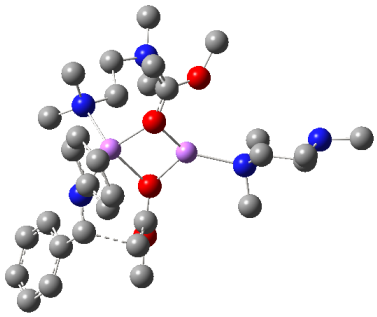

5f
G = -1796.248546
(-60 °C)

Atom	X	Y	Z	Atom	X	Y	Z
C	-2.499206	-1.151011	-3.863819	N	-2.244553	-1.481326	1.110921
O	-1.769102	-0.354649	-2.925329	C	-1.534260	-2.227359	2.059971
C	-1.211325	-0.924199	-1.829776	C	-1.355587	-1.646188	3.337252
O	-0.562873	-0.118232	-1.106597	C	-0.675471	-2.306356	4.353912
Li	1.217900	0.075443	-0.561841	C	-0.136776	-3.579299	4.139750
O	0.928032	0.232871	1.229038	C	-0.297444	-4.171363	2.887368
Li	-0.970662	0.194394	0.953656	C	-0.981099	-3.515410	1.862693
N	-1.565580	2.332674	1.413374	H	-1.079900	-4.015483	0.904363
C	-0.674662	3.076480	0.495184	H	0.115647	-5.160234	2.698391
C	-0.623206	4.608871	0.652821	H	0.395850	-4.096415	4.932943
N	0.280613	5.212782	-0.332061	H	-0.572167	-1.827969	5.325258
C	-0.317064	5.296278	-1.659904	H	-1.793244	-0.667071	3.517599
H	-1.210638	5.952494	-1.689841	C	-2.763096	-2.149938	0.056618
H	0.418411	5.695057	-2.367157	C	-3.989563	-1.604504	-0.610555
H	-0.613634	4.304999	-2.013452	C	-4.320790	-0.244830	-0.576343
C	0.747510	6.524645	0.098621	C	-5.475967	0.224902	-1.201374
H	1.257548	6.439572	1.063914	C	-6.330391	-0.659071	-1.864155
H	1.465319	6.916132	-0.631064	C	-6.019938	-2.020696	-1.892431
H	-0.067511	7.268677	0.203995	C	-4.859897	-2.485469	-1.271895
H	-1.635551	5.054020	0.593138	H	-4.627945	-3.548867	-1.290008
H	-0.232710	4.848636	1.647593	H	-6.685535	-2.722423	-2.389068
H	0.338219	2.688336	0.632040	H	-7.234312	-0.292963	-2.343871

H	-0.985518	2.811369	-0.521498	H	-5.715242	1.285003	-1.163364
C	-1.186188	2.479346	2.827537	H	-3.670707	0.433416	-0.039534
H	-0.136310	2.206284	2.965690	H	-2.838365	-3.239909	0.150974
H	-1.349567	3.501016	3.210684	C	1.887288	0.717877	1.963698
H	-1.798783	1.799954	3.430625	C	2.058656	0.594843	3.299899
C	-2.979455	2.680806	1.232347	H	2.895588	1.023706	3.833253
H	-3.239188	2.629340	0.170308	H	1.357370	-0.016287	3.853094
H	-3.602065	1.964616	1.778484	O	2.783647	1.433211	1.149267
H	-3.225869	3.691601	1.597728	C	3.901548	2.051703	1.767204
H	4.456356	2.558457	0.973281	H	4.550882	1.312033	2.252819
C	7.410952	-1.878612	-1.617080	N	6.124889	-1.784244	-0.937861
H	7.650865	-0.921582	-2.093301	H	3.007945	-1.184851	-3.867255
H	7.439544	-2.666470	-2.396260	H	1.913111	-2.032902	-2.744945
H	8.195947	-2.099898	-0.885928	H	1.394421	-0.521371	-3.516501
C	5.828142	-3.019567	-0.219685	C	3.193867	1.060734	-2.340607
H	4.925158	-2.907755	0.386594	H	4.007686	1.041886	-3.082840
H	5.689299	-3.888824	-0.894032	H	2.347390	1.594514	-2.786701
H	6.654448	-3.248721	0.461008	H	3.525620	1.615520	-1.459227
C	5.064672	-1.401650	-1.869704	H	3.270532	-1.911232	-0.747007
H	5.430403	-0.536049	-2.433951	C	-1.455743	-2.273924	-1.447609
H	4.865520	-2.203531	-2.609951	H	-1.890892	-2.948256	-2.178976
C	3.766120	-1.014258	-1.136602	H	-0.647933	-2.711580	-0.869049
H	4.020786	-0.386612	-0.277186	H	-3.407504	-1.559814	-3.414670
N	2.750667	-0.280830	-1.929421	H	-2.766000	-0.471495	-4.674952
C	2.250023	-1.046562	-3.080043	H	-1.876691	-1.962794	-4.257699
H	3.582423	2.788880	2.514619				

Table A2.9: DFT Optimized geometry, coordinates, and MP2 corrected energy for TMEDA unchleated nitrogen-coordinated closed dimer transition structure **5g**.

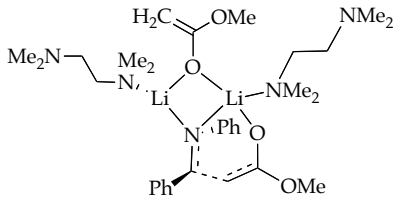

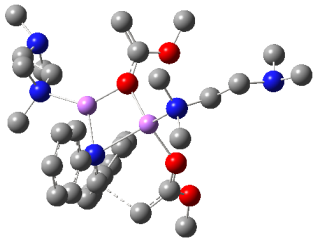

5g
G = -1796.26004
(-60 °C)

Atom	X	Y	Z	Atom	X	Y	Z
C	0.626985	2.291510	4.573910	C	0.507172	1.953803	-2.662571
O	1.215148	1.441800	3.589318	C	0.975274	2.640317	-3.778692
C	1.381756	1.875177	2.312535	C	1.106086	4.032621	-3.756181
O	1.948851	1.070845	1.552454	C	0.762192	4.714752	-2.589089
Li	1.486749	0.290377	-0.111422	C	0.290290	4.036248	-1.464516
O	0.317033	-1.056085	-0.796724	H	0.041767	4.614106	-0.581400
Li	-1.098278	0.054884	-0.978676	H	0.864339	5.796962	-2.545317
N	-3.070775	-0.124519	-1.640711	H	1.472834	4.570148	-4.625798
C	-3.623049	-1.252694	-0.852950	H	1.242860	2.081666	-4.672871
C	-5.037657	-1.738168	-1.224310	H	0.439290	0.867755	-2.691389
N	-5.480978	-2.798643	-0.317138	C	-0.792412	2.487665	0.704773
C	-5.944514	-2.280981	0.965133	C	-1.632831	1.715468	1.668802
H	-6.849357	-1.646990	0.870332	C	-1.449545	0.342740	1.911029
H	-6.185372	-3.117299	1.630224	C	-2.265356	-0.333336	2.821459
H	-5.164997	-1.686565	1.449563	C	-3.280040	0.341640	3.503861
C	-6.498722	-3.646833	-0.924874	C	-3.473314	1.705909	3.270610
H	-6.112202	-4.088183	-1.849544	C	-2.656519	2.382404	2.364607
H	-6.749895	-4.463879	-0.239479	H	-2.813456	3.444514	2.186885
H	-7.436326	-3.106765	-1.165498	H	-4.261882	2.243007	3.791668
H	-5.755433	-0.894871	-1.244260	H	-3.910220	-0.187424	4.213839
H	-5.015332	-2.156093	-2.236483	H	-2.095701	-1.391552	3.001680
H	-2.933305	-2.098358	-0.957465	H	-0.657024	-0.202444	1.406590
H	-3.595458	-0.942903	0.196217	H	-1.161455	3.511089	0.590488
C	-2.962175	-0.434174	-3.076405	C	0.379986	-2.354742	-0.929883

H	-2.428168	-1.380903	-3.204222	C	0.110230	-3.057429	-2.060862
H	-3.941394	-0.508807	-3.575683	H	0.170194	-4.134910	-2.123113
H	-2.392594	0.358836	-3.573523	H	-0.135059	-2.512422	-2.964695
C	-3.792052	1.140555	-1.432829	O	0.769521	-2.950024	0.258054
H	-3.858074	1.351730	-0.361982	C	0.876839	-4.363620	0.290200
H	-3.233238	1.952803	-1.908569	H	1.190984	-4.623795	1.303735
H	-4.808578	1.127515	-1.856204	H	-0.086762	-4.842331	0.071904
N	-0.346963	1.848907	-0.413711	H	1.623065	-4.726195	-0.429108
C	0.135665	2.627847	-1.469876	C	0.825593	3.119813	1.858996
H	0.441474	3.825847	2.588828	H	7.674873	-3.073108	1.726857
H	1.388887	3.577651	1.052073	H	7.557370	-3.224624	-0.044706
H	-0.420677	2.507502	4.341564	H	5.394298	-2.199558	-1.121041
H	0.681301	1.734052	5.510780	H	6.058419	-0.737961	-0.377144
H	1.185810	3.228831	4.677121	H	3.931526	-0.545944	1.022809
N	3.449380	-0.039401	-0.945381	H	3.225181	-1.841445	0.060743
C	3.953706	-1.024203	0.038431	C	4.187156	1.229338	-0.924930
C	5.372089	-1.575177	-0.204892	H	4.202337	1.619052	0.096607
N	5.881063	-2.314245	0.952645	H	5.224016	1.138941	-1.290447
C	5.149709	-3.551340	1.198865	H	3.668269	1.952029	-1.563573
H	5.202085	-4.261773	0.348188	C	3.364765	-0.583633	-2.307014
H	5.568170	-4.049268	2.080285	H	2.777736	-1.506803	-2.298901
H	4.096751	-3.342147	1.404877	H	2.854983	0.142432	-2.947891
C	7.307273	-2.578012	0.820974	H	4.353089	-0.791038	-2.749913
H	7.850669	-1.633659	0.706035				

Table A2.10: DFT Optimized geometry, coordinates, and MP2 corrected energy for unsolvated anion transition structure for triple ion **5h/7b**.

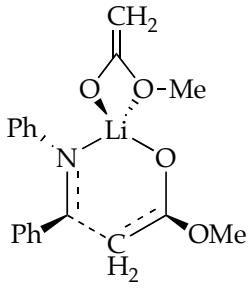

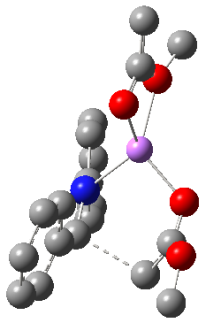

5h (part 1)
7b (part 1)
G = -1096.125087
(-60 °C)

Atom	X	Y	Z	Atom	X	Y	Z
C	3.810699	2.395381	0.723651	C	-2.013357	0.775909	-1.233472
O	2.483869	2.144718	0.323709	H	-1.091884	1.344062	-1.146228
C	1.695557	3.192373	-0.284702	H	-3.128299	2.481143	-1.902509
O	0.500798	2.775007	-0.419258	H	-5.261761	1.223242	-2.188303
Li	0.698764	1.081083	0.440973	H	-5.319626	-1.218879	-1.681644
O	-0.023742	0.380764	2.081382	H	-3.276053	-2.360120	-0.872824
C	-1.103583	-0.245211	2.090215	C	1.496461	-1.604956	-0.521685
C	-1.241959	-1.598676	1.702222	C	2.738452	-1.017697	-0.865591
H	-2.187097	-2.119778	1.814005	C	3.920169	-1.748812	-0.842080
H	-0.353886	-2.203195	1.845220	C	3.921026	-3.098758	-0.470988
O	-2.208492	0.529019	2.386500	C	2.709826	-3.693552	-0.116021
C	-3.482565	-0.080557	2.508750	C	1.518205	-2.968332	-0.136406
H	-4.163467	0.708518	2.840766	H	0.601188	-3.467482	0.158630
H	-3.839436	-0.480077	1.552706	H	2.687628	-4.739130	0.188324
H	-3.474796	-0.886354	3.256407	H	4.846396	-3.669869	-0.451972
N	0.367419	-0.790923	-0.599560	H	4.852918	-1.260585	-1.118833
C	-0.835203	-1.341771	-0.477847	H	2.742436	0.031539	-1.144951
H	-0.953647	-2.423977	-0.594089	C	2.282618	4.378442	-0.602826
C	-2.041741	-0.594119	-0.923914	H	3.330177	4.589913	-0.433980
C	-3.248144	-1.295044	-1.098308	H	1.670658	5.150443	-1.053610
C	-4.399408	-0.652834	-1.549653	H	3.862573	3.229487	1.437418
C	-4.366296	0.714944	-1.836827	H	4.177831	1.481211	1.200169
C	-3.171063	1.418514	-1.676574	H	4.452301	2.635577	-0.137020

Table A2.11: DFT Optimized geometry, coordinates, and MP2 corrected energy for TMEDA dichleated lithium cation of triple ion **5h**.

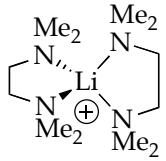

S10

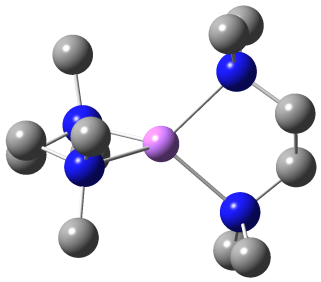

5h (part 2)
G = -700.0090158
(-60 °C)

Atom	X	Y	Z	Atom	X	Y	Z
Li	-0.000036	-0.000067	0.000879	N	-1.582491	1.067730	-1.066734
N	1.582060	-1.073170	-1.061697	C	-2.758167	0.226867	-0.731418
C	2.757437	-0.229782	-0.731708	C	-2.760985	-0.230160	0.726264
C	2.761419	0.234317	0.723736	N	-1.583853	-1.066708	1.067337
N	1.584244	1.072099	1.061734	C	-1.447203	-1.151090	2.535448
C	1.447954	1.162431	2.529548	H	-0.576993	-1.763608	2.790272
H	2.336140	1.617627	2.996896	H	-1.306447	-0.151750	2.956048
H	0.577837	1.776033	2.782081	H	-2.335259	-1.604413	3.004863
H	1.307219	0.164807	2.954208	C	-1.749742	-2.434049	0.531841
C	1.749888	2.437257	0.520654	H	-0.893866	-3.046969	0.824923
H	1.804648	2.420497	-0.571128	H	-2.664699	-2.911287	0.919007
H	0.893850	3.051189	0.811129	H	-1.804431	-2.421852	-0.560012
H	2.664711	2.916255	0.905935	H	-2.756694	0.639919	1.390777
H	2.758126	-0.632537	1.392443	H	-3.698687	-0.774009	0.930332
H	3.699087	0.779508	0.924297	H	-3.696880	0.767202	-0.940262
H	3.696350	-0.770396	-0.938943	H	-2.747164	-0.643266	-1.395845
H	2.745043	0.637153	-1.400280	C	-1.753450	2.433035	-0.527644
C	1.441073	-1.170094	-2.528648	H	-0.899552	3.049646	-0.818718
H	1.297113	-0.174588	-2.957131	H	-2.669827	2.908166	-0.914055
H	2.328628	-1.625568	-2.996929	H	-1.808563	2.417850	0.564130
H	0.571322	-1.786465	-2.775667	C	-1.442536	1.156981	-2.534246

C	1.754332	-2.435543	-0.515680	H	-0.572658	1.771619	-2.785111
H	2.670990	-2.911869	-0.899927	H	-1.299392	0.159200	-2.957685
H	1.809673	-2.414693	0.575979	H	-2.330203	1.610454	-3.004256
H	0.900855	-3.054322	-0.803374				

Table A2.12: DFT Optimized geometry, coordinates, and MP2 corrected energy for TMCDA disolvated open dimer transition structure **7a**.

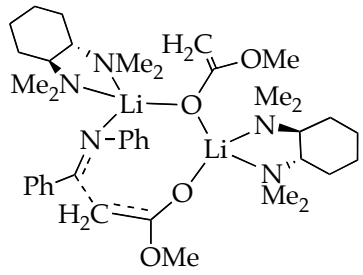

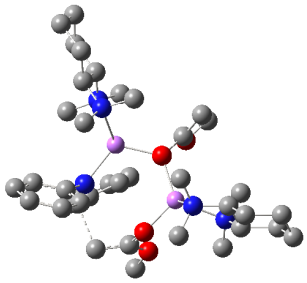

7a
G = -2107.099098
(-60 °C)

Atom	X	Y	Z	Atom	X	Y	Z
C	-1.882295	4.843801	0.414028	C	-0.584057	-0.860684	-2.148942
O	-2.056096	3.428864	0.422712	C	-0.765717	-2.113434	-2.649616
C	-1.438922	2.662951	1.382733	C	-0.427180	3.206533	2.216231
O	-1.750479	1.451784	1.360701	H	-0.338896	4.284110	2.310496
Li	-2.036523	0.082043	0.090695	H	-0.279534	2.662512	3.143242
O	-0.433486	-0.516495	-0.900382	H	-0.851684	5.123042	0.176391
Li	1.354391	-0.250125	-0.091692	H	-2.546103	5.219395	-0.368058
N	1.447563	1.250964	1.370478	H	-2.171689	5.284048	1.376079
C	1.746797	0.737413	2.652802	N	-4.087319	0.291679	-0.865799
C	0.783169	-0.002006	3.365347	C	-4.998878	-0.688599	-0.213450
C	1.072291	-0.539578	4.620364	C	-3.833408	0.029031	-2.290244
C	2.330177	-0.354910	5.199296	C	-4.571780	1.668325	-0.698755
C	3.293672	0.387146	4.510882	C	-4.234594	-1.940016	0.286533
C	3.005243	0.930898	3.258130	C	-6.216728	-1.093393	-1.076808
H	3.758838	1.505578	2.724324	H	-5.393035	-0.174404	0.672061
H	4.276477	0.542527	4.950864	H	-4.718457	0.200115	-2.925476

H	2.555194	-0.777280	6.175076	H	-3.036199	0.696878	-2.626348
H	0.307393	-1.100535	5.153487	H	-3.481029	-0.995373	-2.436021
H	-0.199634	-0.113205	2.917670	H	-3.833849	2.360294	-1.108943
C	1.350234	2.591480	1.348519	H	-5.540244	1.843206	-1.201039
C	1.348144	3.327332	0.048724	H	-4.673656	1.898644	0.364624
C	0.720663	2.823502	-1.101288	C	-5.202461	-2.935425	0.971197
C	0.731929	3.555029	-2.290167	H	-3.804861	-2.437364	-0.594029
C	1.371528	4.795415	-2.358146	N	-3.065830	-1.561557	1.127738
C	2.004480	5.302907	-1.221194	C	-7.158655	-2.062701	-0.352246
C	1.989579	4.574398	-0.030824	H	-5.867587	-1.578032	-1.997603
H	2.483142	4.975174	0.852574	H	-6.760213	-0.191495	-1.384578
H	2.512634	6.263416	-1.260644	C	-6.394435	-3.316602	0.084175
H	1.377736	5.360816	-3.286692	H	-4.653075	-3.835883	1.270568
H	0.231336	3.145689	-3.163675	H	-5.590127	-2.485177	1.894863
H	0.210874	1.866299	-1.069044	C	-2.106432	-2.661682	1.263103
H	1.885367	3.145177	2.129898	C	-3.410347	-1.037501	2.457928
H	-7.593647	-1.572977	0.531491	C	5.931853	-3.595041	-0.784800
H	-7.997904	-2.327933	-1.007569	H	-1.207713	-2.288501	1.764097
H	-6.039081	-3.855105	-0.806643	H	-2.494106	-3.510177	1.853172
H	-7.055109	-4.006870	0.623783	H	-1.819783	-3.020785	0.271601
H	-0.899494	-2.320217	-3.702449	H	-4.142498	-0.231658	2.375314
H	-0.791185	-2.953943	-1.968962	H	-3.807292	-1.810601	3.136243
O	-0.556893	0.261103	-2.981420	H	-2.513100	-0.606645	2.907935
C	-0.684396	0.069382	-4.379353	N	2.463792	-2.297120	0.455394
H	-0.617001	1.060780	-4.834741	H	3.907966	-4.303368	-0.880202
H	0.118253	-0.566740	-4.775612	H	4.510725	-4.130855	0.762573
H	-1.650221	-0.383548	-4.640257	C	5.932382	-2.927013	-2.162419
C	3.831937	-2.263378	-0.129498	H	5.300524	-1.054863	-3.060008
C	1.560320	-3.251711	-0.201831	H	5.936553	-0.911205	-1.427183
C	2.508127	-2.586834	1.894533	C	2.794963	0.203550	-2.816654
C	3.860130	-1.557536	-1.507069	C	4.032866	0.827820	-0.852340
C	4.505750	-3.656021	-0.225204	H	6.577625	-3.023883	-0.101574
H	4.426591	-1.657250	0.567141	H	6.354055	-4.606408	-0.841502
H	1.840829	-4.303971	-0.026750	H	5.366243	-3.549301	-2.871086
H	0.553417	-3.099392	0.191790	H	6.952934	-2.851046	-2.558698

H	1.514122	-3.067967	-1.276703	H	2.239601	1.140511	-2.744164
H	1.503280	-2.491525	2.311449	H	3.650784	0.363598	-3.495303
H	2.871401	-3.604944	2.117729	H	2.135548	-0.552500	-3.251187
H	3.146521	-1.862529	2.405693	H	3.427596	1.726920	-0.727334
C	5.302274	-1.532115	-2.073053	H	4.366624	0.513130	0.139754
H	3.251034	-2.157424	-2.195624	H	4.916229	1.087223	-1.458366
N	3.203684	-0.220880	-1.469462				

Table A2.13: DFT Optimized geometry, coordinates, and MP2 corrected energy for TMCDA dichleated lithium cation of triple ion **7b**.

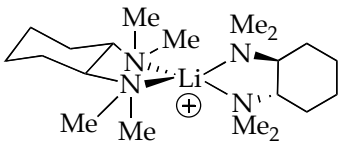

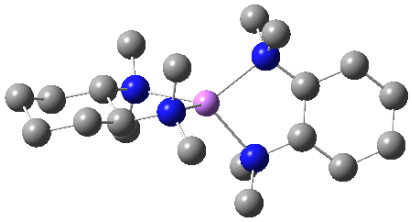

7b (part 2)
G = -1010.821826
(-60 °C)

Atom	X	Y	Z	Atom	X	Y	Z
C	5.507338	0.357428	0.162202	Li	0.000008	0.179886	0.024431
C	4.279239	0.909065	0.896067	C	-2.765206	-0.746662	0.326312
C	2.965687	0.688421	0.110469	C	-2.976633	0.691398	-0.203238
C	2.777506	-0.804014	-0.253213	C	-4.239129	0.779580	-1.091216
C	4.046762	-1.369223	-0.935470	C	-5.495038	0.264232	-0.377987
C	5.322502	-1.135897	-0.116599	C	-5.283836	-1.183015	0.072464
H	5.267274	-1.684865	0.834359	C	-4.057013	-1.284065	0.988452
H	6.183548	-1.540472	-0.660303	H	-3.907555	-2.324283	1.296441
H	3.915683	-2.439734	-1.127606	H	-4.266640	-0.712647	1.901509
H	4.180942	-0.888492	-1.912580	H	-5.148687	-1.826866	-0.808446
H	2.627942	-1.359364	0.683632	H	-6.166269	-1.559707	0.601620
N	1.514464	-1.025008	-1.039580	H	-5.720968	0.894827	0.493669
C	1.162139	-2.458181	-1.078867	H	-6.356261	0.340854	-1.051078
H	0.162494	-2.573941	-1.510675	H	-4.095997	0.180917	-1.999182
H	1.857244	-3.053645	-1.687875	H	-4.385021	1.816341	-1.416630

H	1.153194	-2.868739	-0.066483
C	1.602207	-0.537250	-2.431723
H	1.842325	0.529097	-2.457142
H	2.351298	-1.075956	-3.027371
H	0.634357	-0.681293	-2.917236
H	3.053672	1.246880	-0.829775
N	1.748024	1.255297	0.789427
C	1.716996	0.991970	2.242866
H	0.763657	1.344655	2.644127
H	1.799418	-0.081138	2.440809
H	2.516807	1.507536	2.791158
C	1.672178	2.714265	0.576362
H	2.528503	3.253318	1.008213
H	1.632098	2.933871	-0.494634
H	0.763515	3.104220	1.043714
H	4.215422	0.406850	1.869305
H	4.408430	1.978051	1.101358
H	5.657342	0.896062	-0.784285
H	6.404152	0.532553	0.766930
H	-3.154734	1.335916	0.665626
N	-1.732266	1.235177	-0.852909
C	-1.629102	0.894287	-2.286688
H	-0.654248	1.221285	-2.657730
H	-1.708773	-0.187486	-2.430373
H	-2.397879	1.381604	-2.901548
C	-1.684386	2.704664	-0.718206
H	-2.534487	3.203628	-1.207707
H	-1.683491	2.984709	0.339431
H	-0.766574	3.083640	-1.176311
H	-2.540583	-1.391963	-0.535829
N	-1.545997	-0.837088	1.201197
C	-1.216330	-2.244059	1.504503
H	-1.929292	-2.711846	2.198178
H	-1.199822	-2.830269	0.582642
H	-0.224919	-2.291722	1.967137
C	-1.682965	-0.110881	2.480890
H	-1.840758	0.957370	2.310147
H	-2.504209	-0.488384	3.105011
H	-0.759247	-0.232066	3.051263

REFERENCES II

1. (a) Green, J. R. In *Science of Synthesis*; Georg Thieme Verlag: New York, 2005; Vol. 8a, pp 427-486. (b) Schetter, B.; Mahrwald, R. *Angew. Chem., Int. Ed.* **2006**, *45*, 7506. (c) Arya, P.; Qin, H. *Tetrahedron* **2000**, *56*, 917. (d) Caine, D. In *Comprehensive Organic Synthesis*; Trost, B. M.; Fleming, I., Eds.; Pergamon: New York, **1989**, Vol. 1, p 1. (e) Martin, S. F. *Ibid.*, Vol. 1, pg. 475. (f) *Comprehensive Organic Functional Group Transformations II*; Katritzky, Alan R.; Taylor, Richard J. K., Eds.; Elsevier: Oxford, UK, 1995, pp. 834-835. (g) Cativiela, C.; Diaz-de-Villegas, M. D. *Tetrahedron: Asymmetry* **2007**, *18*, 569.

2. (a) Seebach, D. In Proceedings of the Robert A. Welch Foundation Conferences on Chemistry and Biochemistry; Wiley: New York, 1984; p 93. (b) Seebach, D. Angew. Chem., Int. Ed. Engl. **1988**, 27, 1624. (c) Setzer, W. N.; Schleyer, P. v. R. Adv. Organomet. Chem. **1985**, 24, 353. (d) Williard, P. G. In Comprehensive Organic Synthesis; Trost, B. M.; Fleming, I., Eds.; Pergamon: New York, 1991; Vol. 1, Chapter 1.1.

3. (a) Arnett, E. M.; Moe, K. D. *J. Am. Chem. Soc.* **1991**, *113*, 7288. (b) Arnett, E. M.; Fisher, F. J.; Nichols, M. A.; Ribeiro, A. A. *J. Am. Chem. Soc.* **1990**, *112*, 801. (c) Seebach, D.; Bauer, von W. *Helv. Chim. Acta* **1984**, *67*, 1972. (d) Shobatake, K.; Nakamoto, K. *Inorg. Chim. Acta* **1980**, *4*, 485. (e) den Besten, R.; Harder, S.; Brandsma, L. *J. Organomet. Chem.* **1990**, *385*, 153. (f) Halaska, V.; Lochmann, L. *Collect. Czech. Chem. Commun.* **1973**, *38*, 1780. (g) Golovanov, I. B.; Simonov, A. P.; Priskunov, A. K.; Talalseva, T. V.; Tsareva, G. V.; Kocheshkov, *Dokl. Adka. Nauk. SSSR* **1963**, *149*, 835. (h) Simonov, A. P.; Shigorin, D. N.; Talalseva, T. V.; Kocheshkov, K. A. *Bull. Acad. Sci. USSR Div. Chem. Sci.* **1962**, *6*, 1056. (i) Armstrong, D. R.; Davies, J. E.; Davies, R. P.; Raithby, P. R.; Snaith, R.; Wheatley, A. E. H. *New J. Chem.* **1999**, 35. (j) Suzuki, M.; Koyama, H.; Noyori, R. *Bull. Chem. Soc. Jpn.* **2004**, *77*, 259. (k) Suzuki, M.; Koyama, H.; Noyori, R. *Tetrahedron* **2004**, *60*, 1571. (l) Lochmann, L.; Lim, D. *J. Organomet. Chem.* **1973**, *50*, 9. (m) Pospisil, P. J.; Wilson, S. R.; Jacobsen, E. N. *J. Am. Chem. Soc.* **1992**, *114*, 7585-7587.

4. (a) Jackman, L. M.; Lange, B. C. *J. Am. Chem. Soc.* **1981**, *103*, 4494. (b) Jackman, L. M.; Chen, X. *J. Am. Chem. Soc.* **1997**, *119*, 8681. (c) Jackman, L. M.; Petrei, M. M.; Smith, B. D. *J. Am. Chem. Soc.* **1991**, *113*, 3451. (d) Jackman, L. M.; Bortiatynski, J. *Adv. Carbanion Chem.* **1992**, *1*, 45.

5. The structure and reactivity of lithium enolates during methacrylate polymerizations have garnered considerable attention and have been reviewed: Zune, C.; Jerome, R. *Prog. Polymer Sci.* **1999**, *24*, 631. Also, see: Baskaran, D. *Prog. Polym. Sci.* **2003**, *28*, 521.

6. (a) Streitwieser, A. *J. Mol. Model.* **2006**, *12*, 673. (b) Streitwieser, A.; Wang, D. Z. *J. Am. Chem. Soc.* **1999**, *121*, 6213. (c) Leung, S. S.-W.; Streitwieser, A. *J. Org. Chem.* **1999**, *64*, 3390. (d) Wang, D. Z.; Kim, Y.-J.; Streitwieser, A. *J. Am. Chem. Soc.* **2000**, *122*, 10754. (e) Kim, Y.-J.; Streitwieser, A. *Org. Lett.* **2002**, *4*, 573. (f) Kim, Y.-J.; Wang, D. Z. *Org. Lett.* **2001**, *3*, 2599. (g) Streitwieser, A.; Leung, S. S.-W.; Kim, Y.-J. *Org. Lett.* **1999**, 1, 145. (h) Abbotto, A.; Leung, S. S.-W.; Streitwieser, A.; Kilway, K. V. *J. Am. Chem. Soc.* **1998**, *120*, 10807. (i) Leung, S. S.-W.; Streitwieser, A. *J. Am. Chem. Soc.* **1998**, *120*, 10557. (j) Abu-Hasanayn. F.; Streitwieser, A. *J. Org. Chem.* **1998**, *63*, 2954. (k) Abu-Hasanayn, F.; Streitwieser, A. *J. Org. Chem.* **1996**, *118*, 8136. (l) Gareyev, R.; Ciula, J. C.; Streitwieser, A. *J. Org. Chem.* **1996**, *61*, 4589. (m) Abu-Hasanayn, F.; Stratakis, M.; Streitwieser, A. *J. Org. Chem.* **1995**, *60*, 4688. (n) Dixon, R. E.; Williams, P. G.; Saljoughian, M.; Long, M. A.; Streitwieser, A. *Magn. Reson. Chem.* **1991**, *29*, 509.

7. (a) Reich, H. J. *J. Org. Chem.* **2012**, *77*, 5471. (b) Kolonko, K. J.; Wherritt, D. J.; Reich, H. J. *J. Am. Chem. Soc.* **2011**, *133* 16774.

8. (a) Hsieh, H. L.; Quirk, R. P. *Anionic Polymerization: Principles and Practical Applications*; Marcel Dekker: New York, 1996. (b) *Ions and Ion Pairs in Organic Reactions*; Szwarc, M., Ed.; Wiley: New York, 1972; Vol. 1 and 2. (c) Wardell, J. L. In *Comprehensive Organometallic Chemistry*; Wilkinson, G.; Stone, F. G. A.; Abels, F. W., Eds.; Pergamon: New York, 1982; Vol. 1, Chapter 2. (d) Wakefield, B. J. *The Chemistry of Organolithium Compounds*; Pergamon Press: New York, 1974. (e) Brown, T. L. *Pure Appl. Chem.* **1970**, *23*, 447. (f) Collum, D. B. *Acc. Chem. Res.* **1992**, *25*, 448.

9. Qu, B.; Collum, D. B. *J. Am. Chem. Soc.* **2006**, *128*, 9355 and references cited therein.

10. Ma, Y.; Collum, D. B. *J. Am. Chem. Soc.* **2007**, *129*, 14818 and references cited therein.

11. Liou, L. R.; McNeil, A. J.; Toombes, G. E. S.; Collum, D. B., *J. Am. Chem. Soc.* **2008**, *130*, 17334 and references cited therein.

12. Liou, L. R.; McNeil, A. J.; Ramirez, A.; Toombes, G. E. S.; Gruver, J. M.; Collum, D. B. *J. Am. Chem. Soc.* **2008**, *130*, 4859 and references cited therein.

13. A comprehensive survey of scaled procedures used by Pfizer Process over two decades shows that 68% of all C-C bond formations are carbanion based and 44% of these involved enolates: Dugger, R. W.; Ragan, J. A.; Ripin, D. H. B. *Org. Process Res. Dev.* **2005**, *9*, 253. For other applications of lithium enolates in pharmaceutical chemistry see: Farina, V.; Reeves, J. T.; Senanayake, C. H. Song, J. J. *Chem. Rev.* **2006**, *106*, 2734. Wu, G.; Huang, M. *Chem. Rev.* **2006**, *106*, 2596.

14. (a) *Enantioselective Synthesis of β-Amino Acids*; Juaristi, E., Ed.; Wiley-VCH: New York, 1997. (b) Sewald, N. *Angew. Chem., Int. Ed.* **2003**, *42*, 5794. (c) Ma, J.-A. *Angew. Chem., Int. Ed.* **2003**, *42*, 4290. (d) Liu, M.; Sibi, M. P. *Tetrahedron* **2002**, *58*, 7991. (e) Abele, S.; Seebach, D. *Eur. J. Org. Chem.* **2000**, 1. (f) Cardillo, G.; Tomasini, C. *Chem. Soc. Rev.* **1996**, 117. (g) Cole, D. C. *Tetrahedron* **1994**, *32*, 9517. (h) Juaristi, E.; Quintana, D.; Escalante, J. *Aldrichimica Acta* **1994**, *27*, 3.

15. (a) Michel, K.; Froehlich, R.; Wuerthwein, E.-U.; Eur. *J. Org. Chem.* **2009**, 5653. (b) Hata, S.; Iwasawa, T.; Iguchi, M.; Yamada, K.; Tomioka, K. *Synthesis* **2004**, 1471. (c) Braun, M.; Sacha, H.; Galle, D.; Baskaran, S. *Pure Appl. Chem.* **1996**, *68*, 561. (d) Iwasaki, G.; Shibasaki, M. *Tetrahedron Lett.* **1987**, *28*, 3257.

16. (a) Denmark, S. E.; Nicaise, O. J.-C. In *Comprehensive Asymmetric Catalysis*; Jacobsen, E. N., Pfaltz, A., Yamamoto, Y., Eds; Springer-Verlag: Heidelberg, 1999. Chapter 26.2. (b) Kobayashi, S.; Ishitani, H. *Chem. Rev.* **1999**, *99*, 1069. (c) Enders, D.; Reinhold, U. *Tetrahedron: Asymmetry* **1997**, *8*, 1895. (d) Volkmann, R. A. In *Comprehensive Organic Synthesis*; Trost, B. M.; Fleming, I., Eds; Pergamon: Oxford, 1991; Chapter 1.12. (e) Bloch, R. *Chem. Rev.* **1998**, *98*, 1407. (f) Dugger, R. W.; Ragan, J. A.; Ripin, D. H. B. *Org. Process Res. Dev.* **2005**, *9*, 253. (g) Farina, V.; Reeves, J. T.; Senanayake, C. H.; Song, J. J. *Chem. Rev.* **2006**, *106*, 2734. (h) Wu, G.; Huang, M. *Chem. Rev.* **2006**, *106*, 2596.

17. (a) Gakh, Y. G.; Gakh, A. A.; Gronenborn, A. M. *Magn. Reson. Chem.* **2000**, *38*, 551. (b) McGill, C. A.; Nordon, A.; Littlejohn, D. *J. Process Anal. Chem.* **2001**, *6*, 36. (c) Espinet, P.; Albeniz, A. C.; Casares, J. A.; Martinez-Ilarduya, J. M. *Coord. Chem. Rev.* **2008**, *252*, 2180.

18. ^{19}F NMR spectroscopy has a growing importance in structural and mechanistic organolithium chemistry: (a) Briggs, T. F.; Winemiller, M. D.; Collum, D. B.; Parsons, R. L., Jr.; Davulcu, A. K.; Harris, G. D.; Fortunak, J. D.; Confalone, P. N. *J. Am. Chem. Soc.* **2004**, *126*, 5427. (b) Hoepker, A. C.; Gupta, L.; Ma, Y.; Faggin, M. F.; Collum, D. B. *J. Am. Chem. Soc.* **2011**, *133*, 7135. (c) De Vries, T. S.; Goswami, A.; Liou, L. R.; Gruver, J. M.; Jayne, E.; Collum, D. B. *J. Am. Chem. Soc.* **2009**, *131*, 13142. (d) Ma, Y.; Breslin, S.; Keresztes, I.; Lobkovsky, E.; Collum, D. B. *J. Org. Chem.* **2008**, *73*, 9610. (e) Riggs, J. C.; Ramirez, A.; Cremeens, M. E.; Bashore, C. G.; Candler, J.; Wirtz, M. C.; Coe, J. W.; Collum, D. B. *J. Am. Chem. Soc.* **2008**, *130*, 3406. (f) Ma, Y.; Lobkovsky, E.; Collum, D. B. *J. Org. Chem.* **2005**, *70*, 2335. (g) Ramirez, A.; Candler, J.; Bashore, C. G.; Wirtz, M. C.; Coe, J. W.; Collum, D. B. *J. Am. Chem. Soc.* **2004**, *126*, 14700. (h) Kolonko, K. J.; Guzei, I. A.; Reich, H. J. *J. Org. Chem.* **2010**, *75*, 6163. (i) Kolonko, K. J.; Reich, H. J. *J. Am. Chem. Soc.* **2008**, *130*, 9668.

19. Gruver, J. M.; Liou, L. R.; McNeil, A. J.; Ramirez, A.; Collum, D. B. *J. Org. Chem.* **2008**, *73*, 7743.

20. (a) Kim, Y.-J.; Bernstein, M. P.; Galiano-Roth, A. S.; Romesberg, F. E.; Fuller, D. J.; Harrison, A. T.; Collum, D. B.; Williard, P. G. *J. Org. Chem.* **1991**, *56*, 4435. (b) For a improved procedure see: Ma, Y.; Hoepker, A. C.; Gupta, L.; Faggin; M. F.; Collum, D. B. *J. Am. Chem. Soc.*, **2010**, *132*, 15610.

21. (a) Collum, D. B. *Acc. Chem. Res.* **1993**, *26*, 227. (b) Lucht, B. L.; Collum, D. B. *Acc. Chem. Res.* **1999**, *32*, 1035.

22. Gregory, K; Schleyer, P. v. R.; Snaith, R. *Adv. Inorganic. Chem.* **1991**, *37*, 47. Mulvey, R. E. *Chem. Soc. Rev.* **1991**, *20*, 167.

23. Review of ^{6}Li NMR spectroscopy: Günther, H. *J. Brazil. Chem.* **1999**, *10*, 241.

24. For theoretical investigations of ^{6}Li-^{15}N coupling constants, see: (a) Parisel, O.; Fressigné, C.; Maddaluno, J.; Giessner-Prettre, C. *J. Org. Chem.* **2003**, *68*, 1290. (b) Koizumi, T.; Morihashi, K.; Kikuchi, O. *Bull. Chem. Soc. Jpn.* **1996**, *69*, 305.

25. For leading references and discussions of mixed aggregation effects, see: (a) Tchoubar, B.; Loupy, A. *Salt Effects in Organic and Organometallic Chemistry*; VCH: New York, 1992; Chapters 4, 5, and 7. (b) Caubère, P. *Chem. Rev.* **1993**, *93*, 2317. (c) Gossage, R. A.; Jastrzebski, J. T. B. H.; van Koten, G. *Angew. Chem., Int. Ed.* **2005**, *44*, 1448. (d) Ma, Y.; Hoepker, A. C.; Gupta, L. Faggin, M. F.; Collum, D. B. *J. Am. Chem. Soc.* **2010**, *132*, 15610. (e) See ref 16a and 22b.

26. The concentration of LDA, although expressed in units of molarity, refers to the concentration of the monomer unit (normality). The concentration of TMEDA is expressed as total concentration of free (uncoordinated) ligand.

27. We define the idealized rate law as that obtained by rounding the observed reaction orders to the nearest rational order.

28. The rate law provides the stoichiometry of the transition structure relative to that of the reactants: (a) Edwards, J. O.; Greene, E. F.; Ross, J. *J. Chem. Educ.* **1968**, *45*, 381. (b) Collum, D. B.; McNeil, A. J.; Ramirez, A. *Angew. Chem., Int. Ed.* **2007**, *46*, 3002.

29. Frisch, M. J.; Trucks, G.; W.; Schlegel, H. B.; Scuseria, G. E.; Robb, M. A.; Cheeseman, J. R.; Montgomery, Jr., J. A.; Vreven, T.; Kudin, K. N.; Burant, J. C.; Millam, J. M.; Iyengar, S. S.; Tomasi, J.; Barone, V.; Mennucci, B.;Cossi, M.; Scalmani, G.; Rega, N.; Petersson, G. A.; Nakatsuji, H.; Hada, M.; Ehara, M.; Toyota, K.; Fukuda, R.; Hasegawa, J.; Ishida, M.; Nakajima, T.; Honda, Y.; Kitao, O.; Nakai, H.; Klene, M.; Li, X.; Knox, J. E.; Hratchian, H. P.; Cross, J. B.; Bakken, V.; Adamo, C.; Jaramillo, J.; Gomperts, R.; Stratmann, R. E.; Yazyev, O.; Austin, A. J.; Cammi, R.; Pomelli, C.; Ochterski, J. W.; Ayala, P. Y.; Morokuma, K.; Voth, G. A.; Salvador, P.; Dannenberg, J. J.; Zakrzewski, V. G.; Dapprich, S.; Daniels, A. D.;Strain, M. C.; Farkas, O.; Malick, D. K.; Rabuck, A. D.; Raghavachari, K.; Foresman, J. B.; Ortiz, J. V.; Cui, Q.; Baboul, A. G.; Clifford, S.; Cioslowski, J.; Stefanov, B. B.; Liu, G.; Liashenko, A.; Piskorz, P.; Komaromi, I.; Martin, R. L.; Fox, D. J.; Keith, T.; Al-Laham, M. A.; Peng, C. Y.; Nanayakkara, A.; Challacombe, M.; Gill, P. M. W.; Johnson, B.; Chen, W.; Wong, M. W.; Gonzalez, C.; and Pople, J. A.; Gaussian, Inc., Wallingford CT, 2004. *GaussianVersion 3.09*; revision A.1; Gaussian, Inc.: Wallingford, CT, 2009. Gaussian 03, Revision B.04.

30. Open dimers were first proposed for the isomerization of oxiranes to allylic alcohols by mixed metal bases. See: Mordini, A.; Rayana, E. B.; Margot, C.; Schlosser, M. *Tetrahedron* **1990**, *46*, 2401. For a bibliography of lithium amide open dimers, see Ramirez, A.; Sun, X.; Collum, D. B. *J. Am. Chem. Soc.* **2006**, *128*, 10326 and references cited therein. Open dimer-based mechanisms for 1,2-additions of alkyllithiums have been investigated computationally: (a) Kaufmann, E.; Schleyer, P. v. R.; Houk, K. N.; Wu, Y.-D. *J. Am. Chem. Soc.* **1985**, *107*, 5560. (b) Nakamura, E.; Nakamura, M.; Koga, N.; Morokuma, K. *J. Am. Chem. Soc.* **1993**, *115*, 11016. Mori, S.; Kim, B. H.; Nakamura, M. *Chem. Lett.* **1997**, 1079.

31. For an attempted comprehensive bibliography of anionic triple ions of lithium salts (X-Li-X^-), see: Ma, Y.; Ramirez, A.; Singh, K. J.; Keresztes, I.; Collum, D. B. *J. Am. Chem. Soc.* **2006**, *128*, 15399.

32. Reich, H. J. *J. Org. Chem.* **2012**, *77*, 5471 and references cited therein.

33. Lithium enolates and their mixed aggregates have been examined computationally: (a) Pratt, L. M.; Streitwieser, A. *J. Org. Chem.* **2003**, *68*, 2830. (b) Pratt, L. M.; Newman, A.; Cyr, J. S.; Johnson, H.; Miles, B.; Lattier, A.; Austin, E.; Henderson, S.; Hershey, B.; Lin, M.; Balamraju, Y.; Sammonds, L.; Cheramie, J.; Karnes, J.; Hymel, E.; Woodford, B.; Carter, C. *J. Org. Chem.* **2003**, *68*, 6387. (c) Abbotto, A.; Streitwieser, A.; Schleyer, P. v. R. *J. Am. Chem. Soc.* **1997**, *119*, 11255. (d) Weiss, H.; Yakimansky, A. V.; Müller, A. H. E. *J. Am. Chem. Soc.* **1996**, *118*, 8897. (e) Pratt, L. M.; Khan, I. M. *J. Comput. Chem.* **1995**, *16*, 1067-1080. Dybal, J.; Kříž, J. *Collect. Czech. Chem. Commun.* **1994**, *59*, 1699. (f) Romesberg, F. E.; Collum, D. B. *J. Am. Chem. Soc.* **1994**, *116*, 9187. Rosi, M.; Sgamellotti, A.; Floriani, C. *J. Mol. Struct. (THEOCHEM)* **1998**, *431,* 33. (g) Romesberg, F. E.; Collum, D. B. *J. Am. Chem. Soc.* **1994**, *116*, 2166. (h) Pratt, L. M.; Streitwieser, A. *J. Org. Chem.* **2003**, *68*, 3830. (i) Pratt, L. M.; Nguyen, S. C.; Thanh, B. T. *J. Org. Chem.* **2008**, *73*, 6086. (j) Pratt, L. M.; Nguyen, N. V.; Ramachandran, B. *J. Org. Chem.* **2005**, *70*, 4279. (k) Streitwieser, A.; Reyes, J. R.; Singhapricha, T.; Vu, S.; Shah, K. *J. Org. Chem.* **2010**, *75*, 3821. (k) Pugh, J. K.; Streitwieser, A. *J. Org. Chem.* **2001**, *66*, 1334. (l) Kwan, E. E.; Evans, D. A. *Org. Lett.* **2010**, *12*, 5124. (l) Streitwieser, A.; Reyes, J. R.; Singhapricha, T.; Vu, S.; Shah, K. *J. Org. Chem.* **2010**, *75,* 3821. (m) Streitwieser, A. *J. Org. Chem.* **2009**, *74*, 4433.

34. For a structurally related triple ion bearing a TMEDA-chelated internal lithium, see: Bildmann, U. J.; Muller, G. *Organometallics* **2001**, *20*, 1689.

35. For a discussion of intrinisic reaction coordinate (IRC) calculations, see: Foresman, J. B.; Frisch, A. E. *Exploring Chemistry with Electronic Structure Methods,* 2nd ed.; Gaussian, Inc.: Pittsburgh, 1993.

36. (a) Bauer, W.; Klusener, P. A. A.; Harder, S.; Kanters, J. A.; Duisenberg, A. J. M.; Brandsma, L.; Schleyer, P. v. R. *Organometallics* **1988**, *7*, 552. (b) Köster, H.; Thoennes, D.; Weiss, E. *J. Organomet. Chem.* **1978**, *160*, 1. (c) Tecle´, B.; Ilsley, W. H.; Oliver, J. P. *Organometallics* **1982**, *1*, 875. (d) Harder, S.; Boersma, J.; Brandsma, L.; Kanters, J. A. *J. Organomet. Chem.* **1988**, *339*, 7. (e) Sekiguchi, A.; Tanaka, M. *J. Am. Chem. Soc.* **2003**, *125*, 12684. (f) Linnert, M.; Bruhn, C.; Ruffer, T.; Schmidt, H.; Steinborn, D. *Organometallics* **2004**, *23*, 3668. (g) Fraenkel, G.; Stier, M. *Prepr. Am. Chem. Soc., Div. Pet. Chem.* **1985**, *30*, 586. (h) Ball, S. C.; Cragg-Hine, I.; Davidson, M. G.; Davies, R. P.; Lopez-Solera, M. I.; Raithby, P. R.; Reed, D.; Snaith, R.; Vogl, E. M. *J. Chem. Soc., Chem. Commun.* **1995**, 2147. (i) Wehman, E.; Jastrzebski, J. T. B. H.; Ernsting, J.-M.; Grove, J. M.; van Koten, G. *J. Organomet. Chem.* **1988**, *353*, 145. (j) Bernstein, M. P.; Romesberg, F. E.; Fuller, D. J.; Harrison, A. T.; Williard, P. G.; Liu, Q. Y.; Collum, D. B. *J. Am. Chem. Soc.* **1992**, *114*, 5100.

37. The $(\eta^2\text{-TMEDA})_2Li^+$ is quite stable as evidenced by a number of examples in the crystallographic literature. Of particular interest are triple ions of general structure $[X_2Li]^-/^+Li(TMEDA)_2$. Hosmane, N. S.; Yang, J.; Zhang, H.; Maguire, J. A. *J. Am. Chem. Soc.* **1996**, *118*, 5150. Eaborn, C.; Lu, Z.-R.; Hitchcock, P. B.; Smith, J. D. *Organometallics* **1996**, *15*, 1651.

38. Cohen, A. J.; Mori-Sánchez, P.; Yang, W. *Science* **2008**, *321*, 792.

39. Representative studies of TMCDA in organolithium chemistry: (a) Hodgson, D. M.; Stefane, B.; Miles, T. J.; Witherington, J. *J. Org. Chem.* **2006**, *71*, 8510. (b) Cabello, N.; Kizirian, J.-C.; Gille, S.; Alexakis, A.; Bernardinelli, G.; Pinchard, L.; Caille, J.-C. *Eur. J. Org. Chem.* **2005**, *22*, 4835. (c) Cointeaux, L.; Alexakis, A. *Tetrahedron: Asymmetry* **2005**, *16*, 925. (d) Mealy, M. J.; Luderer, M. R.; Bailey, W. F.; Sommer, M. B. *J. Org. Chem.* **2004**, *69*, 6042. (e) Strohmann, C.; Gessner, V. H. *J. Am. Chem. Soc.* **2007**, *129*, 8952. (f) Strohmann, C.; Gessner, V. H. *J. Am. Chem. Soc.*, **2008**, *130*, 11719. (h) See ref 9 and 38a.

40. (a) Lucht, B. L.; Bernstein, M. P.; Remenar, J. F.; Collum, D. B. *J. Am. Chem. Soc.* **1996**, *118*, 10707. (b) Remenar, J. F.; Lucht, B. L.; Collum, D. B. *J. Am. Chem. Soc.* **1997**, *119*, 5567. (c) Hoffmann, D.; Collum, D. B. *J. Am. Chem. Soc.* **1998**, *120*, 5810. (d) Rutherford, J. L.; Hoffmann, D.; Collum, D. B. *J. Am. Chem. Soc.* **2002**, *124*, 264.

41. We suspect that the η^1-form of TMCDA imparts severe steric congestion (buttressing) owing to the proximity of the Li-NMe_2 moiety with the uncoordinated -NMe_2 moiety. Differences between TMEDA and TMCDA as ligands have also been attributed to the fixed bite-angle of TMCDA: Heuger, G.; Kalsow, S.; Göttlich, R. *Eur. J. Org. Chem.* **2002**, 1848.

42. Analogous relative reactivities of TMEDA and TMCDA were previously interpreted as evidence that both are chelated in the transition structures (ref 3).

43. (a) Kennedy, A. R.; Mulvey, R. E.; O'Hara, C. T.; Robertson, G. M.; Robertson, S. D. *Angew. Chem.* **2011**, *50*, 8375. (b) Garcia-Alvarez, P.; Kennedy, A. R.; O'Hara, C. T.; Reilly, K.; Robertson, G. M. *Dalton Trans.* **2011**, *40*, 5332.

44. Rodriguez-Delgado, A.; Chen, E.Y.-X. *J. Am. Chem. Soc.* **2005**, *127*, 961.

45. The concept of aggregate-based reactions of enolates has been endorsed enthusiastically: (a) Streitwieser, A.; Leung, S. S.-W.; Kim, Y.-J. *Org. Lett.* **1999**, *1*, 145-147. (b) Leung, S. S.-W.; Streitwieser, A. *J. Am. Chem. Soc.* **1998**, *120*, 10557-10558. (c) Solladié-Cavallo, A.; Csaky, A. G.; Gantz, I.; Suffert, J. *J. Org. Chem.* **1994**, *59*, 5343-5346. (d) Wei, Y.; Bakthavatchalam, R. *Tetrahedron* **1993**, *49*, 2373-2390. (e) Wei, Y.; Bakthavatchalam, R.; Jin, X.-M.; Murphy, C. K.; Davis, F. A. *Tetrahedron Lett.* **1993**, *34*, 3715-3718. (f) Solladié-Cavallo, A.; Simon-Wermeister, M.-C.; Schwarz, J. *Organometallics* **1993**, *12*, 3743-3747. (g) Pospisil, P. J.; Wilson, S. R.; Jacobsen, E. N. *J. Am. Chem. Soc.* **1992**, *114*, 7585-7587. (f) Williard, P. G.; Hintze, M. J. *J. Am. Chem. Soc.* **1987**, *109*, 5539-5541. (g) Horner, J. H.; Vera, M.; Grutzner, J. B. *J. Org. Chem.* **1986**, *51*, 4212-4220. (h) Heathcock, C. H.; Lampe, J. *J. Org. Chem.* **1983**, *48*, 4330-4337. (i) House, H. O.; Gall, M.; Olmstead, H. D. *J. Org. Chem.* **1971**, *36*, 2361-2371.

46. Kofron, W. G.; Baclawski, L. M. *J. Org. Chem.* **1976**, *41*, 1879.

47. Bose, A. K.; ANjaneyulc, B.; Bhaitacharya, S. K.; Manhas, M. S. *Tetrahedron* **1967**, *23*, 4769.

CHAPTER III:
Amino Alkoxide-Enolate Mixed Aggregates

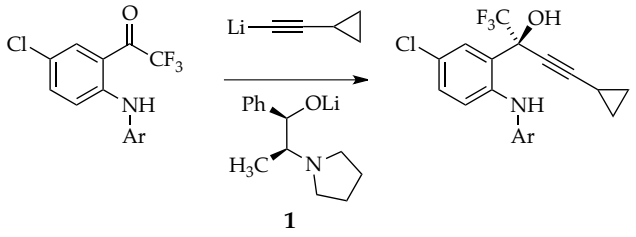

1 (1)

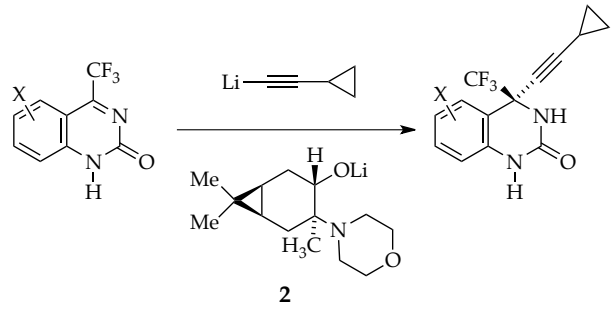

2 (2)

Alkoxides **1** and **2** were used by Merck and DuPont on pilot plant and plant scales to effect the enantioselective 1,2-additions shown in Schemes 1 and 2 in the synthesis of two reverse-transcriptase inhibitors.[1,2] By pre-equilibrating the acetylide and **1**, then cooling back down before adding the trifluoromethyl ketone, Merck was able to achieve 98% e.e. for the alkylation shown in Scheme 1. In ground-breaking work, Collum and coworkers elucidated the most active chiral mixed aggregate as cubic tetramer **3b**, which forms exclusive of **3a** and **3c** when reagents are mixed in a 1:1 ratio.[3] However, **3a** and **3c** can each be formed exclusively by mixing cyclopropylacetylide and amino alkoxide their respective stoichiometric ratios. This turned out to be an important feature of these mixtures that was exploited by DuPont whose most active specie was the 3:1 alkoxide heavy mixed aggregate **3c**. Following

similar protocol, DuPont was able to achieve 99.5% e.e. for the alkylation shown in Scheme 2, exemplifying the broad utility of these chiral auxiliaries.

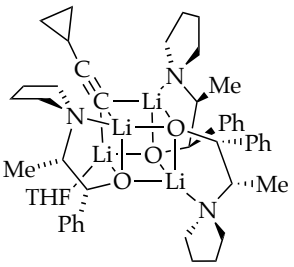

3a

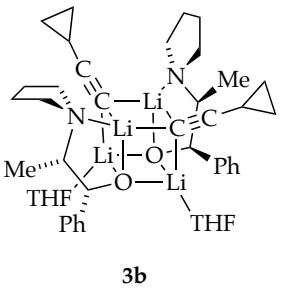

3b

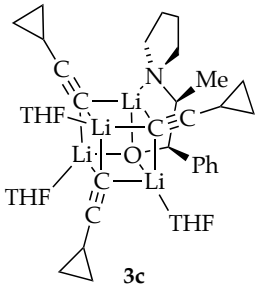

3c

Before we characterized the amino alkoxides themselves (Chapter 1), we initially set out to utilize the alkoxides in a manner analogous to that described above, but for stereoselective enolate chemistry. Asymmetric enolate additions, we believe, should be amenable to analagous aggregation control by replacing the acetylides with enolates (e.g. **4a-4c**).

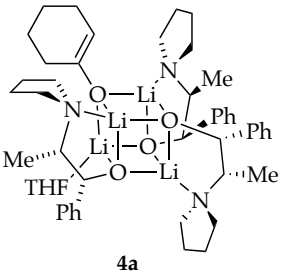

4a

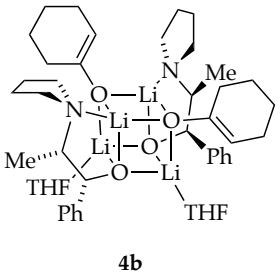

4b

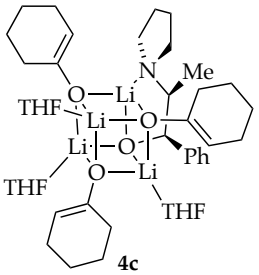

4c

Figure 3.1 shows spectra of mixtures of **1** and acetophenone enolate in varying ratios. Peaks corresponding to the homoaggregates, the 1:3, and the 2:2 mixed aggregates are apparent. The 3:1 amino alkoxide heavy mixed aggregate, however, was not evident. Furthermore, control of the aggregate stoichiometry through control

of the stoichiometry of the mixture, as in the cases of mixtures of amino alkoxides and acetylides, was not observed.

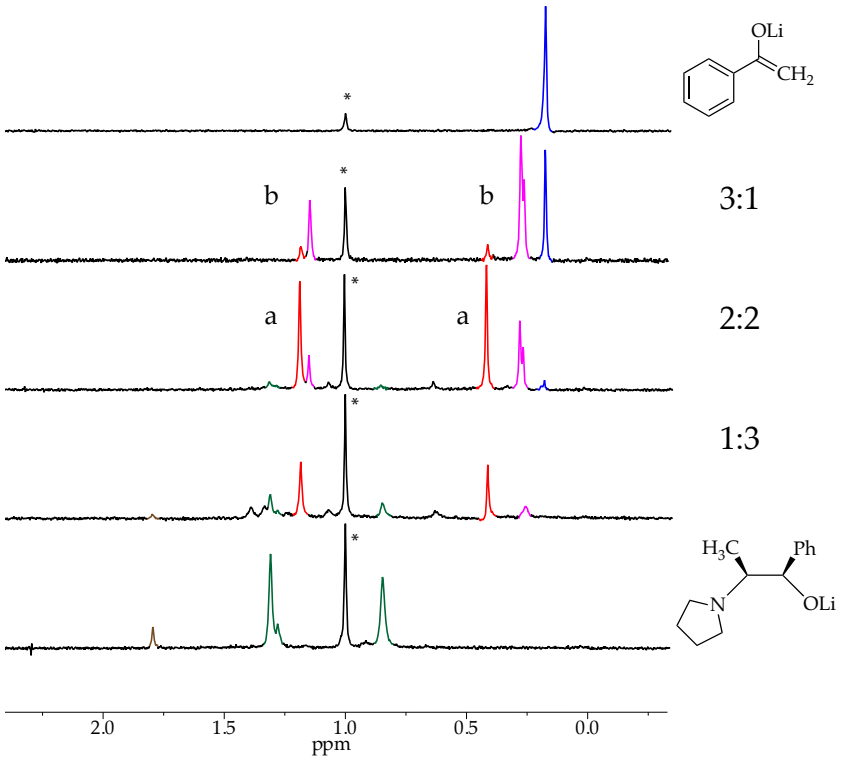

Figure 3.1. ^{6}Li NMR spectra of 0.10 M mixtures of [^{6}Li]acetophenone enolate and amino alkoxide **1** with 0.02 M excess ^{6}LiHMDS (asterisk) in 1.2 M THF with toluene cosolvent at -80 °C. Ratios of enolate to **2** shown. Mixed tetramers: a) (red): 2:2; b) (fuschia): 3:1.

Other mixtures of **1** with various enolates and phenolates gave less clear results. For example, when **1** was mixed with naphthol, numerous unexpected peaks resulted (Figure 3.2), potentially indicating the presence of competing aggregate forms.

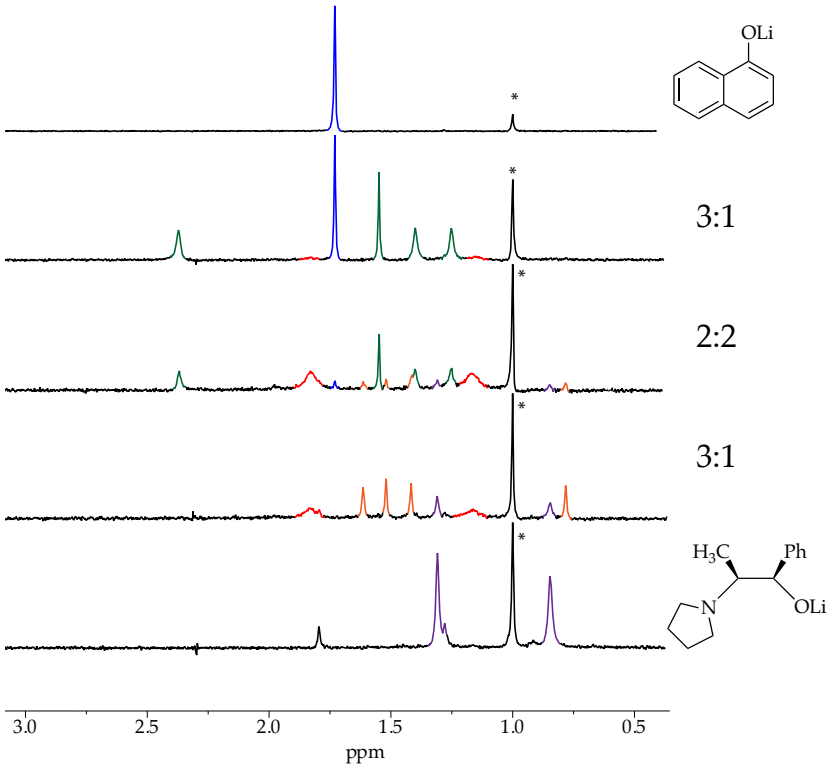

Figure 3.2. ^{6}Li NMR spectra of 0.10 M mixtures of [^{6}Li]naphthol phenolate and amino alkoxide **1** with 0.02 M excess ^{6}LiHMDS (asterisk) in 1.2 M THF with toluene cosolvent at -80 °C. Ratios of enolate to **2** shown. Identically colored peaks appear together, but are uncharacterized.

Mixtures of **2** with enolates and phenolates gave more consistent results. In the case of the mixture of **1** with cyclohexanone enolate, peaks corresponding to the 1:3, 2:2, and 3:1 cubic tetramers (**4a-4c**) were evident, though differences in coalescence temperatures leave peaks for the enolate rich 1:3 aggregate notably broad (Figure 3.3).

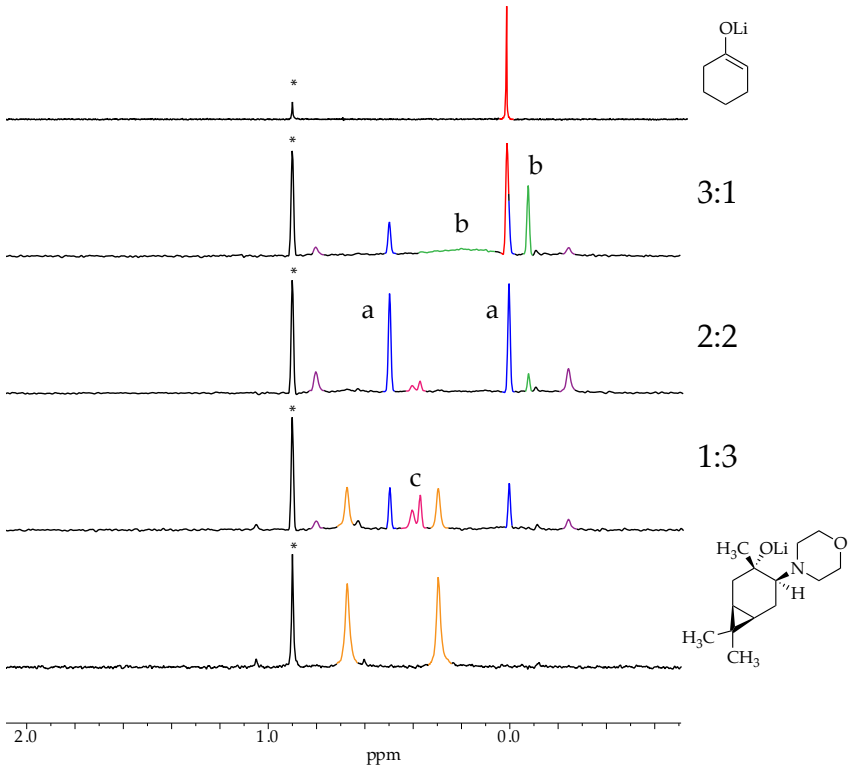

Figure 3.3. ^{6}Li NMR spectra of 0.10 M mixtures of [^{6}Li]cyclohexanone enolate and amino alkoxide **2** with 0.02 M excess ^{6}LiHMDS (asterisk) in 1.2 M THF with toluene cosolvent at -80 °C. Ratios of enolate to **2** shown. Mixed tetramers: a) (blue): 2:2; b) (green): 3:1; c) (fuchsia) 1:3. Purple is suspected 1:1 mixed dimer or isomer of 2:2.

The same peak pattern was observed in corresponding mixtures of **2** with naphthol phenolate (Figure 3.4). In mixtures of **2** with 1-indanone enolate (Figure 3.5) and 4-fluorophenolate (Figure 3.6), we did not observe the 3:1 alkoxide heavy aggregate. However, as previously mentioned, variable temperature work revealed that in some cases the aggregates appear to have different coalescence temperatures, thus some peaks may not appear due to decalescence at the observed temperature. In the case of mixtures of **2** and acetophenone enolate (Figure 3.7), we did see one peak that appears to correspond to the 3:1 alkoxide heavy mixed aggregate, but a second pair of peaks following a 1:1 stoichiometry are also present, indicating there may be

an additional aggregate or 2:2 isomer present. In any case, we are confident in the assignment of most of these mixtures as cubic tetramers analogous to those exploited by Merck and DuPont.

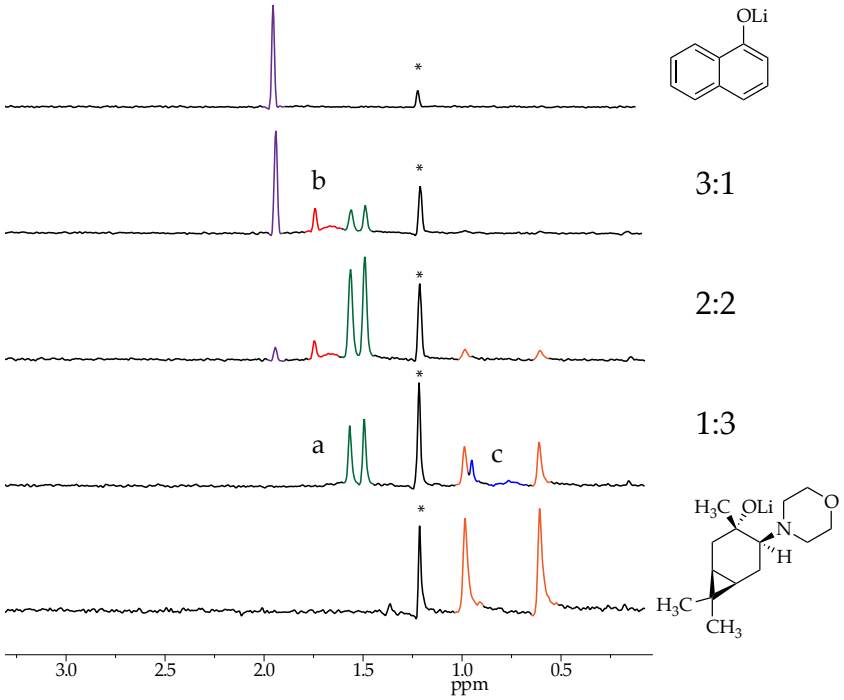

Figure 3.4. ^{6}Li NMR spectra of 0.10 M mixtures of [^{6}Li]naphthol phenolate and amino alkoxide **2** with 0.02 M excess ^{6}LiHMDS (asterisk) in 1.2 M THF with toluene cosolvent at -80 °C. Ratios of phenolate to **2** are shown. Mixed tetramers: a) (green): 2:2; b) (red): 3:1; c) (blue): 1:3.

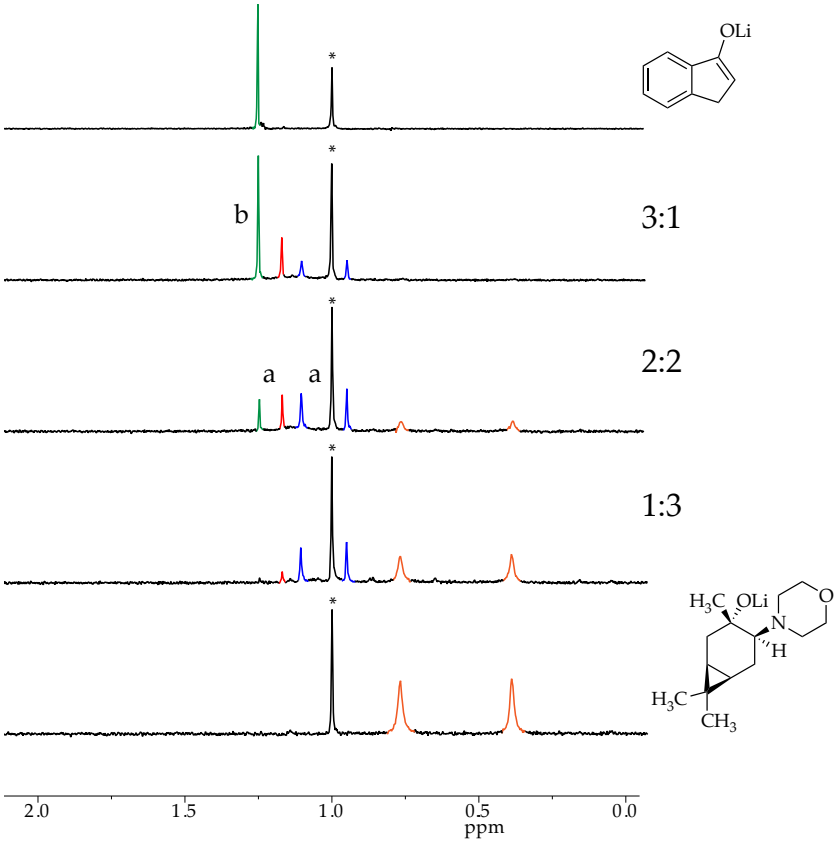

Figure 3.5. ^{6}Li NMR spectra of 0.10 M mixtures of [^{6}Li]1-indanone enolate and amino alkoxide **2** with 0.02 M excess ^{6}LiHMDS (asterisk) in 1.2 M THF with toluene cosolvent at -80 °C. Ratios enolate:**2** are: 1:0, 3:1, 2:2, 1:3 and 0:1 descending. Mixed tetramers: Blue: 2:2; Red: 3:1.

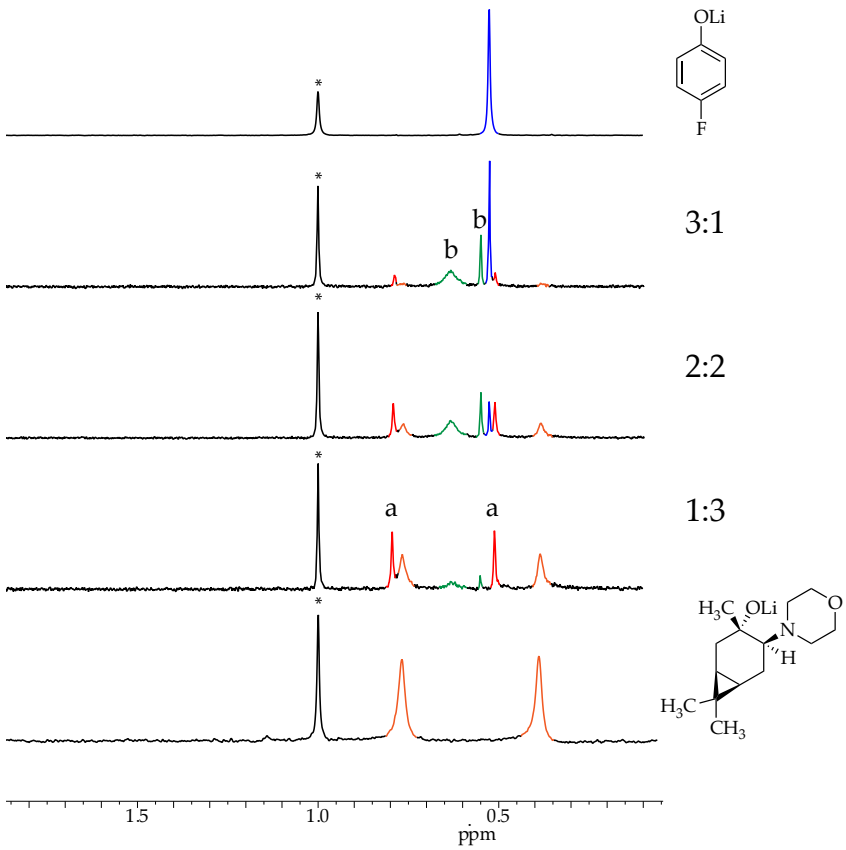

Figure 3.6. ^{6}Li NMR spectra of 0.10 M mixtures of [^{6}Li]4-fluorophenolate and amino alkoxide **2** with 0.02 M excess ^{6}LiHMDS (asterisk) in 1.2 M THF with toluene cosolvent at -80 °C. Ratios of enolate to **2** are shown. Mixed tetramers: a) (red): 2:2; b) (green): 3:1.

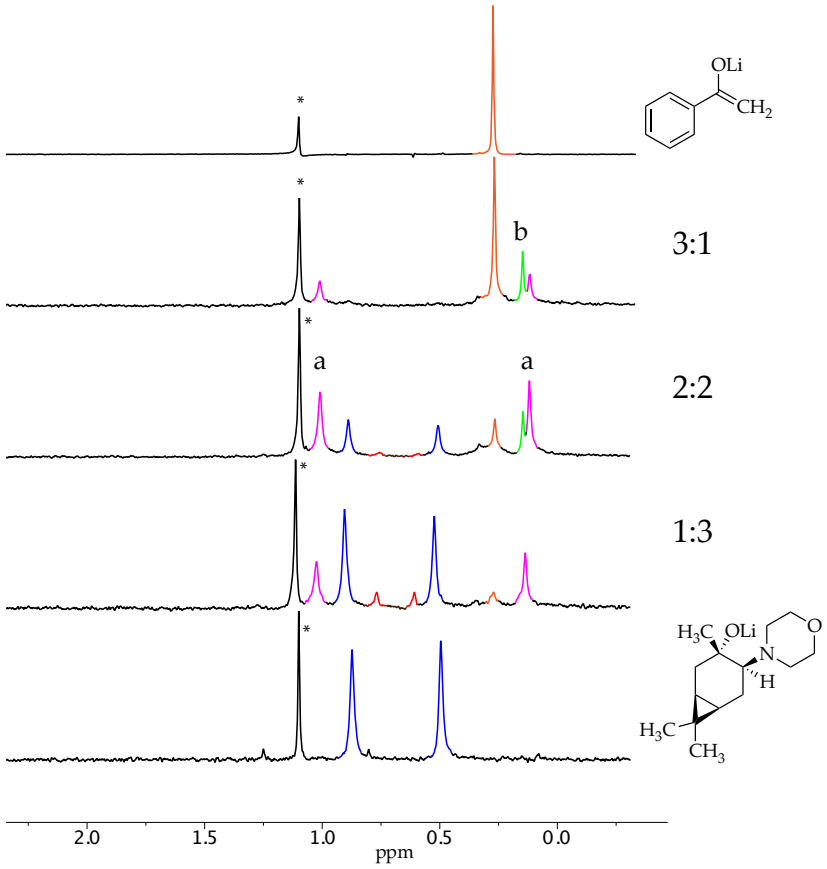

Figure 3.7. ^{6}Li NMR spectra of 0.10 M mixtures of [^{6}Li]acetophenone enolate and amino alkoxide **2** with 0.02 M excess ^{6}LiHMDS (asterisk) in 1.2 M THF with toluene cosolvent at -80 ºC. Ratios of enolate to **2** are shown. Mixed tetramers: a) (fuchsia): 2:2; b) (green): 3:1. Red pair of peaks are minor and unknown.

Unfortunately, with all of the amino alkoxide-enolate mixed aggregates, we were unable to achieve control of aggregate stoichiometry through mixture ratios- when a 1:1 ratio of amino alkoxide to enolate was mixed, for example, all possible mixed aggregates (4a-4c) and homoaggregates were observed simultaneously. This complete lack of stoichiometric control was concerning- we expect that 1:3 mixed

tetramer **5** with one enolate distal to the chelating amino alkoxide, for example, would give little facial preference for an incoming electrophile.

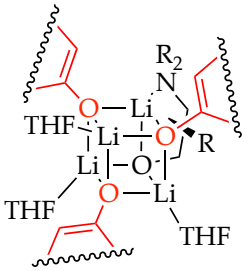

5

In studies of amino alkoxide aggregation presented in Chapter 1 of this thesis, we showed that amino alkoxides exclusively prefer a twist form where chelation is observed in perpendicular rather than in parallel planes (Scheme 3). Interestingly the industrially successful amino alkoxide-acetylide mixed aggregates do not preserve the inherently preferred chelate form of the amino alkoxides (**3a-3c**). Their success is perhaps a bit adventitious. We propose a new approach that may give more consistent control: We will aim to preserve the inherent twist chelate structure by directly inserting chelating enolates to replace the chelating alkoxides (Scheme 4). No rearrangement of the preferred twist structure would be required to accommodate the new chelates. Ongoing studies in the Collum group will explore this approach while aiming to develop a general method for engineering chiral aggregates with potential for highly stereo controlled enolate additions.

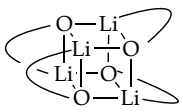

observed

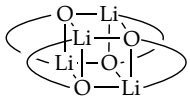

not observed

(3)

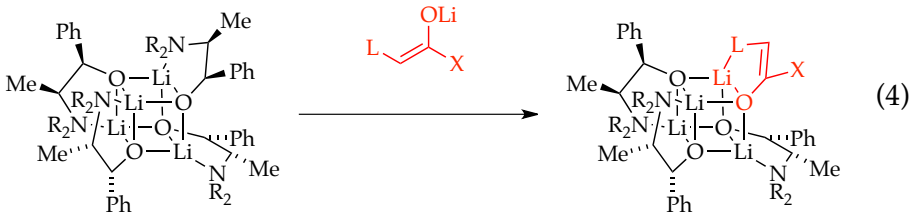
Ph
Me
R2N
Me
Ph
O
Li
Me
R2N
Li
O
R2N
Li
O
Ph
Me
O
Li
N
R2
Me
Ph
OLi
L
X
Ph
Me
L
X
O
Li
R2N
Li
O
R2N
Li
O
Ph
Me
O
Li
N
R2
Me
Ph

(4)

REFERENCES III

1. (a) Grabowski, E. J. J. "Reflections on Process Research". In *Chemical Process Research: The Art of Practical Organic Synthesis*; Abdel-Magid, A. F.; Ragan, J. A., Eds. American Chemical Society, Washington D.C.: USA 2004; pp 1-21.

2. (a) "An Efficient Chiral Moderator Prepared from Inexpensive (+)-3-Carene: Synthesis of the HIV-1 Non-Nucleoside Reverse Transcriptase Inhibitor DPC". Kauffman, G. S.; Harris, G. D.; Dorow, R. L.; Stone, B. R. P.; Parsons, R. L.; Pesti, J. A.; Magnus, N. A.; Fortunak, J. M.; Confalone, P. N.; Nugent, W. A. *Org. Lett.* **2000**, *2*, 3119. (b) "Development of Commercially Viable, Enantioselective Processes for HIV-1 NNRTIs". Parsons, R. L., Jr. *Curr. Opin. Drug Discovery Dev.* **2000**, *3*, 783.

3. (a) "Lithium Ephedrate-Mediated 1,2-Addition of a Lithium Acetylide to a Ketone: Solution Structures and Relative Reactivities of Mixed Aggregates Underlying the High Enantioselectivities". Thompson, A.; Corley, E. G.; Huntington, M. F.; Grabowski, E. J. J.; Remenar, J. F.; Collum, D. B. *J. Am. Chem. Soc*. **1998**, *120*, 2028. (b) "Highly Enantioselective 1,2-Addition of Lithium Acetylide-Ephedrate Complexes: Spectroscopic Evidence for Reaction Proceeding via a 2:2 Tetramer and X-ray Characterization of Related Complexes". Xu, F.; Reamer, R. A.; Tillyer, R.; Cummins, J. M.; Grabowski, E. J. J.; Reider, P. J.; Collum, D. B.; Huffman, J. C. *J. Am. Chem. Soc.* **2000**, *122*, 11212.